UNIVERSITY OF CINCINNATI

Date: January 19, 2006

I, Daekeun Kim **,**

hereby submit this work as part of the requirements for the degree of:

Doctorate of Philosophy (Ph.D.)

in:

Environmental Engineering

It is entitled:

Development of Integrated Treatment Scheme of Adsorption and Biofiltration for VOCs Removal

This work and its defense approved by:

Chair: Dr. George A. Sorial

Dr. Makram T. Suidan

Dr. Dionysios D. Dionysiou

Dr. Albert D. Venosa

Development of Integrated Treatment Scheme of Adsorption and Biofiltration for VOCs Control

A dissertation submitted to the

Division of Research and Advanced Studies
of the University of Cincinnati

in partial fulfillment of the requirements for the degree of

DOCTOR OF PHILOSOPHY

in the Department of Civil and Environmental Engineering
of the College of Engineering

2006

by

Daekeun Kim

M.S., Environmental Engineering, Konkuk University, Seoul, Korea, 2000
B.S., Environmental Engineering, Konkuk University, Seoul, Korea, 1998

Committee Chair: Dr. George A. Sorial

ABSTRACT

Biofiltration for VOC control is best operated at steady loads of contaminants. Variations in contaminant loads are, however, common in real application. As a solution to this limitation in biofiltration system, an innovative integrated technology was proposed to achieve stable contaminant removal efficiency by combining the buffering capacity of a 2-bed cyclic adsorption/desorption unit with a Trickle Bed Air Biofilter (TBAB). The overall goal of the study was accomplished through three specific studies: Characterization of TBAB performance; Development of adsorption process; Application of an integrated technology. First, investigations were made to operate independent lab-scale TBAB systems to remove single VOC. Experimental findings supported the handling limitation of biofilter performance under adverse feeding conditions experienced after biofilter reactor startup, biofilter backwashing as biomass control, fluctuating loads, or non-use periods (starvation and stagnant). Second, the design of the adsorption system was fundamentally based on the results obtained from the adsorption isotherm, which were explored by using Tedlar gas sampling bags as a simple constant volume method. The adsorption system consisted of two fixed beds which are alternately pressurized and depressurized in a 2-step cycle, where adsorption and desorption was simply achieved. Its main function is to dampen VOC concentration pulses in waste streams. Finally, by utilizing an adsorption/desorption cycle in a 2-fixed bed adsorption, an integrated treatment process of the 2-bed adsorption unit followed by the TBAB was developed and extensively tested. It was proven to achieve the goal of reliably treating fluctuating VOC loading with high removal efficiency; and attain more consistent emission compliance and economical design of biofiltration facilities.

ACKNOWLEGEMENT

I would like to express my deepest appreciation to my advisor, Dr. George A. Sorial, for his guidance, help, and support throughout my journey at the University of Cincinnati. His continuous pursuit of perfection and demand for scientific excellence was a major driving force behind this work. I would like to thank my committee members, Dr. Makram T. Suidan, Dr. Dionysios D. Dionysiou, and Dr. Albert D. Venosa, for their contribution, input, and critical review of my work. I gratefully acknowledge the financial assistance I received during the course of my graduate study, from the University Cincinnati and from the National Science Foundation.

I would like also to thank Zhangli Cai, my research partner for his continual support and cooperation throughout this study. I would like to thank Rachael Rhodes for her exceptional help during her work here as co-op student in the project. I would like to thank all my colleagues and friends at University of Cincinnati for making this journey enjoyable and memorable.

I would like to extend my acknowledgement to my previous advisor, Dr. Wan Namkoong at Konkuk University, whose reflective, considerate guidance encouraged me to continue studying at University of Cincinnati. I feel very fortunate to thank all my colleagues and friends in Korea.

I acknowledge my deepest gratitude to my parents, for their continuous faith and support. Only with their generous support and understanding was it possible to finish this seemingly interminable work. I also thank my brother Bonghan and sister Hajeong for routinely but patiently encouraging me to do graduate study. They alone were able to convince me that the personal benefit would make the efforts worthwhile.

To My Parents

TABLE OF CONTENTS

LIST OF TABLES

LIST OF FIGURES

CHAPTER 1

INTRODUCTION

1.1. Background

Primary gases emitted from most processes employing organic or petroleum based solvents have commonly been referred to as volatile organic compounds (VOCs). The release of VOCs into the environment contributes significantly to current air pollution problem. They are responsible for the formation of photo-oxidants such as ground-level ozone, $PM_{2.5}$ (Particulate matter that is 2.5 micrometers or smaller in size), urban smog, and regional haze. Individual VOCs have also significant adverse effects on their own toxicities. VOCs as a class have, therefore, been recommended for addition to the federal list of toxic substances (Hogue 2005; USEPA 2005; Wegman and Sasser 2005).

Anthropogenic source of VOCs are numerous and results form the presence of VOCs in unburned gasoline, solvent evaporation, and industrial emissions. Affected industries include paint booth industries, boat manufacturing facilities, yeast production facilities, plastic industries, pharmaceutical industries, petroleum industries, and many other industries including dry cleaing fertilizer; explosives; textile; food/beverages; leather; pulp and paper (Hines et al. 1993; Kennes and Veiga 2001; USEPA 2003).

VOC emissions have been managed by both federal and provincial initiatives. Policy development work has led to the development of a number of national standard, guidelines, and code of VOC emissions. Particularly, the passage of the 1990 Amendments to the Clean Air Act significantly heightened the interest in the development of innovative technologies for solving current pollution problems and preventing new ones (Lee 1991).

1.1.1. Biofiltration Technology

Since VOCs concentration in industrial off gas is at a low level in most cases, biological technologies have been recognized to be attractive as compared with other controls such as thermal incineration, carbon adsorption, liquid scrubbing, condensation, and catalytic incineration (Chou and Hsiao 1998; Deshusses et al. 1995; Devinny et al. 1996). In recent years, biofiltration has been recognized as a cost-effective technology for the purification of air contaminated with low concentrations of biologically degradable organic compounds (Leson and Winer 1991; Ottengraf et al. 1986; Smith et al. 1998).

Biofilters are reactors in which a humid polluted air stream is passed through a porous packed bed on which a mixed culture of microorganisms is immobilized (Deshusses 1997; Eweis et al. 1998). Biofilters are typically suitable to remove VOCs with moderate to low Henry's constants (Deshusses and Johnson 2000; Zhu et al. 2004). Biofiltration had been also applied to hot gas streams (more than 40 ^{o}C) (Kong et al. 2001). Conventional biofilters use a natural organic medium such as peat, compost, leaves, wood bark, and soil. The natural organic medium is impregnated with nutrients and buffers, and the bed moisture is maintained at a constant level by humidifying air (Devinny et al. 1996).

Trickle bed air biofilter (TBAB) is conceptually an identical process to conventional biofilters. TBABs employ synthetic inorganic or polymeric media as microbial attachment and allow intermittent delivery of nutrient and buffer to the media bed. The concept of the TBAB allows consistent nutrient and pH control for optimizing the waste utilizing kinetics for micro-organisms. TBABs are especially applicable for treating VOC at high loading and they achieved consistent VOC removal efficiencies exceeding 99 % at high VOC loadings (Smith et al. 1996; Sorial et al. 1995). Lu and his coworkers (Lu et al. 2000; Lu et al. 2001) also demonstrated that

TBAB appears to be an effective treatment process for removing both single and mixed VOCs with low to high loadings.

Although biofilters have been used successfully for many applications, several design and operational challenges remain. These challenges include understandings of the biomass control in the biofilter and dynamically-varying waste gas stream due to the unsteady-state nature of the industrial processes.

TBABs performance decreased substantially, with build up of back pressure due to accumulation of excess biomass within the medium bed (Delhomenie et al. 2003; Smith et al. 1996; Weber and Hartmans 1996). The control of biomass was necessary for attaining stable, long-term high removal efficiencies for the biofilter. For this reason, many researchers have focused on the biomass control for long-term operation of biofiltration. Reported biomass control strategies included bed irrigation (Jorio et al. 2000), stimulation of protozoan predation (Cox and Deshusses 1999), mechanical methods employing bed stirring and bed washing (Delhomenie et al. 2003), and NaOH washing (Weber and Hartmans 1996), and periodic backwashing with full-medium fluidization (Smith et al. 1996; Smith et al. 1998; Sorial et al. 1995; Sorial et al. 1998). Specifically, the studies reporting periodic backwashing strategy demonstrated that long term performance of biofilters could be maintained at high removal efficiencies in the 99 % level for a toluene loading of 4.1 kg COD/m^3·day (Smith et al. 1998) and for a styrene loading of 4.26 kg COD/ m^3·day (Sorial et al. 1998). However, most of these methods have major drawbacks such as the subsequent reduction in biofilter performance due to the loss of active biomass (Delhomenie et al. 2003).

In practice most off gas or treatment streams contaminated with VOCs have variable flowrates, unsteady loading, and various contaminant compositions, which limit the handling efficiency of the biofiltration (Fitch et al. 2002; Mohseni and Allen 1999). The biofilter is also

exposed to the non-use conditions (e.g. substrate starvation) due to the shut down for equipment repair or during weekends and holidays. Generally, the original removal efficiencies after the non-use periods can be recovered more quickly than those seen in the original acclimation at the start-up. A study of microbial activity in a biomass recycle reactor revealed that starvation resulted in variation on bacterial numbers and microbial community as well as their physiological state (Konopka et al. 2002).

1.1.2. Innovative Biofiltration Technology

To overcome erratic performance of the biofilter during these kinds of transient loads, the development of an innovative biofilteration technology to achieve stable contaminant removal efficiency is significant for accomplishing the increasing stringent environmental legislation. Some studies (Moe and Qi 2004; Woertz et al. 2002) suggested that a fungal biofilter should be an effective alternative to conventional abatement technologies under discontinuous loading conditions. Irvine and Moe (2001) proposed periodical operated biofilter during unsteady state loading. This system imposed a diverse array of operating conditions of a sequencing batch reactor. Song and Kinney (2001) improved the biomass distribution and the stability of bioreactors by a directionally switching mode such that the contaminant air stream direction is periodically reversed through the reactor. Park and Kinney (2001) evaluated the slip feed system for biofilter. In this system, reacclimation periods were reduced after a shutdown period. Al-Rayes et al. (2001) applied load dampening system to dampen the contaminant during transient feed conditions. Lee et al. (2001) developed a horizontal biofilter without back-mixing to allow a shorter residence time. Yang and his coworkers (Yang et al. 2002; Yang et al. 2004) developed a rotating drum biofilter for even distribution of the VOC loading, biomass, and nutrient. Most of

these studies have shown the possibility of applying their systems for VOC removal, but little studies have achieved long-term extended, high removal performance.

Researchers have reported that the use of "treatment trains" or "coupled systems" may be advantageous compared with any single biological technology. Manninen et al. (2003) found that a liquid treatment reactor coupled with a biofilter provided an average VOC removal efficiency of 96 % at a VOC loading rate of 79 $g/m^3 \cdot hr$. Other researchers reported that a combined system of a biofilter preceded by a carbon filter can provide an effective solution for VOC control of emissions with unstable pollutant load (Amanullah et al. 2000; Chang et al. 2001; Li and Moe 2004; Weber and Hartmans 1995). Weber and Hartmans (1995) applied activated carbon as a buffer in biofiltration of waste gases with fluctuating contaminant content. Li and Moe (2004) installed a single column of GAC in series before a biofilter, demonstrating that the GAC can dampen effectively the effects of the intermittent loading. However, when larger fluctuation of the contaminant loading is encountered, the buffer capacity of a single bed of carbon adsorption will be quickly exhausted. Furthermore, since contaminants are mostly captured in the adsorption column before the biofilter, the biofilter will be exposed to substrate starvation condition until breakthrough in the adsorption column is achieved. Further attention should be implemented towards the design of the buffer unit for successful application of an integrated system of a adsorption unit and a biofilter.

Since the buffer capacity of the adsorbents depends on the desired concentration range of the adsorbate and on the time available for desorption (Weber and Hartmans 1995), long-term maintenance of the adsorption unit is not practical without a regeneration step. Hence the successful operation of adsorption system is determined by the sufficient regeneration (i.e., desorption). The possible modes of desorption depend on economic factor and technical considerations (Ruthven et al. 1994).

1.2. Research Objectives

The overall objective of the proposed study is to develop a novel technology for VOCs removal from waste gas with long-term, stable, high removal (>99 %) performance. An integrated treatment scheme of a 2-fixed bed adsorption unit followed by a TBAB unit was proposed for this purpose. It is expected that the operating cycle of adsorption and desorption for the 2-fixed bed adsorption unit minimizes fluctuations in removal performance in the TBAB unit and improves the overall efficiency of the biofiltration treatment process. Typical contaminants in paint booth operation were represented as model VOCs. The specific objectives of this study are addressed in three major phases:

Phase I: Characterization of TBAB performance under adverse operating conditions: 1) Determine the critical loading capacity of TBAB for each contaminant. 2) Determine the impact of non-use periods under different loading rates.

Phase II: Development of a 2-bed adsorption process for dampening contaminant fluctuations: The purpose of this phase is to develop a system to dampen VOC concentration pulses in waste air. In order to achieve a more steady effluent composition, the following specific goals were studied: 1) Determine the adsorption isotherms of VOCs of concern; 2) Evaluate the performance of adsorption and desorption cycles for a 2-fixed bed adsorption unit.

Phase III: Application of the integrated technology to the removal of VOC: The performance of an integrated treatment scheme of a TBAB unit preceded by a 2-fixed bed adsorption unit was explored under dynamic loadings of the contaminant.

1.3. Structure of Dissertation

Chapter 1 introduces the research background and the objectives. Phase I for this study specifies TBAB performance, which is presented in Chapters 2, 3, and 4. Chapter 2 provides characteristics of TBAB performance for single VOC removal and the significance of this study. The effects of step-changes in influent concentration of VOCs and non-use periods on biofilter performance were investigated. In Chapter 3, biofilter response for each VOC removal was compared based on the results obtained from Chapter 2. In Chapter 4, the role of biomass distribution and activity in biofilter performance was explored.

For Phase II, the adsorption study is provided in Chapters 5 and 6. Chapter 5 presents a study on gas phase adsorption isotherm to determine the equilibrium adsorption capacities of different types of adsorbent for VOCs. In Chapter 6, 2-fixed bed adsorption system was designed based on the results obtained from Chapter 5, and the operating cycles of adsorption and desorption in a 2-fixed bed adsorption system were evaluated. Phase III is presented in Chapter 7. The integrated performance of a 2-fixed bed adsorption system followed by a TBAB was investigated. The final chapter, Chapter 8, presents a summary of this research and the conclusions. Chapter 9 provides recommendations for future study. The structure of dissertation was delineated in Figure 1.1.

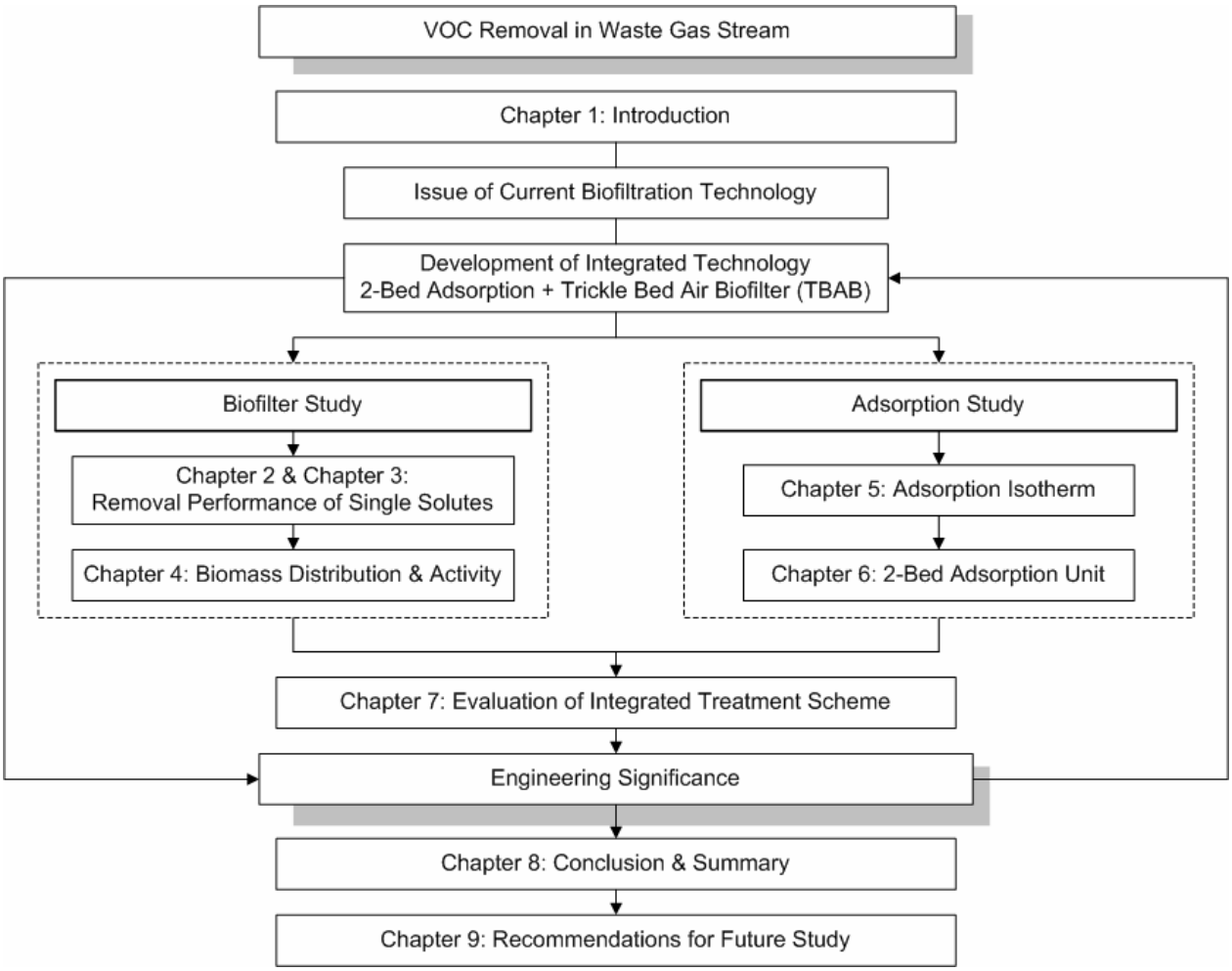

Figure 1-1 Schematic diagram of structure of dissertation

1.4. References

Al-Rayes, A. W., Kinney, K. A., Seibert, A. F., and Corsi, R. L. (2001). "Load dampening system for vapor phase bioreactors." *Journal of Environmental Engineering-Asce*, 127(3), 224-232.

Amanullah, M., Viswanathan, S., and Farooq, S. (2000). "Equilibrium, kinetics, and column dynamics of methyl ethyl ketone biodegradation." *Industrial & Engineering Chemistry Research*, 39(9), 3387-3396.

Chang, K. S., Lu, C. Y., and Lin, M. R. (2001). "Treatment of volatile organic compounds from polyurethane and epoxy manufacture by a trickle-bed air biofilter." *Journal of Bioscience and Bioengineering*, 92(2), 126-130.

Chou, M. S., and Hsiao, C. C. (1998). "Treatment of styrene-contaminated airstream in biotrickling filter packed with slags." *Journal of Environmental Engineering-Asce*, 124(9), 844-850.

Cox, H. H. J., and Deshusses, M. A. (1999). "Chemical removal of biomass from waste air biotrickling filters: Screening of chemicals of potential interest." *Water Research*, 33(10), 2383-2391.

Delhomenie, M. C., Bibeau, L., Gendron, J., Brzezinski, R., and Heitz, M. (2003). "A study of clogging in a biofilter treating toluene vapors." *Chemical Engineering Journal*, 94(3), 211-222.

Deshusses, M. A. (1997). "Biological waste air treatment in biofilters." *Current Opinion in Biotechnology*, 8(3), 335-339.

Deshusses, M. A., Hamer, G., and Dunn, I. J. (1995). "Behavior of biofilters for waste air biotreatment .1. dynamic- model development." *Environmental Science & Technology*, 29(4), 1048-1058.

Deshusses, M. A., and Johnson, C. T. (2000). "Development and validation of a simple protocol to rapidly determine the performance of biofilters for VOC treatment." *Environmental Science & Technology*, 34(3), 461-467.

Devinny, J. S., Deshusses, M. A., and Webster, T. S. (1996). *Biofiltration for air pollution control*, Lewis Publishers, Boca Raton, FL.

Eweis, J. B., Ergas, S. J., Chang, D. P. Y., and Schroeder, E. D. (1998). *Bioremediation Principles*, WCB/McGraw-Hill, Boston.

Fitch, M. W., England, E., and Zhang, B. (2002). "1-butanol removal from a contaminated airstream under continuous and diurnal loading conditions." *Journal of the Air & Waste Management Association*, 52(11), 1288-1297.

Hines, A. L., Ghosh, T. K., Loyalka, S. K., and Warder, R. C. (1993). *Indoor air quality and control*, PTR Prentice Hall, Englewood cliffs, NJ.

Hogue, C. *Cancer risk*. In Chemical & Engineering News, 83, 2005

Irvine, R. L., and Moe, W. M. (2001). "Period biofilter operation for enhanced performance during unsteady-state loading conditions." *Water Science and Technology*, 43(3), 231-239.

Jorio, H., Bibeau, L., and Heitz, M. (2000). "Biofiltration of air contaminated by styrene: Effect of nitrogen supply, gas flow rate, and inlet concentration." *Environmental Science & Technology*, 34(9), 1764-1771.

Kennes, C., and Veiga, M. C. (2001). *Bioreactors for waste gas treatment*, Kluwer Academic Publishers, Boston.

Kim, D., Cai, Z., and Sorial, G. A. (2005). "Evaluation of trickle bed air biofilter performance under periodic stressed operating conditions as a function of styrene loading." *Journal of the Air & Waste Management Association*, 55(2), 200-209.

Kong, Z., Farhana, L., Fulthorpe, R. R., and Allen, D. G. (2001). "Treatment of volatile organic compounds in a biotrickling filter under thermophilic conditions." *Environmental Science & Technology*, 35(21), 4347-4352.

Konopka, A., Zakharova, T., and Nakatsu, C. (2002). "Effect of starvation length upon microbial activity in a biomass recycle reactor." *Journal of Industrial Microbiology & Biotechnology*, 29(5), 286-291.

Lee, B. (1991). "Highlights of the clean-air act amendments of 1990." *Journal of the Air & Waste Management Association*, 41(1), 16-19.

Lee, D. H., Lau, A. K., and Pinder, K. L. (2001). "Development and performance of an alternative biofilter system." *Journal of the Air & Waste Management Association*, 51(1), 78-85.

Leson, G., and Winer, A. M. (1991). "Biofiltration - an innovative air-pollution control technology for voc emissions." *Journal of the Air & Waste Management Association*, 41(8), 1045-1054.

Li, C. N., and Moe, W. M. "Effect of activated carbon as a buffer for biofilters treating dynamically varying VOC concentrations." *Air & Waste Management Association's 97th Annual Conference & Exhibition*, Indianapolis, IN.

Lu, C. Y., Chu, W. C., and Lin, M. R. (2000). "Removal of BTEX vapor from waste gases by a trickle bed biofilter." *Journal of the Air & Waste Management Association*, 50(3), 411-417.

Lu, C. Y., Lin, M. R., and Lin, J. C. (2001). "Removal of styrene vapor from waste gases by a trickle-bed air biofilter." *Journal of Hazardous Materials*, 82(3), 233-245.

Manninen, M. R., Niemi, B. A., and Kleinheinz, G. T. (2003). "Use of a coupled biological system to treat a chemically complex air stream." *Archives of Environmental Contamination and Toxicology*, 45(1), 1-10.

Moe, W. M., and Qi, B. (2004). "Performance of a fungal biofilter treating gas-phase solvent mixtures during intermittent loading." *Water Research*, 38(9), 2259-2268.

Mohseni, M., and Allen, D. G. (1999). "Transient performance of biofilters treating mixtures of hydrophilic and hydrophobic volatile organic compounds." *Journal of the Air & Waste Management Association*, 49(12), 1434-1441.

Ottengraf, S. P. P., Meesters, J. J. P., Vandenoever, A. H. C., and Rozema, H. R. (1986). "Biological elimination of volatile xenobiotic compounds in biofilters." *Bioprocess Engineering*, 1(2), 61-69.

Park, J., and Kinney, K. A. (2001). "Evaluation of slip feed system for vapor-phase bioreactors." *Journal of Environmental Engineering-Asce*, 127(11), 979-985.

Ruthven, D. M., Farooq, S., and Knaebel, K. S. (1994). *Pressure swing adsorption*, VCH Publishers, Weinheim, New York.

Smith, F. L., Sorial, G. A., Suidan, M. T., Breen, A. W., Biswas, P., and Brenner, R. C. (1996). "Development of two biomass control strategies for extended, stable operation of highly efficient biofilters with high toluene loadings." *Environmental Science & Technology*, 30(5), 1744-1751.

Smith, F. L., Sorial, G. A., Suidan, M. T., Pandit, A., Biswas, P., and Brenner, R. C. (1998). "Evaluation of trickle bed air biofilter performance as a function of inlet VOC concentration and loading, and biomass control." *Journal of the Air & Waste Management Association*, 48(7), 627-636.

Song, J., and Kinney, K. A. (2001). "Effect of directional switching frequency on toluene degradation in a vapor-phase bioreactor." *Applied Microbiology and Biotechnology*, 56(1-2), 108-113.

Sorial, G. A., Smith, F. L., Suidan, M. T., Biswas, P., and Brenner, R. C. (1995). "Evaluation of trickle-bed biofilter media for toluene removal." *Journal of the Air & Waste Management Association*, 45(10), 801-810.

Sorial, G. A., Smith, F. L., Suidan, M. T., Pandit, A., Biswas, P., and Brenner, R. C. (1998). "Evaluation of trickle-bed air biofilter performance for styrene removal." *Water Research*, 32(5), 1593-1603.

USEPA. *Toxic release inventory program*. available on the World Wide Web at http://www.epa.gov/tri/index.htm (accessed on accessed on April 2005)

USEPA. (2005). "Guidelines for Carcinogen Risk Assessment." *EPA/630/P-03/001B*, U.S. Environmental Protection Agency, Washingto, D.C.

Weber, F. J., and Hartmans, S. (1995). "Use of activated carbon as a buffer in biofiltration of waste gases with fluctuating concentrations of toluene." *Applied Microbiology and Biotechnology*, 43(2), 365-369.

Weber, F. J., and Hartmans, S. (1996). "Prevention of clogging in a biological trickle-bed reactor removing toluene from contaminated air." *Biotechnology and Bioengineering*, 50(1), 91-97.

Wegman, L., and Sasser, E. *The path toward clean air: Implementing new standards for ozone and fine particles*. In The magazine for environmental managers, April 2005

Woertz, J. R., Kinney, K. A., Kraakman, N. J. R., van Heiningen, W. N. M., van Eekert, M. H. A., and van Groenestijn, J. W. (2002). "Mite growth on fungus under various environmental conditions and its potential application to biofilters." *Experimental and Applied Acarology*, 27(4), 265-276.

Yang, C. P., Suidan, M. T., Zhu, X., and Kim, B. J. "Development and evaluation of rotating drum biofilter for VOC removal." *Water Environment Federation*, Alexandria, VA.

Yang, C. P., Suidan, M. T., Zhu, X. Q., and Kim, B. J. (2004). "Removal of a volatile organic compound in a hybrid rotating drum biofilter." *Journal of Environmental Engineering-Asce*, 130(3), 282-291.

Zhu, X. Q., Suidan, M. T., Pruden, A., Yang, C. P., Alonso, C., Kim, B. J., and Kim, B. R. (2004). "Effect of substrate Henry's constant on biofilter performance." *Journal of the Air & Waste Management Association*, 54(4), 409-418.

CHAPTER 2

TBAB STUDY FOR SINGLE VOC REMOVAL

2.1. Abstract

This study evaluated the impact of two nonuse periods, i.e., starvation (without VOCs loading) and stagnant (no flow passing through the biofilter), on biofilter performance as a function of VOCs loading. The obtained results were compared against consistently high efficient performance of the biofilter by employing backwashing as biomass control. The study was conducted by using the following VOCs-two aromatic compounds, namely, toluene and styrene, and two oxygenated compounds, namely, methyl ethyl ketone (MEK) and methyl isobutyl ketone (MIBK).

High performance (over 99% removal) of the biofilter had been observed for all experimental strategies (backwashing, starvation, and stagnant) for toluene loading up to 3.52 kg COD/m^3·day (corresponding to an inlet concentration of 250 ppmv); styrene loading up to 1.27 kg COD/m^3·day (100 ppmv); MEK loading up to 3.52 kg COD/m^3·day (250 ppmv); and MIBK loading up to 2.17 kg COD/m^3·day (100 ppmv). Up to these loadings rates, no substantial negative impact of nonuse periods on the biofilter performance was revealed. However, when higher VOCs loading was employed, the coordinated biomass control was subsequently unavoidable for attaining consistently high removal efficiency. As VOCs loading increased, reacclimation of the biofilter to reach the 99 % removal efficiency following backwashing or the nonuse periods was delayed; which was a critical factor in biofilter performance. Biofilter response after the nonuse periods was apparently different to that after backwashing. It was strongly dependent on the active biomass in the biofilter.

2.2. Introduction

This chapter presents the results of the first phase of this research. The effects of adverse operating conditions on biofilter performance were explored by using lab-scale trickle bed air biofilters treating different single VOC, namely, Toluene, Styrene, Methyl ethyl ketone, and Methyl isobutyl ketone. The impact of non-use period (starvation and stagnant) was investigated under different VOC loading rates. The obtained results were compared against a consistent high efficient performance of the biofilter by employing backwashing as biomass control. The study results can be considered in the design and operation of the biofilter for further application. The evaluation for each VOC is focused on the following operational parameters: (1) VOC loading and removal, (2) the response of biofilter performance after backwashing and non-use periods, and (3) development of preliminary kinetic data based on removal with biofilter depth.

2.3. Materials and Methods

2.3.1. Experimental Biofilter System

Experimental work was performed on four independent lab-scale reactors for controlling single contaminants. The schematic diagram of the experimental system for the lab-scale TBAB is presented in Figure 2-1. The biofilter was constructed of seven cylindrical glass sections (Ace Glass Inc., Vineland, NJ) with an internal diameter of 76 mm and a total length of 130 cm. The sections were connected with high pressure clamps (75psi). Each section was equipped with a sampling port that extends to the centre of the column. A head space section in the top section was designed for VOC-containing air inlet and for housing the nutrient spray nozzle, while a bottom space at a bottom section was designed for the outlet of treated air and leachate. Each space had sampling ports to allow sampling of stream entering and leaving the biofilter, as well

as axially along the medium bed four gas-sampling ports, which were located at 7.6 cm, 23 cm, 38 cm, and 53 cm from the bottom of bed of the reactor.

The reactor was packed with pelletized diatomaceous earth biological support media (Celite® 6 mm R-635 Bio-Catalyst Carrier; Celite Corp., Lompoc, CA) to a depth of about 60 cm. The pelletized media was demonstrated to be significantly superior to the other media such as a compost mixture and a synthetic, monolithic media (Sorial et al. 1993). The pellets of R-635 were made from sintered diatomaceous earth and are therefore principally silica (SiO_2). Their physical properties were measured in other study (Smith et al. 1996) performed at University of Cincinnati. They had a circular cross-section with a nominal diameter of 0.635 cm, length of 0.64 cm (mean), a sphericity of 0.84, and a specific surface of 11.9 cm^2/cm^3. The measured pellet internal and external void fractions were about 0.65 and 0.34, respectively, and the bulk density was about 0.62 g/cm^3. The biofilters were maintained at a constant operating temperature of 20 ^oC in a constant temperature chamber. The biofilters were operated in a co-current gas and liquid downward flow mode.

The air supplied to the biofilter was purified with complete removal of water, oil, carbon dioxide, VOCs, and particles by Balston FTIR purge gas generator (Paker Hannifin Corporation, Tewksbury, MA). The air pressure was reduced to 20 psi (140 kPa) by a pressure control valve, both for safety and for isolating the biofilter from any pressure fluctuations in the upstream air supply. The air flow to the biofilter was regulated by a mass flow controller (MKS Model 247C four-channel read-out mass flow controller, Andover, Mass). Liquid VOC was injected via a syringe pump (Harvard Apparatus, model NP 70-2208, Holliston, MA) into the air stream where it vaporized, and entered the biofilter through the topmost side port of the column.

The biofilter was equipped with an independent system for feeding 1.5 L/day (initial setup value) of a buffered nutrient solution. This solution was made from deionized and activated

carbon filtered water, according to a formulation that contains all necessary macronutrients, micronutrients, and buffers. Detailed composition of the various components in the buffered nutrient solution is summarized in Appendix I. Sufficient nitrogen and phosphorus were supplied to sustain the microbial activity during all experimental periods. Initially, the nutrient formulation for the biofilter was adjusted to contain the same amount (wt/wt) of nutrient-nitrogen (N) and phosphorus (P) for a given VOC loading (COD/N = 50 and N/P = 4). As the sole source of nutrient-nitrogen, nitrate (NO_3-N) was used because the use of nitrate (NO_3-N) instead of ammonia (NH_3-N) can be effective in reducing the observed biomass yield and provided better performance of biofilter (Smith et al. 1996). 1 M $NaHCO_3$ was used as a pH buffer. The solution was circulated by a stainless steel gear pump from a 20-L feed tank through a solenoid operated 3-way valve and back to the feed tank. A programmable controller (Danaher Controls, Eagle Signal Model MX 190, Gurnee, IN) activated the solenoid once per minute to divert the feed to the biofilter so that a set feeding rate was provided per day. The feed was sprayed as a fine mist onto the top of the medium bed through a spray nozzle (Corrigan Corporation, Northbrook, IL).

2.3.2. Selection of VOCs

The research was conducted by using the following VOCs-two aromatic compounds, namely, toluene and styrene, and two oxygenated compounds, namely, methyl ethyl ketone (MEK) and methyl isobutyl ketone (MIBK). These contaminants are common solvents employed in the industry and are major components of paints and varnishes. The VOCs of concern in this study were reagent grades: toluene (C_7H_8, 99.8 % purity), styrene (C_8H_8, 99.0 % purity), methyl ethyl ketone (MEK, C_4H_8O, 99.0 % purity), and methyl isobutyl ketone (MIBK, $C_6H_{12}O$, 98.5 % purity) (Fisher Scientific, Fair Lawn, N.J). Detailed physical and chemical properties of VOCs studied are described in Appendix II.

2.3.3. Analytical Methods

Gas phase samples for toluene analysis and CO_2 analysis were analyzed by using a gas chromatograph (GC) equipped with a flame ionization detector (FID) and a thermal conductivity detector (TCD), respectively. Liquid phase samples were analyzed for nitrate, total carbon (TC), inorganic carbon (IC), and volatile suspended solid (VSS). The VSS concentrations in the effluent and backwashing solution were determined according to Standard Methods 2540 G (APHA/AWWA/APCF 1998). pH was determined using a Fisher Accumet pH meter, Model 50 (Fisher Scientific Co., Inc., Fair Lawn, NJ). The pH meter has been calibrated by using buffers (pH 4.0, 7.0, and 10.0) supplied by the manufacturer. Pressure drop along the biofilter was monitored by a digital manometer (Modus Instruments, Inc., Clinton, MA). Details about analytical methods are summarized in Appendix III of analysis methods for gas and liquid samples.

2.3.4. Microbial Seed

The biofilters were initially seeded with an aerobic microbial culture, which was obtained from the secondary clarifier of an activated sludge system at a municipal wastewater treatment plant (Millcreek wastewater treatment plant, Cincinnati, OH). Prior to seeding, 100 g/L of a glucose solution was poured in the biofilter bed and was allowed to stay within the bed for a period of 30 minutes. The glucose solution was then drained. The decanted water of the collected activated sludge was then poured in the biofilter bed and was allowed to stay within the bed for a period of 30 minutes. The decanted water was then drained. The biofilter system was then started by introducing the buffered nutrient solution and the contaminated air.

2.3.5. Experimental Plan

The biofilters were operated with three different experimental strategies according to the inlet concentration and VOC loading. The first strategy involves the study of the performance of a biofilter under backwashing as a biomass control. The remaining two focus on two different types of non-use periods (namely, starvation period and stagnant period).

Backwashing: The backwashing was conducted while the biofilter was off line by first using 18 L of the buffered nutrient solution to induce full medium fluidization at about 50 % bed expansion for a defined time period. Finally, the recycle was shut off and 18 L of the buffered nutrient solution was passed through the column as a rinse. The backwashing duration and frequency were initially set at 1 hour per one time per week for each VOC loading (if necessary, 2 hour per one time per week). Compressed air at a rate of about 20 L /min was introduced at the bottom of the biofilter when necessary for shearing off the excess biomass. A schematic diagram of the backwashing system is shown in Figure 2-2.

After backwashing, the biofilter reacclimation period was investigated. Reacclimation was considered to have been achieved when 99 % of the original biofilter performance was attained. VOC profile with the depth of the biofilters was investigated 1 day following backwashing.

Starvation period: This experimental strategy involves the period without contaminant loading, which means pure air with nutrient flow through the biofilter. The duration and frequency for this strategy were two days per week for a period of three weeks at each VOC loading.

Stagnant period: This experimental strategy reflects no flow (VOC, nutrient, and air) passing through the biofilter. The duration and frequency for this strategy were two days per week for a period of three weeks at each VOC loading.

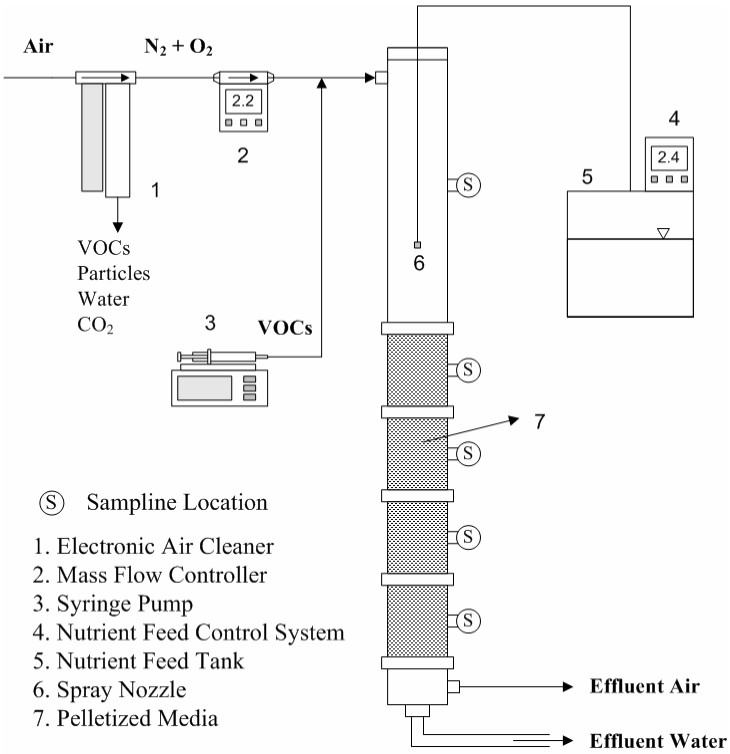

Figure 2-1 Schematic diagram for TBAB study

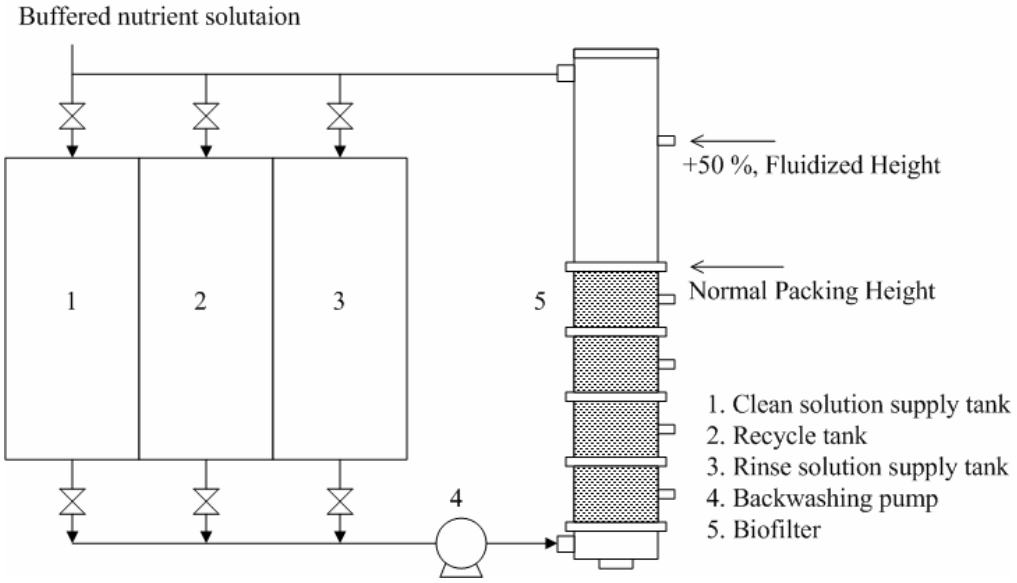

Figure 2-2 Schematic diagram for backwashing system

2.4. Results and Discussion

2.4.1. Toluene Removal

***Biofilter Performance*:** The conditions and strategies for this experiment are summarized in Table 2-1. The biofilter performance with respect to toluene removal is shown in Figure 2-3.

The first operation, stage (I), was recognized as a start-up period, which demonstrates the acclimation period at startup. Stage (II) was conducted under a toluene loading rate of 0.70 kg COD/m^3·day. The overall toluene removal efficiency reached over the 99 % level for all three experimental strategies (backwashing, starvation, and stagnant). When a toluene loading rate was increased to 1.41 kg COD/m^3·day (stage III), a period of 10 days was required to acclimate the biofilter. After that, the biofilter was maintained at the 99 % removal efficiency for all experimental strategies. During the non-use period strategies for VOC loading rates of 0.70 and 1.41 kg COD/m^3·day, the 99 % removal efficiency was attained without backwashing. For a toluene loading rate of 3.52 kg COD/m^3·day (stage IV), a period of 15 days was required for acclimating the biofilter. After the acclimation period, the biofilter maintained the 99 % removal efficiency. During the non-use period strategies for a toluene loading of 3.52 kg COD/m^3·day, the removal efficiency dropped occasionally below 90 % and demanded other means of biomass control. It is interesting to note that the behavior of the biofilter depended on biomass control because its performance decreased substantially with build up of back pressure due to accumulation of excess biomass (Jorio et al. 2000; Smith et al. 1996; Sorial et al. 1995). During stage V period, the overall toluene removal efficiency had not reached above 99 % even by using backwashing. The work by Smith et al. (2002) demonstrated that oxygen limitation might occur in the biofilter operated over 500 ppmv of inlet toluene concentration, resulting in its failure. A further experiment was performed for a toluene loading of 5.64 kg COD/m^3·day (stage VI). A poor performance for toluene removal was obtained (see Figure 2-3).

The toluene removal capacity with respect to loading rate is presented in Figure 2-4. Figure 2-4 confirms that a corresponding inlet toluene concentration of 500 ppmv leads to a significant deterioration of the biofilter performance. A generalized summary of biofilter performance with respect to the experimental strategies is presented in Figure 2-5. It is worthwhile to note that the non-use period strategies provided similar biofilter performance as the backwashing strategy for toluene loading rates of 0.70 and 1.41 kg COD/m^3·day. Irvine and Moe (2001) found that a biofilter loaded periodically can be operated without any contaminant breakthrough. Cox and Deshusses (2002) demonstrated that the biomass content in the reactor decreased during starvation, but this decrease was not critical for future reacclimation of the biofilter performance. Thus the non-use periods can be considered as another means of the biomass control at relatively low toluene loading rate.

***Biofilter Response after Backwashing and Non-use Periods*:** The biofilter response after restart-up following backwashing and non-use periods was explored by collecting effluent samples at prescheduled time intervals to determine the time varying response of the biofilter (see Figure 2-6). The following observation can be deduced from Figure 2-6.

For the backwashing strategy, the overall removal efficiency was initially below the 30 % range but it increased over the 90 % range within 600 min at all toluene loading rates. The biofilter performance immediately after backwashing was unexpectedly poor due to the loss of active biomass. Based on this point of view, it is interesting to discuss the carbon balance during each experimental strategy (see Table 2-2). It was found that there was a greater loss of biomass during the backwashing strategy as compared to the two non-use period strategies.

For the two different non-use strategies, the biofilter initially had relatively high removal efficiency as compared to the backwashing strategy. This may be due to the active biomass

retained within the biofilter. During the non-use strategies, less loss of biomass was encountered as shown in the carbon balance (Table 2-2). It is interesting to observe that for a toluene loading rate of 3.52 kg COD/m^3·day, biofilter responses after non-use periods were different to those for other loading rates. It is speculated that toluene adsorption on biofilm could have contributed to this initial response due to deeper biomass formation in the biofilter bed, and after a certain period, toluene removal could be due biodegradation. These observations suggested that the preservation of biomass could reduce the period of reacclimation of the biofilter performance after non-use periods. However, high accumulated biomass could lead to channeling and hence deterioration in performance. It is shown in Table 2-2 that the ratio of unaccounted carbon to carbon equivalent of VOC removed increased with toluene loading rates. Although backwashing is helpful to remove the accumulated biomass in the biofilter, the remaining biomass retained in the biofilter could be the unaccounted carbon in the carbon balance.

Kinetic Analysis of Biofilter Performance: The removal performances as a function of depth in the biofilter were studied one day following the backwashing and non-use periods. The obtained data were used to develop the first-order reaction rate constant as a function of depth in the biofilter for each experimental strategy (For details about kinetic analysis for toluene removal, see Appendix IV). The obtained results are shown in Figure 2-7. It is seen that the first-order reaction rate constants decreased with an increase in the toluene inlet loading. Assuming that aerobic heterotrophic organisms accounted for the toluene consumption as the substrate, a higher loading of toluene could result in a substrate inhibition effect on the growth of microorganisms, as demonstrated by Schroder et al. (1997). At a low toluene loading, the non-use periods provided higher first-order reaction constants than backwashing strategy, indicating that the active biomass retained in the biofilter could have played an important role in this effect.

However, this behavior was not achieved for a toluene loading rate of 5.64 Kg COD/m^3·day, speculating that it was due to high accumulated biomass.

Table 2-1 Experimental conditions and strategies for toluene biofiltration

	I	II	III	IV	V	VI
Experimental Condition						
Inlet Conc., ppmv	50	50	100	250	500	400
Loading, kg COD/m^3·day	1.14	0.70	1.41	3.52	7.03	5.64
EBRT, min	0.76	1.23	1.23	1.23	1.23	1.23
Experimental Strategy (Operational periods in days)						
Backwashing*	1-46	47-51	92-114	154-191	238-272	273-300
Non-use period**						
Starvation	-	52–71	115-133	192-210	-	
Stagnant	-	72–91	134-153	211-237	-	

* Backwashing frequency and duration were set at 1 hour once per week.

** The frequency and duration for each non-use period were 2 day per week.

Table 2-2 Carbon recovery* at different toluene loading rates and experimental strategies

Loading Rate**	Experimental Strategy	$^aC_{CO2}$ %	$^bC_{IC}$ %	$^cC_{TOC}$ %	$^dC_{VSS}$ %	$C_{unaccounted}$ %
0.70	Backwashing	79.9	0.4	1.5	14.3	4.0
	Non-use periods	83.0	0.7	1.3	0.8	14.2
1.41	Backwashing	75.0	0.6	0.8	12.3	11.3
	Non-use periods	88.2	0.8	0.5	0.2	10.1
3.52	Backwashing	69.2	0.2	0.0	15.4	15.2
	Non-use periods	80.9	0.5	0.2	0.2	18.2
5.64	Backwashing	69.6	0.3	1.5	12.0	16.6
7.03	Backwashing	63.2	0.3	0.1	15.5	20.9

* Carbon balance: $C_{VOC\ removed} = {}^aC_{CO2\ in\ effluent\ gas} + {}^bC_{Inorganic\ carbon\ in\ effluent\ liquid} + {}^cC_{Total\ organic\ carbon\ in\ effluent\ liquid} + {}^dC_{VSS\ in\ effluent\ liquid\ and\ backwashing\ solution} + C_{Biomass\ retained\ in\ the\ reactor}$. A typical cellular composition for a heterogeneous microorganism can be represented as $C_5H_7O_2N$.

** Kg COD/m^3·day

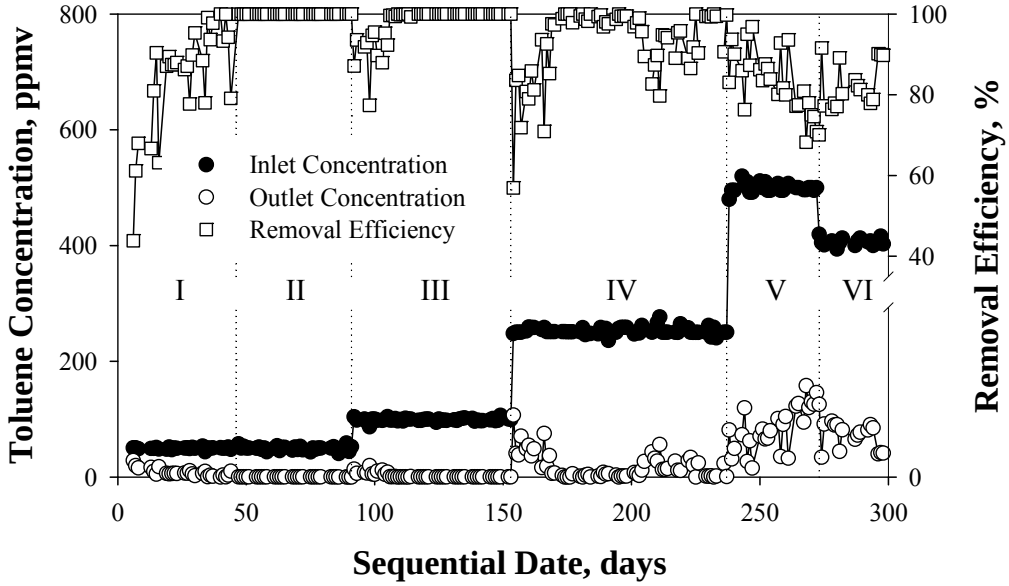

Figure 2-3 Biofilter performance with respect to toluene removal

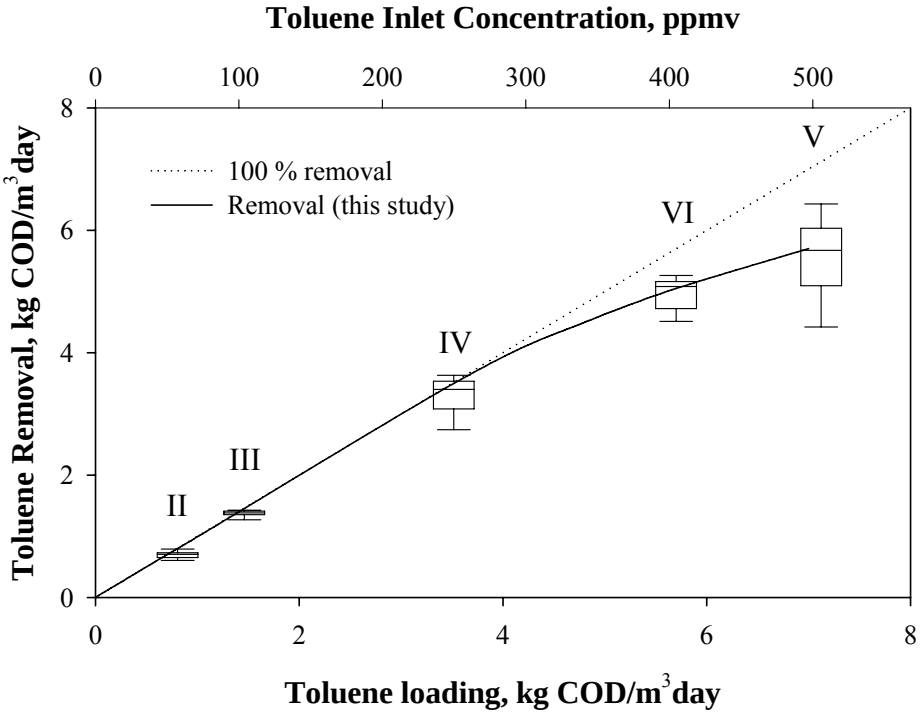

Figure 2-4 Toluene removal capacity with respect toluene loading (under the backwashing strategy)

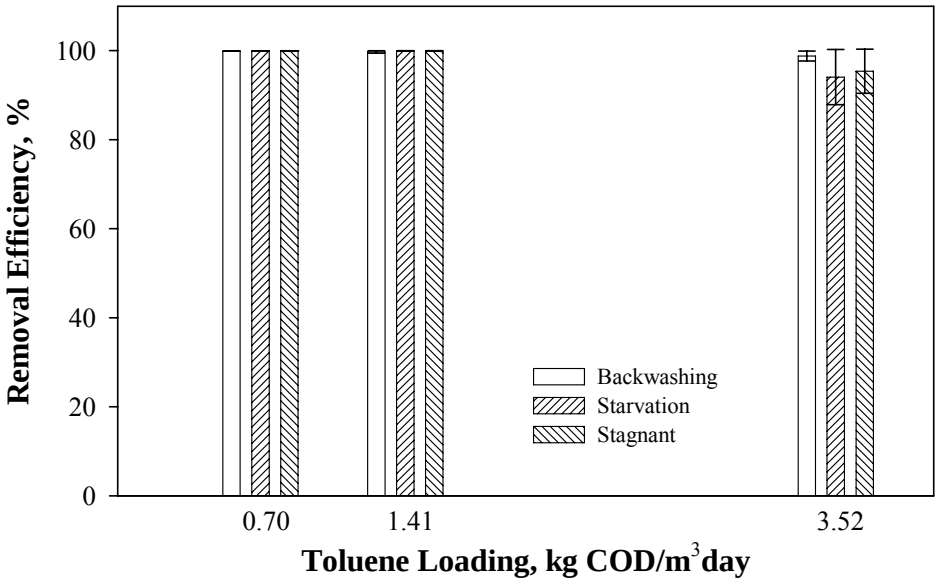

Figure 2-5 Toluene removal efficiency with respect to experimental strategies

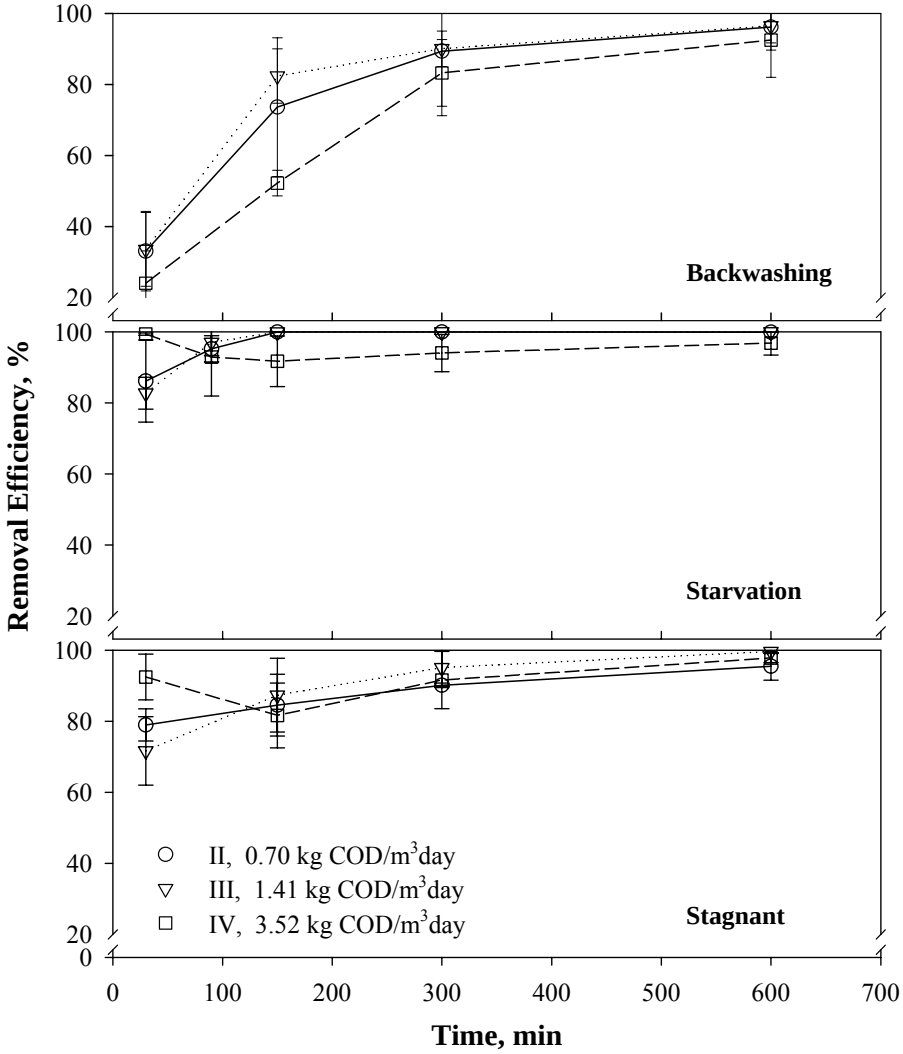

Figure 2-6 Toluene biofilter response after the restart-up after each experimental strategy

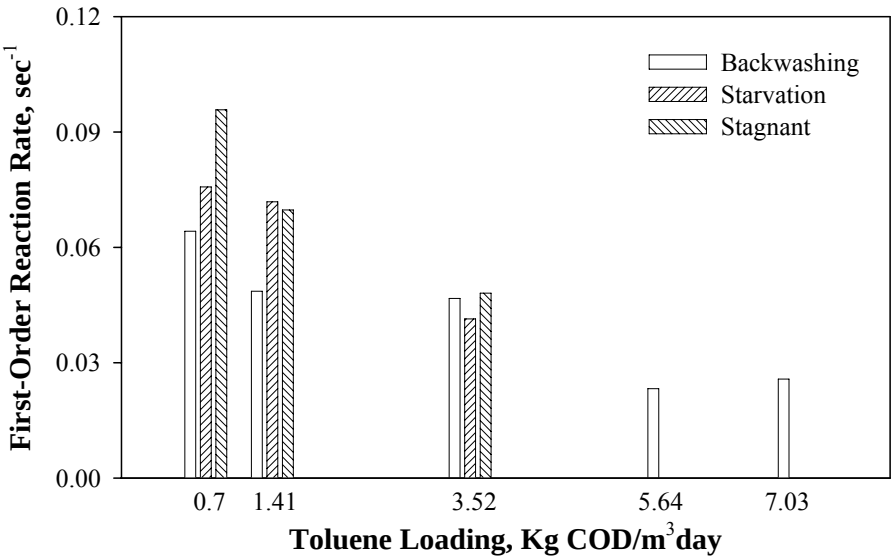

Figure 2-7 First-order reaction rate constants as a function of toluene loading

2.4.2. Styrene Removal

***Biofilter Performance*:** The conditions and strategies for this experiment are summarized in Table 2-3. The biofilter performance with respect to styrene removal is shown in Figure 2-8.

The biofilter was started up using an influent styrene concentration of 50 ppmv, 0.76 min EBRT (1.27 kg COD/ m^3·day), and 2.25 mmol NO_3-N per day as the sole nitrogen source (stage I), which was recognized as a start-up period. On day 44, when backwashing was conducted, the EBRT was increased to 1.51 min and the inlet styrene concentration was still maintained at 50 ppmv corresponding to a loading of 0.64 kg COD/m^3·day (Stage II). The removal efficiency increased to the 99 % level and remained stable at this level with the coordinated biomass control strategy of 1 hour backwashing every week. For non-use period strategies, the removal efficiencies have remained above 99 % and the pressure drop stabilized at about 1 cm of water, indicating that excess biomass had been within the system.

When the inlet concentration was increased to 100 ppmv corresponding to a loading of 1.27 kg COD/m^3·day (Stage III), the removal efficiency dropped to below 90 % and the biofilter did not reach the 99 % performance level for 12 days. In order to recover the desired high removal efficiency, on day 104, the feed rate of the buffered nutrient solution was increased from 1.5 L/day to 2.4 L/day, corresponding to a 7.2 mmol/day of NO_3-N feed rate. On the third day, the overall removal efficiency was over 99 % and remained at this level. A similar behavior was observed by Zhu et al. (2001) in their biofiltration study for diethyl ether removal. They indicated that a higher flow rate of nutrient liquid might result in better biofilter performance due to the increase in the nutrient diffusion driving force. For non-use period strategies at the styrene loading of 1.27 kg COD/m^3·day, the removal efficiencies have remained at the 99 % removal level.

For a styrene loading of 3.17 kg COD/m^3·day (Stage IV) with corresponding inlet concentration of 250 ppmv, the removal efficiency did not reach the 99 % level even though it had risen to 99 % just after backwashing. On day 195, the EBRT was increased to 2.02 min and styrene loading was still maintained at 3.17 kg COD/m^3·day corresponding to an inlet styrene concentration of 330 ppmv (Stage V). Subsequently, styrene removal efficiency increased to 99 % one day after backwashing, but it dropped to as low as 80 % by the day prior to the following backwashing. For the starvation strategy at this loading rate, the overall removal efficiencies have ranged from 85 % to 96 %. This poor performance might be due to the excess biomass that had accumulated within the biofilter. This indicated that the active biomass control such as backwashing is not unavoidable at this styrene loading rate. When the active biomass control, i.e. backwashing was considered on 223 day, the removal efficiency increased to 98 % by the next day. However, when the stagnant strategy was conducted without coordinated backwashing, the overall removal efficiency decreased to about 70 %.

For a styrene loading of 1.9 kg COD/m^3·day (Stage VI), the removal efficiency generally remained at 99 % with backwashing at a rate of 1hour once per week. In a study of styrene biofiltration by (Sorial et al. 1998) using backwashing with a duration of 2 hr every other day, the maximum styrene removal rate was 4.26 kg COD/m^3·day (57.8 g/m^3·hr) with removal efficiencies in the 97-99 % level. Thus more frequent and longer duration of backwashing was perceived as contributing to consistent high removal efficiency at higher styrene loadings. Smith et al. (2002) discussed that an excess of oxygen as an electron acceptor has to exist throughout the entire biofilm in order to avoid biofilter failure. Based on the maximum equilibrium concentration of oxygen in the biofilm at the air-biofilm interface, the maximum practical concentration for styrene in the biofilm at the interface was deduced to be 257 ppmv at 32.2 °C (Sorial et al. 1998). The styrene removal capacity with respect to loading rate is presented in

Figure 2-9. It is shown in Figure 2-9 that styrene loadings above 1.9 kg COD/m^3·day led to a decrease in biofilter efficiency. It is, therefore, speculated that at inlet styrene concentration over 200 ppmv for 2.02 min EBRT (or 150 ppmv for 1.51 EBRT), an unfavorable performance of biofilter is manifested.

In Table 2-4, the carbon recovery is summarized in terms of CO_2, IC, TOC, VSS, and unaccounted carbon according to styrene loading rates and experimental strategies. It can be speculated from Table 2-4 that most inlet carbon was converted to CO_2 as the reaction product for energy production and part of inlet carbon was converted to the VSS as cell synthesis. For the non-use strategies, larger conversion of inlet carbon to CO_2 was found as compared to the backwashing strategy. This could indicate that during the non-use strategies, chemoheterotrophs contributing to degrading styrene used the inlet carbon as an energy source for maintenance of microbial viability rather than as a carbon source for cell growth. Assuming that the unaccounted carbon in the carbon balance contributes to the accumulation of biomass in the biofilter, the larger unaccounted carbon in the non-use strategies could be attributed to biomass accumulation in the biofilter bed. As styrene loading rate increased, biomass accumulation was found to increase.

***Biofilter Response after Backwashing and Non-use Periods*:** Figure 2-10 shows the effluent response corresponding to backwashing and non-use periods for each inlet styrene loading of 0.64, 1.27, and 3.17 kg COD/m^3·day studied. Reacclimation of overall biofilter performance was delayed primarily as styrene loading increased.

For styrene loadings of 0.64 and 1.27 kg COD/m^3·day, the sequence of reacclimation period was in the same sequence of the experimental strategies with backwashing > starvation period > stagnant period. For a styrene loading of 3.17 kg COD/m^3·day, higher removal efficiency was

observed in the initial time after the restart-up following non-use periods (starvation period and stagnant period). It is speculated that initially, adsorption of styrene on the biomass might have occurred because more biomass was available on the biofilter media. After a certain period likely after breakthrough, the biofilter performance was similar to that after backwashing.

Kinetic Analysis of Biofilter Performance: The removal performances as a function of depth in the biofilter were studied one day following the backwashing and the non-use periods. The obtained data were used to develop the first-order reaction rate constant as a function of depth in the biofilter for each experimental strategy (For details about kinetic analysis for styrene removal, see Appendix IV). The obtained results are summarized in Figure 2-11. It is seen from Figure 2-11 that the styrene reaction rate constant decreased as the styrene loading increased. For lower styrene loadings, the non-use strategies showed higher reaction rates than those for the backwashing strategy. However, for a styrene loading of 3.17 kg COD/m^3·day, the non-use strategies showed lower reaction rates than that for the backwashing strategy. This could indicate that the active biomass preserved in the biofiler during non-use periods would provide favorable performance of the biofilter, while for higher substrate loadings, the non-use periods had negative effect on the performance of biofilter due to excess accumulation of biomass.

Table 2-3 Experimental conditions and strategies for styrene biofiltration

	I	II	III	IV	V	VI
Experimental Condition						
Inlet Conc., ppmv	50	50	100	250	330	200
Loading, kg COD/m^3·day	1.27	0.64	1.27	3.17	3.17	1.90
EBRT, min	0.76	1.51	1.51	1.51	2.02	2.02
Experimental Strategy (Operational periods in days)						
Backwashing*	1-43	44 - 50	92 - 113	155-194	195 - 210	258 - 272
Non-use period**						
Starvation	-	51 - 70	114 - 134		211-231	
Stagnant	-	71 - 91	135 - 154		232-257	

* Backwashing frequency and duration were set at 1 hour once per week.

** The frequency and duration for each non-use period were 2 day per week.

Table 2-4 Carbon recovery* at different styrene loading rates and experimental strategies

Loading Rate**	Experimental Strategy	$^aC_{CO2}$ %	$^bC_{IC}$ %	$^cC_{TOC}$ %	$^dC_{VSS}$ %	$C_{unaccounted}$ %
0.64	Backwashing	81.4	0.5	1.1	13.9	3.1
	Non-use periods	82.0	0.8	1.0	0.4	15.9
1.27	Backwashing	68.6	0.6	0.5	16.3	14.0
	Non-use periods	81.5	0.9	0.4	0.5	16.7
1.90	Backwashing	71.6	0.6	0.2	18.3	9.3
3.17	Backwashing	63.5	0.6	0.6	16.9	18.4
	Non-use periods***	84.1	0.8	1.0	9.5	4.6

* Carbon balance: $C_{VOC\ removed} = {}^aC_{CO2\ in\ effluent\ gas} + {}^bC_{Inorganic\ carbon\ in\ effluent\ liquid} + {}^cC_{Total\ organic\ carbon\ in\ effluent\ liquid} + {}^dC_{VSS\ in\ effluent\ liquid\ and\ backwashing\ solution} + C_{Biomass\ retained\ in\ the\ reactor}$. A typical cellular composition for a heterogeneous microorganism can be represented as $C_5H_7O_2N$.

** Kg COD/m^3·day

*** Backwashing has been coordinated due to excess biomass accumulation in the biofilter bed

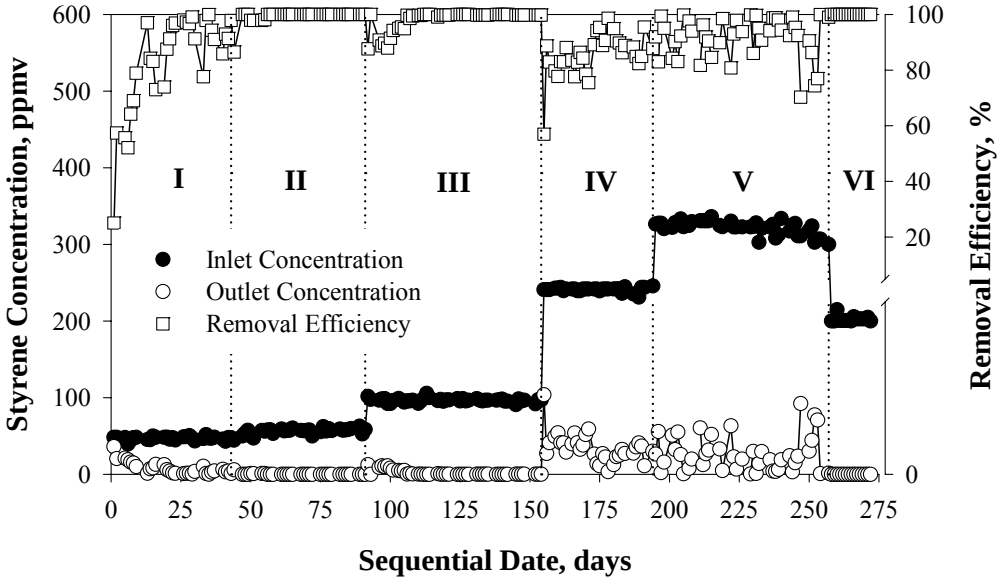

Figure 2-8 Biofilter performance with respect to styrene removal

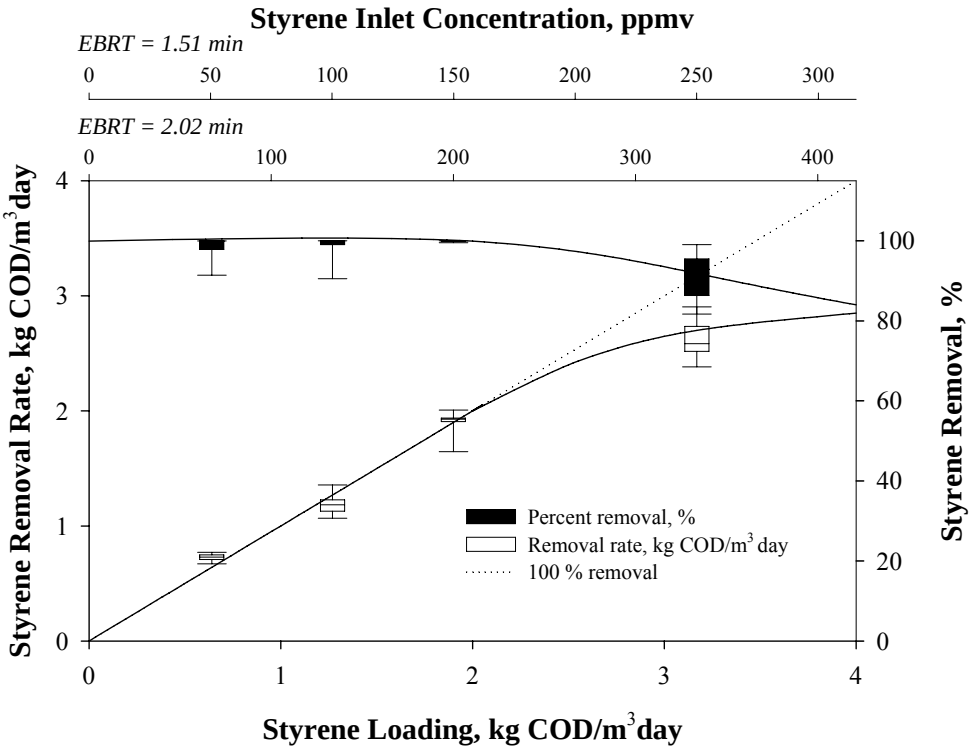

Figure 2-9 Styrene removal capacity with respect styrene loading (under the backwashing strategy)

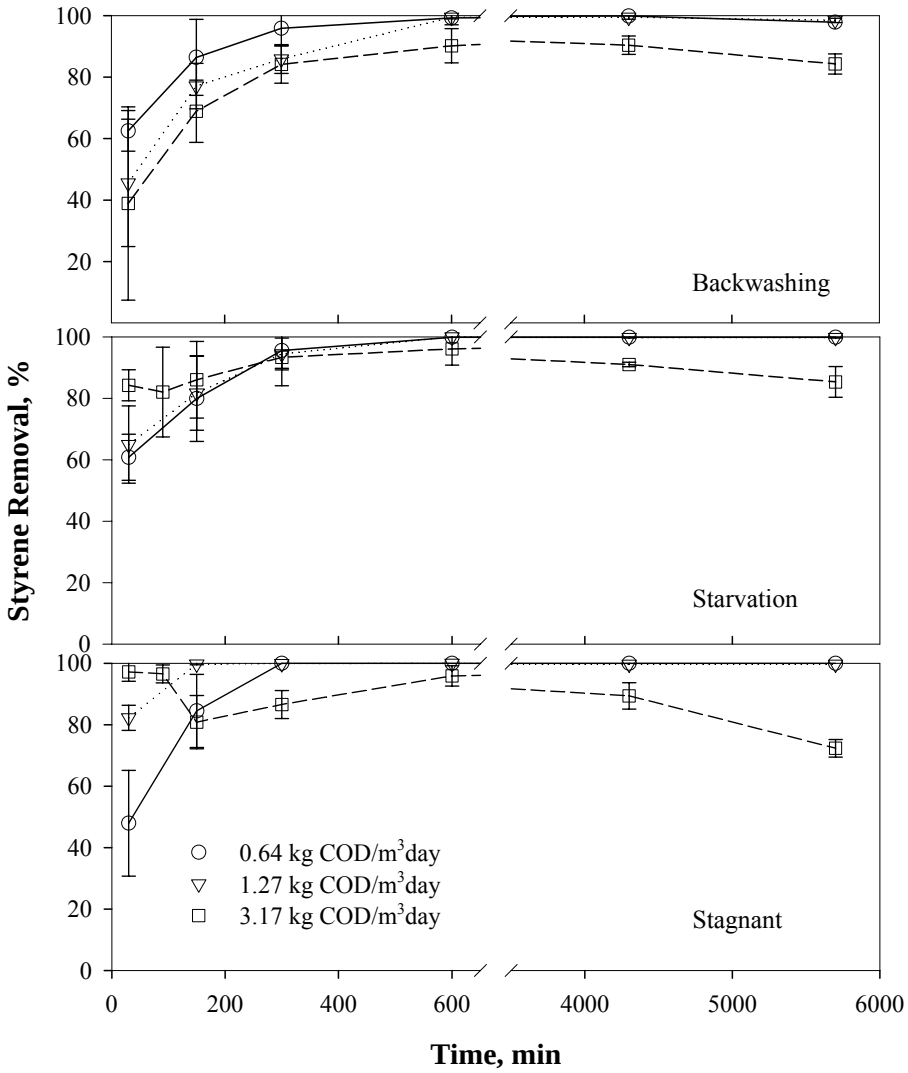

Figure 2-10 Styrene biofilter response after the restart-up after each experimental strategy

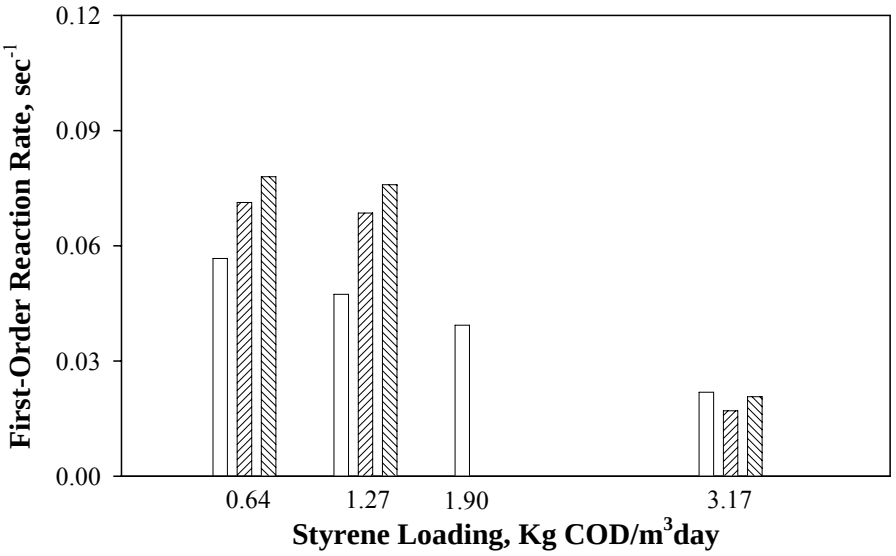

Figure 2-11 First-order reaction rate constants as a function of styrene loading

2.4.3. Methyl Ethyl Ketone Removal

***Biofilter Performance*:** The conditions and strategies for this experiment are summarized in Table 2-5. The biofilter performance with respect to MEK removal is shown in Figure 2-12.

In stage (I) under an employed loading rate of 0.70 kg COD/m^3·day, after about 20 days from start-up period, the biofilter maintained consistently high removal efficiency above 99%. This efficiency was maintained for all three strategies (backwashing, starvation, and stagnant). On day 80, the loading rate was increased to 1.41 kg COD/m^3·day. No apparent acclimation period to the new higher loading rate was observed. The biofilter attained stable removal efficiency above 99% for all three strategies. On day 136, the employed loading rate was increased to 3.52 kg COD/m^3·day. A period of 5 days was apparently required to acclimate to the new loading condition. After that, the biofilter attained consistently over 99 % removal efficiency for all three operating strategies. It is important to note that the corresponding nitrate feeding mass was increased to adjust the ratio of COD to nitrogen (COD/N) to 30 from an initial value of 50 due to high consumption of nitrate. On day 197, after backwashing was conducted, the employed loading rate was increased further to 7.03 kg COD/m^3·day. The biofilter could not be maintained at the 99% removal level. During the backwashing strategy, the biofilter recovered to the 99% removal level just after backwashing, and then its efficiency decreased gradually to around 60% removal just prior to the next backwashing. Since high consumption of nitrate was simultaneously observed, nitrate feed mass was subsequently increased to adjust a COD/N to 10.

During the non-use strategies for MEK loading rate of 7.03 kg COD/m^3·day, backwashing was coordinated as the active biomass control because high accumulation of biomass was found. However, the biofilter could not be maintained at 99% removal level. It decreased to 60-70% removal efficiency just prior to the next backwashing. Therefore, backwashing once a week was thought to be not enough to remove excessive accumulated biomass under the current 7.03 kg

COD/m^3·day loading rate. To maintain consistent 99% removal efficiency, more frequent backwashing operation was required which is, however, not practical for the real application. It was then deduced that the employed 7.03 kg COD/m^3·day loading rate exceeded the maximum elimination capacity under the current operating parameters. On day 269 after backwashing, the loading rate was decreased to 5.64 kg COD/m^3·day. After a period of one week acclimation, the biofilter maintained a 99% removal level during a period of 5 weeks with backwashing once a week.

MEK biofilter performance at different loading rates depicted in Figure 2-13 indicates that up to 5.63 kg COD/m^3·day of an organic loading rate, stable performance over 99% removal efficiency was attained by using backwashing. Table 2-6 shows the carbon recovery at different MEK loading rates and experimental strategies. It is interesting to note that carbon recovery deteriorated as the MEK loading rate increased. This indicates that at higher MEK loading rate, the biomass synthesized accumulated within the bed media, causing biofilter performance to deteriorate.

***Biofilter Response after Backwashing and Non-use Periods*:** Figure 2-14 shows the effluent response corresponding to backwashing and two non-use periods at different MEK loading rates. It can be deduced that for loading rates up to 3.52 kg COD/m^3·day, reacclimation of the biofilter was within a short time (< 90 min) and the non-use periods did not show negative effect on reacclimation. These results indicate that the non-use operation could be conducted as another means for biomass control for loading rates less than 3.52 kg COD/m^3·day. For a loading rate of 7.04 kg COD/m^3·day, the biofilter initially reacclimated but its performance kept decreasing with time for all experimental strategies. It is speculated that for a high loading rate, the initial response mainly resulted from MEK adsorption on the biomass, not from the real MEK

biodegradation. At this loading rate, non-use periods might have caused channeling within the media due to excess biomass accumulation.

Kinetic Analysis of Biofilter Performance: The removal performances as a function of depth in the biofilter were studied one day following backwashing and non-use periods. The obtained data were used to develop the first-order reaction rate constant as a function of depth in the biofilter for each experimental strategy (For details about kinetic analysis for MEK removal, see Appendix IV). The obtained results shown in Figure 2-15 indicate that the reaction rate constants decreased as the substrate loading increased. The effect of non-use periods showed apparent transition from positive to negative as the substrate loading rate increased. It can be deduced that non-use strategies showed higher reaction rates than backwashing strategy due to more available biomass. However, when a high loading rate was employed, non-use strategies showed lower removal rates due to excessive accumulation of biomass in the biofilter bed which would eventually lead to channeling within the media.

Table 2-5 Experimental conditions and strategies for MEK biofiltration

	I	II	III	IV	V
Experimental Condition					
Inlet Conc., ppmv	50	100	250	500	400
Loading, kg COD/m^3·day	0.7	1.41	3.52	7.03	5.64
EBRT, min	0.76	0.76	0.76	0.76	0.76
Experimental Strategy (Operational periods in days)					
Backwashing*	1-35	80-95	136-154	197-225	269-309
Non-use period**					
Starvation	36-56	96-112	155-174	226-244	-
Stagnant	57-79	113-135	175-196	245-268	-

* Backwashing frequency and duration were set at 1 hour once per week.

** The frequency and duration for each non-use period were 2 day per week

Table 2-6 Carbon recovery* at different MEK loading rates and experimental strategies

Loading Rate**	Experimental Strategy	$^aC_{CO2}$ %	$^bC_{IC}$ %	$^cC_{TOC}$ %	$^dC_{VSS}$ %	$C_{unaccounted}$ %
0.70	Backwashing	86.2	0.1	5.9	7.0	0.8
	Non-use periods	73.3	1.2	2.1	0.3	23.1
1.41	Backwashing	70.9	1.1	1.2	13.5	13.3
	Non-use periods	75.9	1.5	1.1	0.2	21.3
3.52	Backwashing	62.3	2.0	0.9	20.9	13.9
	Non-use periods	75.1	3.3	1.1	0.2	20.3
5.64	Backwashing	54.8	3.8	0.9	17.9	22.6
7.03	Backwashing	46.9	3.8	1.9	14.1	33.3
	Non-use periods***	52.9	4.1	1.3	14.4	27.3

* Carbon balance: $C_{VOC\ removed} = {}^aC_{CO2\ in\ effluent\ gas} + {}^bC_{Inorganic\ carbon\ in\ effluent\ liquid} + {}^cC_{Total\ organic\ carbon\ in\ effluent\ liquid} + {}^dC_{VSS\ in\ effluent\ liquid\ and\ backwashing\ solution} + C_{Biomass\ retained\ in\ the\ reactor}$. A typical cellular composition for a heterogeneous microorganism can be represented as $C_5H_7O_2N$.

** Kg COD/m^3·day

*** During an experimental period for this strategy, backwashing strategy has been coordinated due to excess biomass accumulation in the biofilter bed.

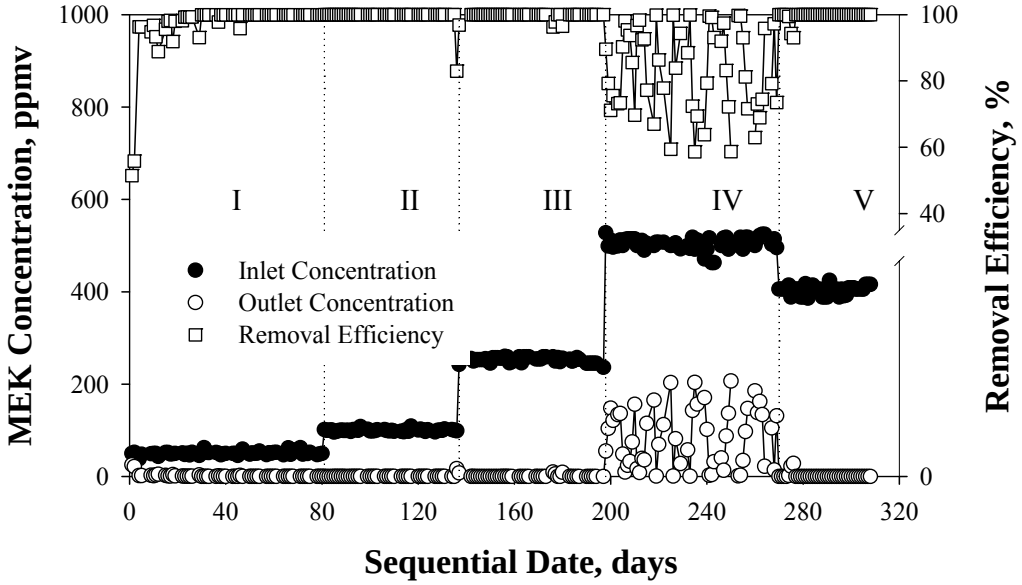

Figure 2-12 Biofilter performance with respect to MEK removal

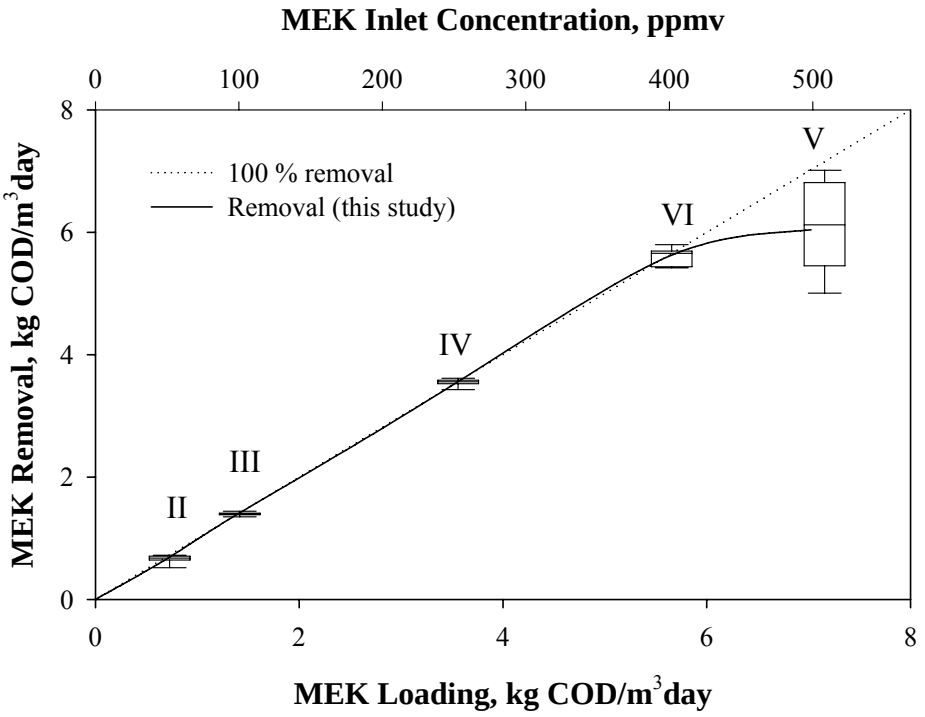

Figure 2-13 MEK removal capacity with respect MEK loading (under the backwashing strategy)

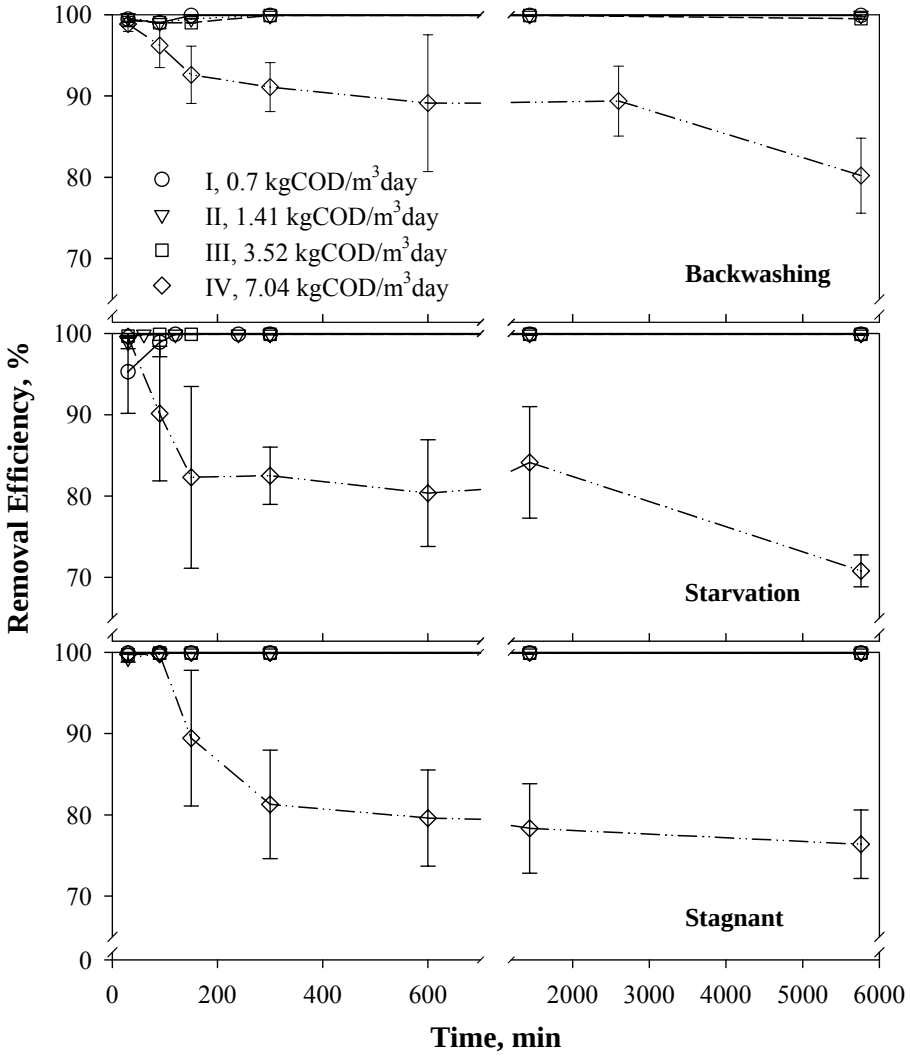

Figure 2-14 MEK biofilter response after the restart-up after each experimental strategy

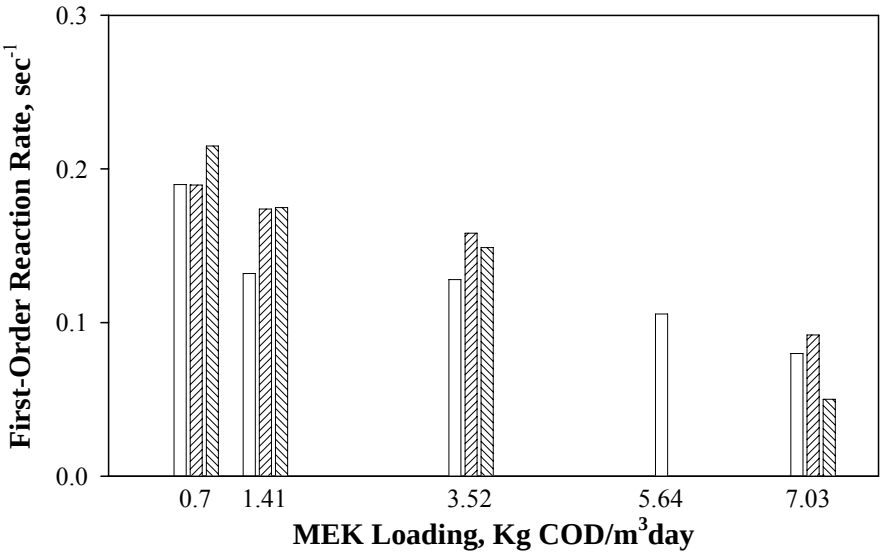

Figure 2-15 First-order reaction rate constants as a function of MEK loading

2.4.4. Methyl Isobutyl Ketone Removal

***Biofilter Performance*:** The conditions and strategies for this experiment are summarized in Table 2-7. The biofilter performance with respect to MIBK removal is shown in Figure 2-16.

In stage (I) under an employed loading rate of 1.09 kg COD/m^3·day, after about 14 days from start-up period, the biofilter had provided over 99 % removal efficiency. The overall removal efficiencies have remained at this level under the backwashing strategy and the two non-use period strategies. When the inlet concentration was increased to 100 ppmv (loading rate of 2.17 kg COD/m^3·day), the biofilter recovered to over 99 % removal efficiency within 90 min. The overall removal efficiencies have remained at this level with coordinated backwashing at a rate of 1 hour once a week. Under the starvation strategy, the biofilter still provided a stable performance with over 99 % removal. However, when the first cycle of stagnant strategy was employed, the overall removal efficiency decreased to 95 %, and dropped to as low as 88 %. It is speculated that the excess biomass accumulation caused channeling or short circuiting. For a solution to the problem, backwashing was coordinated with the next stagnant cycle. The biofilter recovered to 99 % level, and had been maintained at this level.

When the inlet concentration was increased to 250 ppmv with a corresponding loading of 5.43 kg COD/m^3·day, the removal efficiency ranged from 99 % to as low as 65 % even under the backwashing strategy. High consumption of nitrate was observed from effluent liquid nitrate analysis. An increase in nitrate feeding mass (up to COD/N of 25 initially from 50) was, therefore, unavoidable to maintain the microbial activity. Correspondently, the overall removal efficiency increased to the 99 % level, but it decreased gradually as low as 80 % just prior to the next backwashing. It seemed to be difficult to maintain a consistent 99 % level of removal efficiency under the current MIBK loading rate (5.43 kg COD/m^3·day). To avoid excess accumulation of

biomass during the non-use period strategies, backwashing at a rate of 1 hour once a week was employed. However, the biofilter didn't provide the stable high removal performance.

At an inlet concentration of 200 ppmv (correspondingly, 4.34 kg COD/ m^3·day), the overall removal efficiency reached the 99 % removal level. But it decreased to as low as 86% prior to the next backwashing. At an inlet concentration of 150 ppmv (corresponding MIBK loading rate of 3.26 kg COD/m^3·day), the removal efficiency remained over 99% with coordinated backwashing at a rate of 1 hour once a week. It is interesting to note that nitrate feeding mass was increased up to 10 COD/N ratio due to high consumption of nitrate. Details about nitrogen utilization are discussed in Chapter 3.

The MIBK biofilter performance at different loading rates depicted in Figure 2-17 indicates that up to 4.34 kg COD/m^3·day of an organic loading rate, stable performance over 99 % removal efficiency was attained by using backwashing. Table 2-8 shows the carbon recovery at different MIBK loading rates and experimental strategies. It is interesting to note that the carbon recovery deteriorated as the MIBK loading rate increased, speculating that the biomass unwashed was accumulated in the biofilter bed even if backwashing was coordinated for a high MIBK loading rate. The unaccounted carbon in the carbon balance might have contributed to the accumulation of biomass in the biofilter. Furthermore, excess biomass accumulation during the non-use strategies resulted in larger unaccounted carbon as compared to the backwashing strategy.

Biofilter Response after Backwashing and Non-use Periods: Figure 2-18 shows the effluent response corresponding to backwashing strategy and two non-use strategies. Due to the high biomass accumulation for 5.43 kg COD/m^3·day loading rate, backwashing was coordinated with the starvation and stagnant operation. It can be deduced from Figure 2-18 that the reacclimation of biofilter after a specific strategy was delayed as the employed loading rate increased. For

loading rates of 1.09 and 2.17 kg COD/m^3·day, reacclimation had no apparent difference between backwashing strategy and two non-use strategies. For a loading rate of 5.43 kg COD/m^3·day, no full recovery was encountered for all the three strategies. It is interesting to note that at 5.43 kg COD/m^3·day, channeling or short circuiting could dominate due to excess accumulation of biomass, which caused failure of complete recovery.

Kinetic Analysis of Biofilter Performance: The removal performances as a function of depth in the biofilter were studied one day following the backwashing and the non-use periods. The obtained data were used to develop the first-order reaction rate constant as a function of depth in the biofilter (For details about kinetic analysis for MIBK removal, see Appendix IV). Figure 2-19 represents plots of the MIBK first-order reaction rate constants under the different loading rates. This indicates that the reaction rate was dependent on the substrate loading rate. It is important to note that the non-use strategies had a significant negative effect on the biofilter performance when higher loading rates were employed. It is worthwhile noting that excess biomass accumulation was observed for higher substrate loadings. When biofilters are exposed to intermittent operating conditions (i.e., weekend shutdown), backwashing was deemed necessary in order to improve the bifilter performance for high substrate loadings.

Table 2-7 Experimental conditions and strategies for MIBK biofiltration

	I	II	III	IV	V
Experimental Condition					
Inlet Conc., ppmv	50	100	250	200	150
Loading, kg COD/m^3·day	1.09	2.17	5.43	4.34	3.26
EBRT, min	0.76	0.76	0.76	0.76	0.76
Experimental Strategy (Operational periods in days)					
Backwashing*	1-29	70-85	126-158	204-232	233-298
Non-use period**					
Starvation	30-50	86-106	159-179	-	-
Stagnant	51-69	107-125	180-203	-	-

* Backwashing frequency and duration were set at 1 hour once per week.

** The frequency and duration for each non-use period were 2 day per week

Table 2-8 Carbon recovery* at different MIBK loading rates and experimental strategies

Loading Rate**	Experimental Strategy	$^aC_{CO2}$ %	$^bC_{IC}$ %	$^cC_{TOC}$ %	$^dC_{VSS}$ %	$C_{unaccounted}$ %
1.09	Backwashing	89.5	0.6	2.1	7.3	0.5
	Non-use periods	68.0	1.1	2.2	0.3	28.4
2.17	Backwashing	67.1	0.9	0.8	17.5	13.8
	Non-use periods	74.7	1.2	0.6	0.3	23.2
3.26	Backwashing	55.6	3.6	1.4	22.4	17.0
4.34	Backwashing	45.8	3.3	2.3	26.2	22.4
5.43	Backwashing	59.4	2.1	1.5	14.2	22.8
	Non-use periods***	67.1	2.8	0.4	10.5	19.2

* Carbon balance: $C_{VOC\ removed} = {}^aC_{CO2\ in\ effluent\ gas} + {}^bC_{Inorganic\ carbon\ in\ effluent\ liquid} + {}^cC_{Total\ organic\ carbon\ in\ effluent\ liquid} + {}^dC_{VSS\ in\ effluent\ liquid\ and\ backwashing\ solution} + C_{Biomass\ retained\ in\ the\ reactor}$. A typical cellular composition for a heterogeneous microorganism can be represented as $C_5H_7O_2N$.

** Kg COD/m^3·day

*** During an experimental period for this strategy, backwashing strategy has been coordinated due to excess biomass accumulation in the biofilter bed.

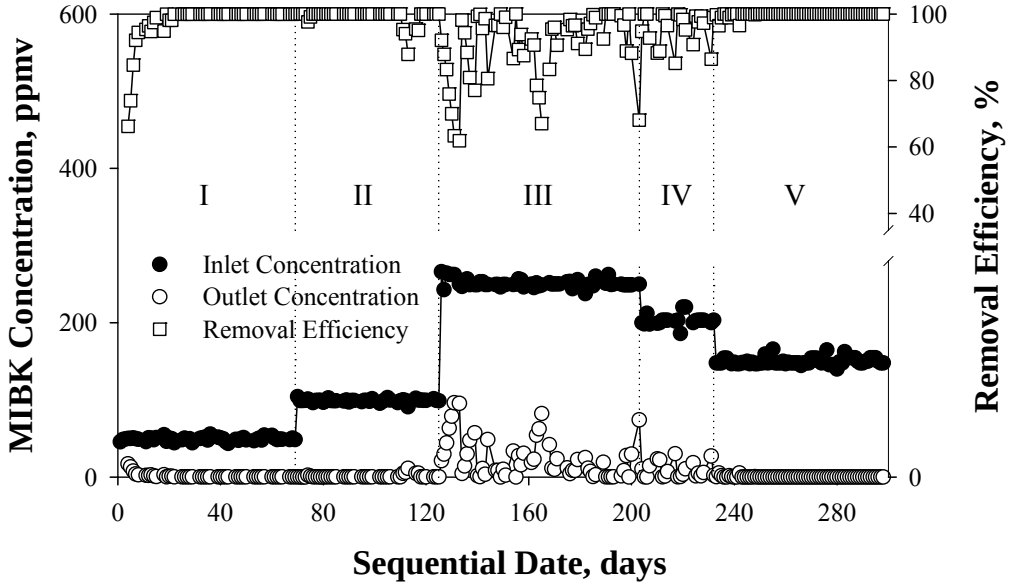

Figure 2-16 Biofilter performance with respect to MIBK removal

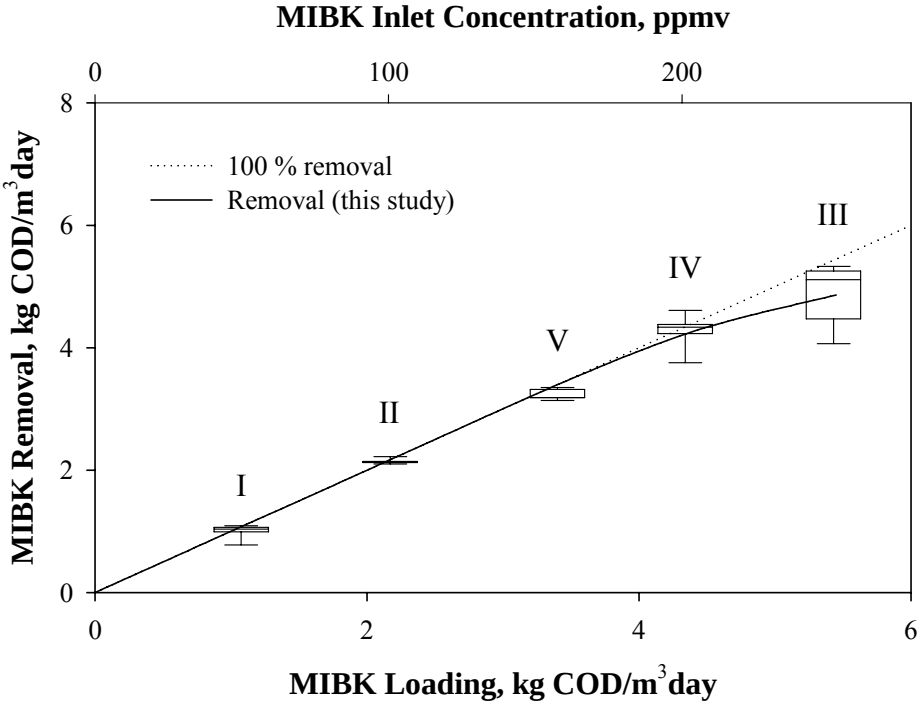

Figure 2-17 MIBK removal capacity with respect MIBK loading (under the backwashing strategy)

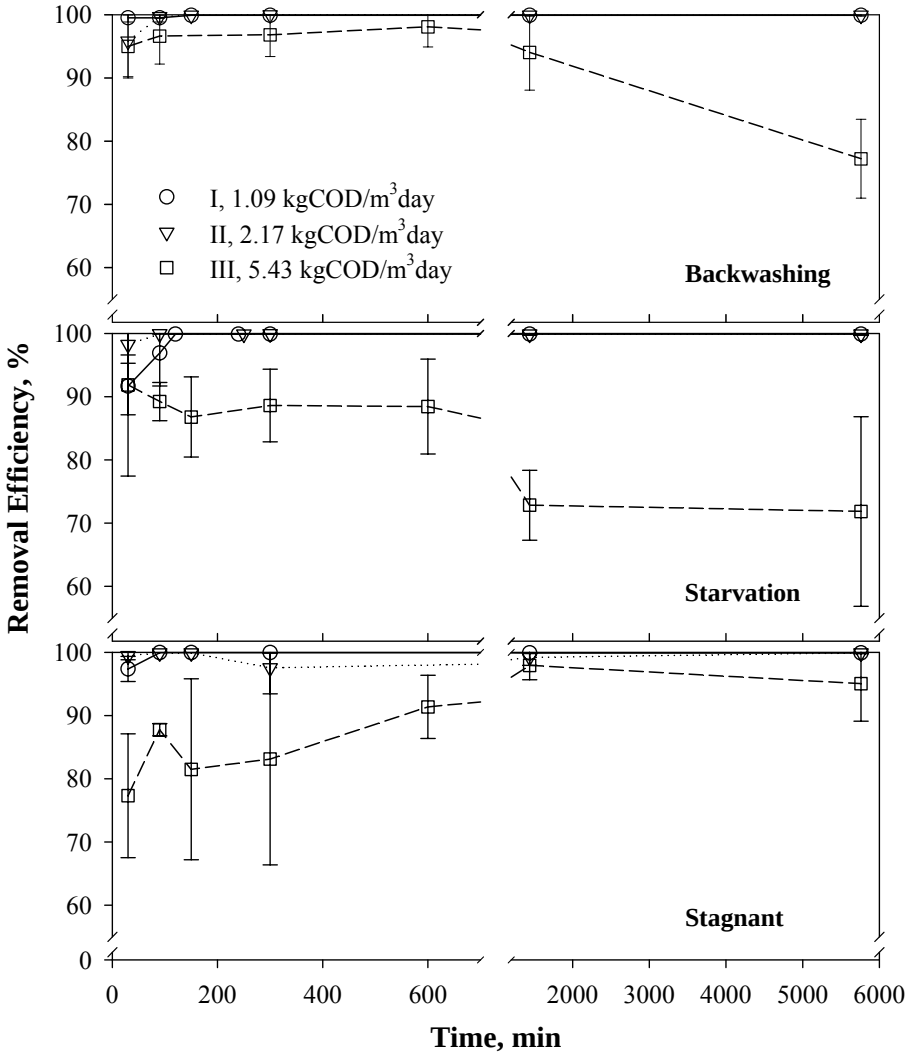

Figure 2-18 MIBK biofilter response after the restart-up after each experimental strategy

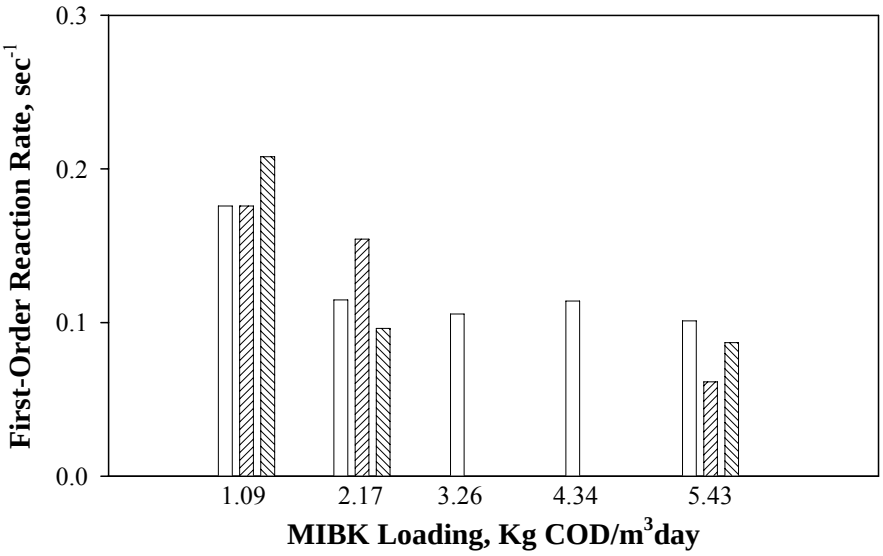

Figure 2-19 First-order reaction rate constants as a function of MIBK loading

2.5. Conclusions

Specific conclusions that can be drawn from this study include the following:

1. High performance (over 99% removal) of the biofilter had been observed for all experimental strategies (backwashing, starvation, and stagnant) for toluene loading up to 3.52 kg COD/m^3·day (corresponding to an inlet concentration of 250 ppmv); for styrene loading up to 1.27 kg COD/m^3·day (100 ppmv); for MEK loading up to 3.52 kg COD/m^3·day (250 ppmv); for MIBK loading up to 2.17 kg COD/m^3·day (100 ppmv).
2. For a step-increase in VOCs loading rate, the acclimation period to reach the original removal performance elongated to period of a number of days.
3. After restart-up following backwashing and non-use periods, a period of reacclimation to reach a 99 % removal level became longer as the VOC loading increased. Reacclimation performance after the non-use periods was apparently different to that after backwashing. The biofilter restart-up response after non-use periods was strongly dependent on the active biomass in the biofilter.
4. The first-order reaction rate decreased with an increase in the VOC loading rate. For a low VOC loading rate, the non-use strategies showed superior reaction kinetics than the backwashing strategy.
5. The non-use periods can be practically utilized as another means of biomass control for a low VOC loading rate where the biofilter does not potentially encounter clogging problem due to accumulation of excess biomass.
6. No significant difference between the effects of two different non-use periods on biofilter performance was observed during the period of this study. As a final engineering view, significant energy saving would be made by shutting down the air blower and liquid pump during a period of non-use. However, operators should notice that long-term of the shut

down cause problems of anaerobic condition in the biofilter bed, i.e., changes in microbial community, biofilm decay, and odor generation.

7. For complying with air regulation consistently, development of novel treatment technology is significant to overcome erratic performance of the biofilter during transient contaminant loadings.

2.6. References

APHA/AWWA/APCF. (1998). *Standard methods for the examination of water and wastewater*, American Public Health Association/American Water Works Association/Water Pollution Control Federation, Washington, D.C.

Cox, H. H. J., and Deshusses, M. A. (2002). "Effect of starvation on the performance and re-acclimation of biotrickling filters for air pollution control." *Environmental Science & Technology*, 36(14), 3069-3073.

Delhomenie, M. C., Bibeau, L., Gendron, J., Brzezinski, R., and Heitz, M. (2003). "A study of clogging in a biofilter treating toluene vapors." *Chemical Engineering Journal*, 94(3), 211-222.

Irvine, R. L., and Moe, W. M. (2001). "Period biofilter operation for enhanced performance during unsteady-state loading conditions." *Water Science and Technology*, 43(3), 231-239.

Jorio, H., Bibeau, L., and Heitz, M. (2000). "Biofiltration of air contaminated by styrene: Effect of nitrogen supply, gas flow rate, and inlet concentration." *Environmental Science & Technology*, 34(9), 1764-1771.

Schroder, M., Muller, C., Posten, C., Deckwer, W. D., and Hecht, V. (1997). "Inhibition kinetics of phenol degradation from unstable steady- state data." *Biotechnology and Bioengineering*, 54(6), 567-576.

Smith, F. L., Sorial, G. A., Suidan, M. T., Biswas, P., and Brenner, R. C. (2002). "Development and demonstration of an explicit lumped-parameter biofilter model and design equation incorporating Monod kinetics." *Journal of the Air & Waste Management Association*, 52(2), 208-219.

Smith, F. L., Sorial, G. A., Suidan, M. T., Breen, A. W., Biswas, P., and Brenner, R. C. (1996). "Development of two biomass control strategies for extended, stable operation of highly

efficient biofilters with high toluene loadings." *Environmental Science & Technology*, 30(5), 1744-1751.

Sorial, G. A., Smith, F. L., Suidan, M. T., Biswas, P., and Brenner, R. C. (1995). "Evaluation of trickle-bed biofilter media for toluene removal." *Journal of the Air & Waste Management Association*, 45(10), 801-810.

Sorial, G. A., Smith, F. L., Suidan, M. T., Pandit, A., Biswas, P., and Brenner, R. C. (1998). "Evaluation of trickle-bed air biofilter performance for styrene removal." *Water Research*, 32(5), 1593-1603.

Sorial, G. A., Smith, F. L., Suidan, M. T., Smith, P. J., Biswas, P., and Brenner, R. C. "Evaluation of biofilter media for treatment of air streams contanin VOCs." *Proceedings of Water Environment Federation 66th Annual Conference and Exposition*, Anaheim, CA, 429-439.

Zhu, X., Suidan, M. T., Alonso, C., Yu, T., Kim, B. J., and Kim, B. R. (2001). "Biofilm structure and mass transfer in a gas phase trickle-bed biofilter." *Water Science and Technology*, 43(1), 285-293.

CHAPTER 3

COMPARISON OF TBAB PERFORMANCES FOR VOC REMOVAL

3.1. Abstract

VOCs removal and biomass growth in the biofilter strongly related to the physicochemical properties of VOCs treated. The availability of VOCs into the biofilm, which can be described by Octanol-water partition coefficient and Henry's constant, was a critical factor to understand VOCs removal in the biofilter. Large biomass yield was found in the biofilters treating oxygenated compounds as compared to aromatic compounds. Nitrate utilization was a strong function of the substrate loading rate and was different according to the VOC treated. Specifically, scaling up the ratio of nitrate utilization to nitrate usage for biomass yield was observed as loading rates of oxygenated compounds increased, of which observation otherwise would have resulted in oxygen limitation and development of denitrification due to deeper biofilm formation. Correspondingly, the substrate inhibition of microbial growth and activity was observed as substrate loading rates increased.

3.2. Introduction

In the previous chapter (Chapter 2), trickle bed air biofilter performances for the removal of four single VOCs were evaluated. The objective of this chapter is to compare their removal performances in the biofilters. The comparisons were focused on the following operational parameters: (1) VOCs removal capacity, (2) nitrogen utilization and biomass yield, (3) CO_2 production, and (4) reaction kinetics.

3.3. Materials and Methods

See 2.3 Materials and Methods in Chapter 2.

3.4. Results and Discussion

3.4.1. VOC Removal Capacity

The removal capacities of VOCs were explored as a function of their loadings over the entire experimental period for the backwashing strategy. Removal capacities for VOCs of concern as a function of their loadings are depicted in Figure 3-1. The error bars in the experimental data points shown in Figure 3-1 represent the standard deviation. From Figure 3-1, the critical loading rate was defined as the maximum allowable loading rate at which the biofilter attains 100 % of the removal efficiency. The critical loading rates were determined to be 3.52 kg COD/m^3·day (46.9 g/m^3·hr), 1.9 kg COD/m^3·day (25.8 g/m^3·hr) , 5.64 kg COD/m^3·day (96.3 g/m^3·hr) , and 4.34 kg COD/m^3·day (66.5 g/m^3·hr) for toluene, styrene, MEK, and MIBK, respectively. To identify a correlation between VOC removal performance by means of the critical loading to the biofilter and the physical-chemical properties of VOC, the explored critical loading rates for VOCs were plotted as a function of octanol-water partition coefficients, Henry's law constants, and ecotoxicity (see Figure 3-2). The octanol-water partition coefficient is a significant predictor of the behavior of environmental contaminant (Watts 1997). Specifically in the biofilter, it is a possible descriptor of phase transfer between the liquid phase and biomass (Aizpuru et al. 2002). The Henry's law constant is the indicator of the tendency of physical transfer between gas phase and liquid phase. Deshusses and Johnson (2000) found that the elimination of VOCs in the biofilter was strongly correlated with Henry's law constant and octanol-water partition coefficient. Zhu et al. (2004) demonstrated that removal of a VOC generally increased with a decrease in its Henry's raw constant. In this study, it can be seen from

Figure 3-2 that the obtained critical loading rate is well correlated with the octanol-water partition coefficient ($r^2 = 0.922$) and ecotoxicity ($r^2 = 0.909$). Even if weak correlation ($r^2 = 0.512$) between the Henry's raw constant and the critical loading rate is seen, this relation shows the general trend that the critical load increases with a decrease in Henry's raw constant. It is interesting to note that if there is no oxygen limitation in the biofilm, the availability of VOCs to the biofilm can be the most significant factor that affects its removal in the biofilter. The biofilter conceptually has gas, aqueous, and solid (biofilm) phase in itself. The physical transfer of VOC between gas phase and aqueous phase (Henry's law constant) could be less significant to describe the mass transfer occurring in the biofilter as compared to the phase transfer from the aqueous or gas phase to the biomass. Zhu et al. (2001) found that the phase transport of gas phase compounds into the biofilm can not be limited by the aqueous phase. Alonso et al. (1998) demonstrated that for compounds with Henry's law constant of less than approximately 0.01, effects of substrate Henry's constants on the biofilter performance was less significant. Since the octanol-water partition coefficient is well correlated with aquatic bioconcentration factors, toxicity, and sorption to soils and sediments (Watts 1997), it can be considered as a more significant factor to understand the availability of VOC into biofilm. This can be confirmed by observing the good correlation between ecotoxicity and the critical loading rate (see Figure 3-2).

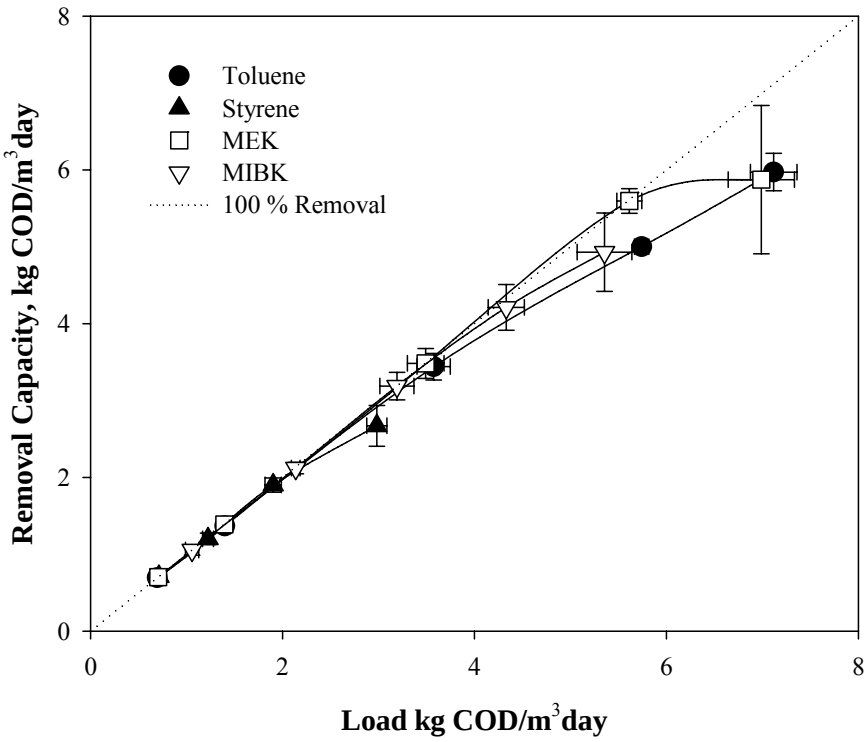

Figure 3-1 Removal capacities for VOCs of concern as a function of their loadings: The vertical and horizontal bars represent the standard error of the mean across the range of experimental period

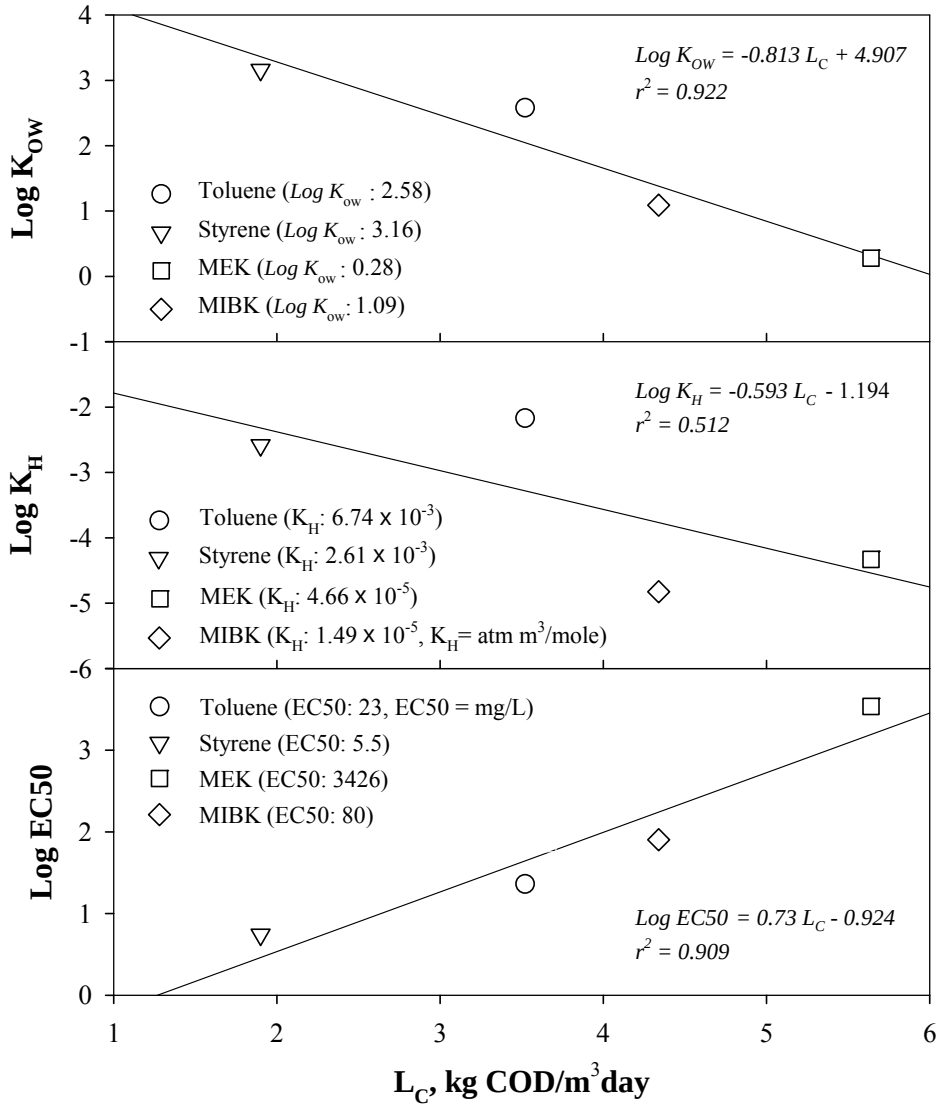

Figure 3-2 Correlation between critical loading rates (L_C) for VOCs and their physicochemical properties: Octanol-water partition coefficient (Log K_{ow}) and Henry's law coefficient (K_H, atm·m^3/mole) were obtained from Watts (1997). Ecotoxicity (EC50, mg/L) of VOCs to photobacterium phosphoreum by the Microtox® test was obtained from the ecotoxicity reviews data (Devillers 1994). The line of best linear fit is included in each plot.

3.4.2. Nitrate Utilization and Biomass Yield

Nitrogen is critical to sustain biomass growth in the biological treatment process (Song et al. 2003). Empirically, nitrogen makes up the largest fraction of dry cell mass (about 12.4 % for a bacterial cell formula of $C_5H_7O_2N$) (Rittmann and McCarty 2001). For biological growth kinetics, the biomass yield coefficient is a good parameter for evaluation of the relation between the rate of substrate utilization and the rate of cell growth. In this study, nitrate was used as the sole source of nutrient-nitrogen because the use of nitrate instead of ammonia can be effective in reducing the observed biomass yield (Smith et al. 1996) and shows no inhibition effect on biofilter performance even at high concentration of nitrate (Yang et al. 2002).

Nitrate feed and nitrogen utilization across the entire experimental period for the backwashing strategy are summarized in Table 3-1. The net N utilization was calculated by subtracting the amounts for the N species in the effluent from the N species present in the nutrient feed. For all compounds, larger nitrogen utilization was generally found when the biofilters had higher VOC loadings. In Table 3-1, the biofilters treating the oxygenated compounds (MEK and MIBAK) were found to utilize much more nitrate as compared to those for aromatic compounds (toluene and styrene). It should be noted that biodegradation of oxygenated compounds in the biofilter was effectively attained when excess nitrate was supplied to sustain the microbial activity, which corresponded to high inlet COD/N value.

Figure 3-3 was developed to observe the relation between nitrogen utilization and nitrate usage for biomass yield at different VOC loading rates. Nitrate usage for biomass yield was estimated by the measurement of biomass loss in the effluent and in the backwashing solution as Zhu et al. (2004) proposed by assuming that nitrogen makes up 12.4 % of the dry biomass. It is also assumed that the biomass was not accumulated within the biofilter bed because excess biomass was periodically removed through biofilter backwashing. For hydrophobic compounds

(toluene and styrene), the ratio of nitrate utilization to nitrate usage for biomass yield was relatively constant regardless of VOC loading rates. However, for hydrophilic compound (MEK and MIBK) the ratio of nitrate utilization to nitrate usage increased with VOC loading rates. It is speculated for hydrophilic compounds that the large nitrate utilization could be attributed to denitrification. MEK and MIBK have dimensionless Henry's constant values of 0.00194 and 0.00062, respectively. Zhu et al. (2004) discussed that O_2 limitation in biofilm could be encountered when biofilters treat VOCs with substrate Henry's constant less than 0.03, causing the accumulation of denitrifiers in the biofilm. These results, therefore, demonstrate that nitrate utilization and biomass growth are not only affected by substrate VOC loading, but also VOC availability in the biofilm.

In Figure 3-4, plots of estimated data of nitrate usage for biomass yield as a function of substrate COD removal are shown for the VOCs studied. COD removal was calculated as the difference between the COD of feed and the COD of the effluent gas and liquid stream. The influent COD was calculated as the sum of the COD equivalent of substrate present in the inlet gas stream and the COD measured in the nutrient feed. Similarly, the effluent COD was calculated as the sum of COD-equivalent VOC present in the outlet gas and the COD measured in the effluent liquid. To evaluate the relation between the rate of substrate utilization and the rate of cell growth, the estimated ratio of COD removal to Nitrate usage for biomass was obtained from the inverse of the slope of the regression line of Figure 3-4, and then the biomass yield coefficient (gVSS/gCOD) was estimated by assuming that nitrogen makes up about 12.4 % for a bacterial cell formula of $C_5H_7O_2N$. Estimated values of COD/N and biomass yield coefficient are summarized in Table 3-2. For oxygenated compounds such as MEK and MIBK, which have dimensionless Henry's constant values of 0.00194 and 0.00062, respectively, higher microbial yield was obtained as compared to aromatic compounds such as toluene and styrene, which have

dimensionless Henry's constant values of 0.28 and 0.109, respectively. This behavior could provide more evidence that the biodegradation of oxygenated compounds in the biofilter utilized much larger nitrogen for cell growth as compared to aromatic compounds.

Table 3-1 Nitrate feeding and nitrate utilization

	Operation Condition		Observation	
	VOC load * KgCOD/m^3·day	Nitrate feed ** g N/day	Nitrate utilization g N/day	COD/N *** g COD/g N
Toluene	0.7 (9.3)	0.04 (50)	0.020 ± 0.003	92.6 ± 1.3
	1.41 (18.8)	0.08 (50)	0.043 ± 0.007	89.9 ± 17.6
	3.52 (46.9)	0.2 (50)	0.098 ± 0.014	92.9 ± 19.2
	5.63 (75.1)	0.3 (50)	0.139 ± 0.043	89.5 ± 33.9
	7.03 (93.7)	0.38 (50)	0.143 ± 0.041	118.9 ± 37.9
Styrene	0.64 (8.7)	0.04 (50)	0.019 ± 0.008	94.2 ± 23.7
	1.27 (17.2)	0.08 (50)	0.045 ± 0.008	75.6 ± 19.5
	1.9 (25.8)	0.2 (25)	0.128 ± 0.048	47.9 ± 20.1
	3.17 (43.0)	0.2 (50)	0.131 ± 0.026	58.5 ± 13.2
MEK	0.7 (11.9)	0.04 (50)	0.034 ± 0.008	58.1 ± 12.3
	1.41 (24.1)	0.09 (50)	0.075 ± 0.014	52.6 ± 13.3
	3.52 (60.1)	0.3 (30)	0.269 ± 0.231	26.0 ± 6.9
	5.6 (95.6)	1.2 (10)	1.168 ± 0.233	12.7 ± 5.4
	7.04 (120.2)	1.5 (10)	1.276 ± 0.231	12.3 ± 3.0
MIBK	1.09 (16.7)	0.06 (50)	0.043 ± 0.002	67.4 ± 2.5
	2.17 (33.3)	0.11 (50)	0.087 ± 0.009	67.7 ± 8.0
	3.26 (49.9)	0.9 (10)	0.894 ± 0.163	10.0 ± 2.3
	4.34 (66.6)	1.0 (10)	0.986 ± 0.157	11.6 ± 2.0
	5.43 (83.3)	0.6 (25)	0.586 ± 0.239	26.1 ± 17.7

* Mass loading rate of VOC (g VOC/m^3·hr) is provided in parenthesis.

** For the nitrogen source, nitrate was supplied in the biofilter. The values in parenthesis indicates the ratio of inlet COD/N (g inlet COD to g inlet nitrate) for a given VOC loading.

*** The ratio of substrate COD removal to nitrate utilization

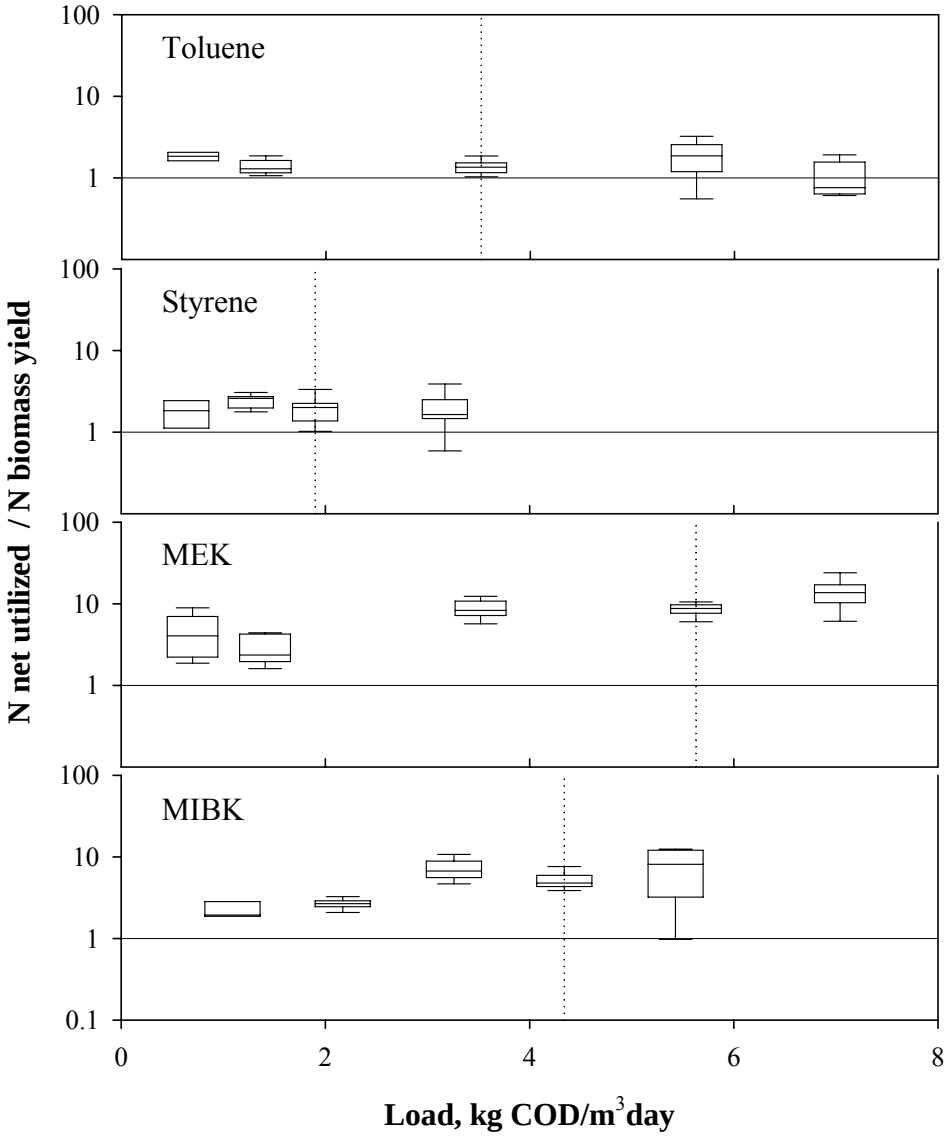

Figure 3-3 Ratio of net utilized nitrogen to estimated nitrogen usage for biomass yield with respect to VOC loadings: The box plot provides the value of $N_{net\ utilized}/N_{biomass\ yield}$ across the range of experimental periods, stretching from the lower hinge (defined as the 5th percentile) to the upper hinge (the 95th percentile). The dotted lines represent the critical VOCs loadings.

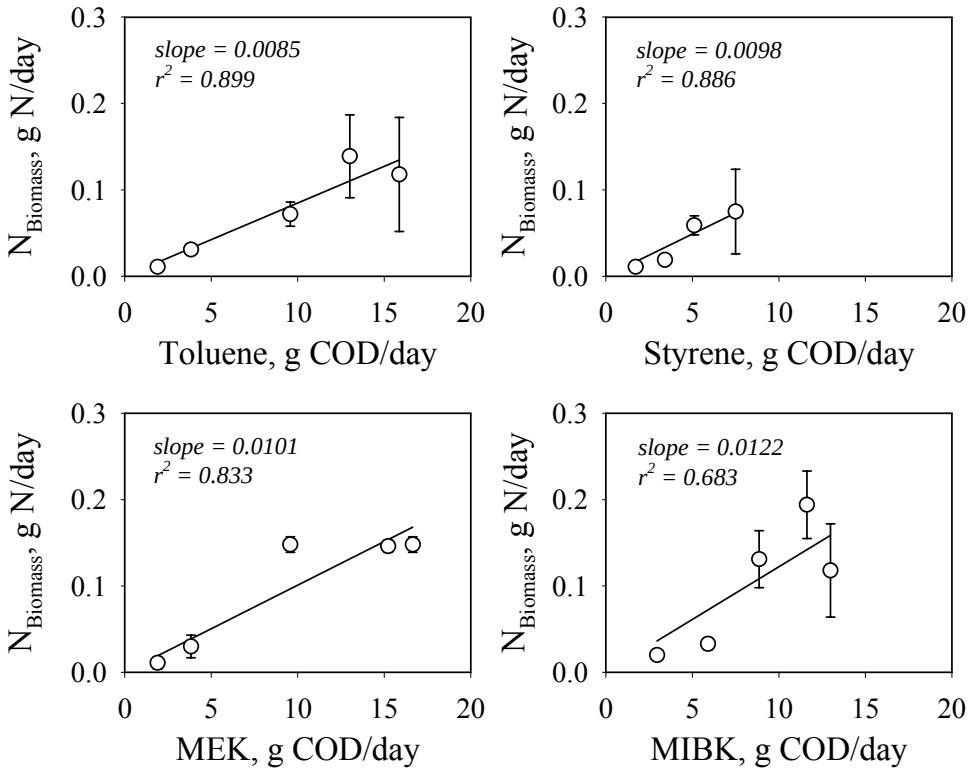

Figure 3-4 Estimated nitrate usage for biomass growth as a function of substrate COD removal: The slope of regression line represents the inverse of COD/N.

Table 3-2 COD removal to Nitrate usage for biomass (gCOD/g$N_{biomass\ yield}$) and equivalent biomass yield coefficient (gVSS/gCOD)

	$COD/N_{biomass\ yield}$ gCOD/gN	Biomass Yield, *Y* gVSS/gCOD
Toluene	117.6	0.069
Styrene	102.0	0.079
MEK	99.0	0.081
MIBK	82.0	0.098

3.4.3. CO_2 Production

In biological processes, a portion of the consumed substrate is converted to new cells (synthesis) and the remaining is oxidized to inorganic (mostly, CO_2 for energy generation), and organic end products (Rittmann and McCarty 2001). The analysis of CO_2 production can be used to provide a good estimate of biological activity in biological processes. In this study, the net production of CO_2 was developed in Figure 3-5 as a function of the substrates consumed. From the slope of the regression line of Figure 3-5, the ratios of CO_2 produced to VOC consumed were found to be 4.67, 6.33, 2.03, and 2.65 for toluene, styrene, MEK, and MIBK, respectively. As seen in Table 3-3, in the aerobic oxidation of VOCs to CO_2 and water, 1 mole of VOC theoretically produces 7, 8, 4, and 6 moles of CO_2 for toluene, styrene, MEK, and MIBK, respectively.

In Table 3-3, the difference between the observed and theoretical values would result in the consumption of substrate for cell synthesis and endogenous respiration (e.g., denitrification). Interestingly, the ratios of observed values to theoretical values were found to be higher for aromatic compounds (toluene and styrene) than those for oxygenated compounds (MEK and MIBK). Correspondingly, in the analysis of biomass yield in the previous section (3.4.2 Nitrate utilization and biomass yield), oxygenated compounds were found to have high biomass yield as compared with aromatic compounds.

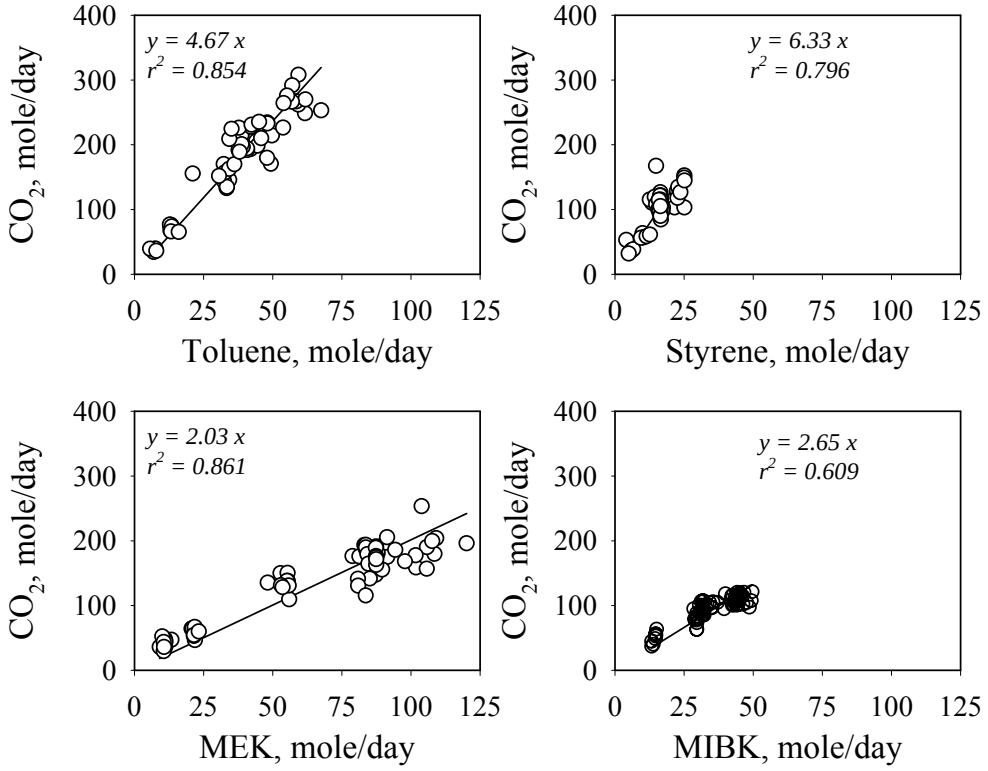

Figure 3-5 CO_2 production as a function of substrate consumed

Table 3-3 Theoretical* and observed CO_2 production** in the biofilters

	Theoretical CO_2 production mole CO_2/mole $VOC_{consumed}$	Observed CO_2 production mole CO_2/mole $VOC_{consumed}$	Obser./Theor. %
Toluene	7	4.67	66.7
Styrene	8	6.33	79.1
MEK	4	2.03	50.8
MIBK	6	2.65	44.2

* Aerobic oxidation of VOC studied to CO_2 and water: Toluene, $C_7H_8 + 9O_2 \rightarrow 7CO_2 + 4H_2O$; Styrene, $C_8H_8 + 10O_2 \rightarrow 8CO_2 + 4H_2O$; MEK, $C_4H_8O + 11/2O_2 \rightarrow 4CO_2 + 4H_2O$; MIBK, $C_6H_{12}O + 17/2O_2 \rightarrow 6CO_2 + 6H_2O$

** The slope of the regression line of Figure 3-5

3.4.4. Reaction Kinetics

In Chapter 2, the first-order reaction rate constants for VOCs studied were investigated. Details are presented in Appendix III. The obtained results are summarized in Figure 3-6 to compare the reaction rates of VOCs studied. For all compounds, the first-order reaction rates were dependent on the substrate inlet concentration. Since high substrate inlet concentration cause a problem of a substrate inhibition effect on the microbial growth or activity (Schroder et al. 1997), lower reaction rates were found at higher substrate loading. On the other hand, since clogging problem due to excessive accumulation of biomass in the biofilter would be encountered for higher substrate loading, substrate utilization rates can decrease as substrate loading rates increase. It is also shown in Figure 3-6 that aromatic compounds such as toluene and styrene had lower reaction rates than oxygenated compounds such as MEK and MIBK, which well corresponds with those obtained in section 3.4.1 for VOC removal capacity.

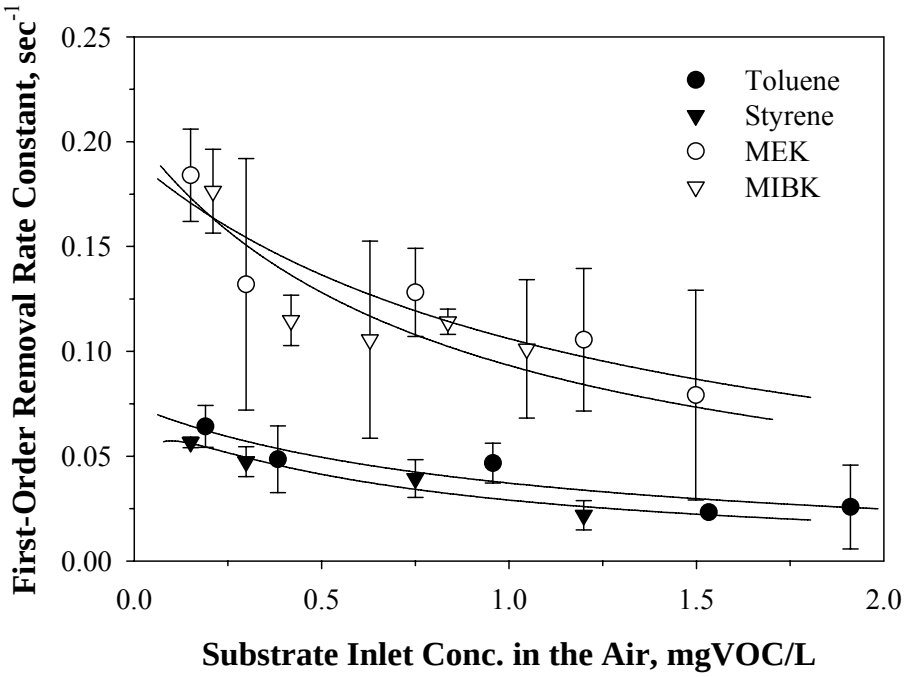

Figure 3-6 First-order reaction rate constants for VOCs studied

3.5. Conclusions

Biofilter performances linked with VOCs removal and biomass growth strongly depended on the physicochemical properties of VOCs treated. Most of all, the availability of VOCs into biofilm, which can be described by Octanol-water partition coefficient and Henry's constant, was a critical factor for understanding VOCs removal in the biofilter. In this study, high correlation (r^2 = 0.922) between Octanol-water partition coefficient and critical loading rate to the biofilter was found.

Large biomass yield was found in the biofilters treating oxygenated compounds (MEK and MIBK) as compared to those for aromatic compounds (toluene and styrene). For the removal of oxygenated compounds, the ratio of nitration utilization to nitrate usage for biomass yield increased as substrate loading increased, which might result in oxygen limitation and development of denitrification due to deeper biofilm formation. Correspondingly, the substrate inhibition of microbial growth and activity was observed as substrate loading rates increased.

3.6. References

Aizpuru, A., Malhautier, L., and Fanlo, J. L. (2002). "Quantitative structure-activity relationship modeling of biofiltration removal." *Journal of Environmental Engineering-Asce*, 128(10), 953-959.

Alonso, C., Suidan, M. T., Kim, B. R., and Kim, B. J. (1998). "Dynamic mathematical model for the biodegradation of VOCs in a biofilter: Biomass accumulation study." *Environmental Science & Technology*, 32(20), 3118-3123.

Deshusses, M. A., and Johnson, C. T. (2000). "Development and validation of a simple protocol to rapidly determine the performance of biofilters for VOC treatment." *Environmental Science & Technology*, 34(3), 461-467.

Devillers, J. (1994). "Handbooks of ecotoxicological data." Ecotoxicity of chemicals to photobacterium phosphoreum, K. L. E. Kaiser and J. Devillers, eds., Gordon and Breach Science Publishers.

Rittmann, B. E., and McCarty, P. L. (2001). *Environmental biotechnology : principles and applications*, McGraw-Hill, Boston :.

Schroder, M., Muller, C., Posten, C., Deckwer, W. D., and Hecht, V. (1997). "Inhibition kinetics of phenol degradation from unstable steady- state data." *Biotechnology and Bioengineering*, 54(6), 567-576.

Smith, F. L., Sorial, G. A., Suidan, M. T., Breen, A. W., Biswas, P., and Brenner, R. C. (1996). "Development of two biomass control strategies for extended, stable operation of highly efficient biofilters with high toluene loadings." *Environmental Science & Technology*, 30(5), 1744-1751.

Song, J., Ramirez, J., and Kinney, K. A. (2003). "Nitrogen utilization in a vapor-phase biofilter." *Water Research*, 37(18), 4497-4505.

Watts, R. J. (1997). *Hazardous wastes: sources, pathways, receptors*, John Wiley & Sons, Inc.

Yang, H., Minuth, B., and Allen, D. G. (2002). "Effects of nitrogen and oxygen on biofilter performance." *Journal of the Air & Waste Management Association*, 52(3), 279-286.

Zhu, X., Suidan, M. T., Alonso, C., Yu, T., Kim, B. J., and Kim, B. R. (2001). "Biofilm structure and mass transfer in a gas phase trickle-bed biofilter." *Water Science and Technology*, 43(1), 285-293.

Zhu, X. Q., Suidan, M. T., Pruden, A., Yang, C. P., Alonso, C., Kim, B. J., and Kim, B. R. (2004). "Effect of substrate Henry's constant on biofilter performance." *Journal of the Air & Waste Management Association*, 54(4), 409-418.

CHAPTER 4

ROLE OF BIOMASS DISTRIBUTION AND ACTIVITY IN TBAB PERFORMANCE

4.1. Abstract

The effects of temporal and spatial changes in biological activity and biomass amount on biofilter performance were investigated in a lab-scale trickle bed air biofilter (TBAB) at a toluene loading of 46.9 $g/m^3 \cdot hr$ under two different experimental strategies, namely, periodic backwashing and starvation. Even spatial distribution of biomass along the bed media through periodic *in-situ* backwashing with media fluidization was deemed necessary to attain consistent high removal performance in the biofilter. Analysis of the overall reaction for toluene biodegradation revealed that cell synthesis was more preferable than toluene oxidation in the inlet section of the biofilter. However, toluene oxidation became predominant in the whole biofilter bed with time. After 2 days of starvation, the concentration of the biofilm EPS (protein and carbohydrates) in the total biomass increased along the media bed depth, while the total biomass in the media bed subsequently decreased. The presence of sufficient biomass and microbial activity favorably influenced biofilter reacclimation after restart-up following starvation. Our findings indicate that microbial activity linked with biomass amount was found to contribute significantly for consistent high removal performance of the biofilter.

4.2. Introduction

The amount of biomass reflects the biological activity in the biofilter ((Devinny et al. 1996). Active microorganisms could be found in the biofilter where biomass is accumulating rapidly. Subsequently, excess accumulation of biomass causes severe biofilter operating problems including a increase in airflow resistance within the bed and low contaminant removal efficiencies (Iliuta and Larachi 2004; Smith et al. 1996; Weber and Hartmans 1996). Thus, coordinated biomass control is deemed necessary for achieving long-term performance of the biofilter. However, subsequent loss of active biomass following biomass control was found to lead to a temporary decrease in biofilter performance (Delhomenie et al. 2003; Kim et al. 2005b). Hence further investigation of biomass activity and accumulation is required to better assess and predict the long-term efficacy of biomass control methods.

In liquid phase bioreactors, starvation led to changes in cells numbers, community composition, and physiological state (Konopka et al. 2002). During starvation in liquid phase bioreactor, the cells produced new extracellular polymeric substances (EPS), but also consumed easily biodegradable EPS in order to satisfy their maintenance of energy requirements (Lobos et al. 2005; Zhang and Bishop 2003). A few studies reported the effect of starvation on biological activity and biomass variation in gas phase bioreactors (Cox and Deshusses 2002; Martin and Loehr 1996; Metris et al. 2001). As observed by Cox and Deshusses (2002), 10 to 50 % of their biomass was lost during 7 days of starvation. During a period of starvation, the rate of endogenous respiration was found to decrease exponentially (Metris et al. 2001). After starvation, reacclimation time to original biofilter performance is hours to days according to the duration of starvation and the presence of alternative carbon source (Martin and Loehr 1996). Since biofilter performance is affected by any changes in biological activity associated with biomass amount

during starvation, further detailed investigations will provide clear understandings of biological activity and biomass variation in gas phase bioreactors during a starvation condition.

This chapter presents the results of investigations on the role of biological activity and biomass distribution in air biofilter performance when periodic *in-situ* backwashing with media fluidization was employed as the biomass control strategy, and when the biofilter was exposed to periods of non-use, i.e., starvation without substrate loading. For this purpose, temporal and spatial changes in biomass activity and accumulation were explored using a trickle bed air biofilter (TBAB) subjected to the toluene removal.

4.3. Materials and Methods

4.3.1. Experimental Biofilter System

Experimental work was performed on a lab-scale TBAB for controlling toluene as a single solute. Details about biofilter system are found in the section 2.3.1 of Experimental Biofilter System. The air flow to the biofilter was set up at 2.22 L/min, corresponding to empty bed retention time (EBRT) of 1.23 min. The liquid flow to the biofilter was set up at the rate of 2.4 L/day of a buffered nutrient solution.

4.3.2. Biofilter Operation

The biofilter continued to be operated without reconditioning the media used in a previous experimental run (Kim et al. 2005c). In order to maintain a constant high removal efficiency, the biofilter received influent air with a 250 ppmv concentration of toluene, corresponding to a loading of 46.9 $g/m^3 \cdot hr$. This loading was found to yield constant high biofilter performance in Chapter 3. A periodic *in-situ* backwashing was considered as the biomass control strategy. Backwashing was conducted while the biofilter was offline by using 18 L of the buffered nutrient

solution to induce full medium fluidization at about 50 % bed expansion for a defined time period. The details of the backwashing were described elsewhere (Kim et al. 2005b; Smith et al. 1996; Sorial et al. 1998). The backwashing duration and frequency were set at 1 hour once per week for a period of three weeks. To avoid significant reduction in media bed volume through media sampling for biomass analysis, the media bed was replenished with flesh pellets during the operation of backwashing. No significant decrease in biofilter performance has been observed subsequent to the replenishment of the media.

After a period of three cycles of backwashing, the starvation strategy was coordinated without other strategies of biomass control such as backwashing. The starvation strategy involves the period without toluene loading, i.e., pure air with nutrient flow through the biofilter. The duration and frequency for starvation were two days per week for a period of two weeks.

4.3.3. Analytical Methods

Gas phase samples for toluene and carbon dioxide analyses were analyzed by using a GC equipped with a FID and a TCD, respectively. Liquid phase samples were analyzed for nitrate, TC, IC, and VSS. Details about analytical methods are found in Appendix III. Biomass analysis was performed to determine spatial variations in volatile solids (VS) as total biomass, and total carbohydrates and proteins as the biofilm EPS. Seven (±1) grams of bed media covered with biomass was carefully collected from each sampling port in the biofilter. VS was determined according to Standard Method 2540G (APHA/AWWA/APCF 1998). Total carbohydrate concentration was determined by phenol reaction described by Daniels et al. (1994). 0.5 to 1.0 g of each wet media sample was mixed with 1 mL MilliQ water in the reaction vial. The sample was mixed with phenol and sulfuric acid and allowed to cool. The absorbance at 488 nm was compared to a glucose standard curve to determine the mass of carbohydrates per dry media mass.

Proteins concentration was determined using Coomassie® Plus Proteins Assay Reagent (#23236) (Pierce Biotechnology, Rockford, IL). 0.5 to 1.0 g of each wet media sample was mixed with 2 mL MilliQ water in the reaction vial. 2-mL of the reagent was added and the solution was sonicated for 10 minutes. The absorbance at 595 nm was compared to a bovine serum albumin standard curve to determine the mass of proteins per dry media mass. All analyses were duplicated in order to ensure reproducibility.

4.4. Results and Discussion

4.4.1. Biofilter performance

The biofilter performance for the three cycles of backwashing is summarized in Figure 4-1. Figure 4-1 provides toluene loading and removal, CO_2 production, and biomass loss as equivalent carbon in mol/m^3·hr as a function of sequential time following backwashing. Nitrogen utilization is also presented in Figure 4-1. CO_2 production was estimated as the net analysis of influent and effluent in the gas streams and liquid streams coupled with inorganic carbon. Biomass loss was estimated as the VSS loss from the effluent liquid by assuming that a typical cellular composition for a heterogeneous microorganism can be represented by $C_5H_7O_2N$. Figure 4-1 clearly shows that the biofilter achieved constant high removal performance. The average removal efficiency was 97.5±1.5 %. A slight increase in CO_2 production rate was observed during the initial days following backwashing, while the nitrogen utilization rate decreased slightly (detailed analysis is provided in next section – biological activity). Generally, it has been observed that the detachment rate of biomass increases with an increase in biomass accumulation (Trulear and Characklis 1982), however, in this study no significant changes in biomass loss was observed (see Figure 4-1). This behavior could indicate that media backwashing was effective in shearing off excess biomass. Total biomass washed out through three times of backwashing amounted to

4.36 ± 0.83 g VSS, which accounts for 13.5 % of the net carbon of the toluene consumed as seen in Table 4-1.

It is speculated that the 37.8 % unaccounted nitrogen reported in Table 4-1 could be due to nitrate utilization as electron acceptor for energy production in addition to oxygen. This observation could lead to denitrification. It has been reported that denitrification activity was responsible for the degradation of significant portion of organic carbon in an aerobic biofilter (du Plessis et al. 1998; Zhu et al. 1998). As the biomass retained within the system increased, it is speculated that denitrifying environment would develop due to deeper biofilm formation.

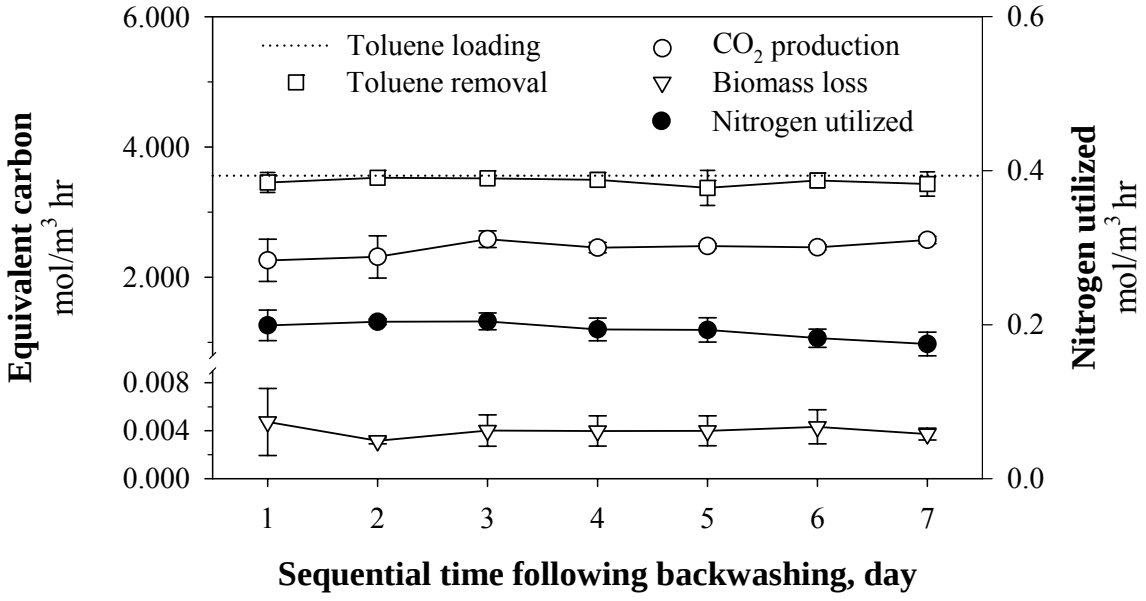

Figure 4-1 Biofilter performance for three cycles of backwashing: The dotted line represents the corresponding toluene loading rate of 3.56 mol/m^3·hr (3.52 kg COD/m^3·day) as carbon. The symbols represent the average experimental value and the error bars represent the standard deviation for three cycles of backwashing.

Table 4-1 Carbon recovery* and nitrogen recovery** during the experimental run with media backwashing

Carbon Recovery, %					Nitrogen Recovery, %		
$^{a}C_{CO_2}$	$^{b}C_{VSS}$	$^{c}C_{TOC}$	$^{d}C_{Backwashing}$	$C_{unaccounted}$	^{e}N	$^{f}N^{***}$	$N_{unaccounted}$
72.3	0.1	1.6	13.5	12.5	47.5	14.7	37.8

* Carbon balance: $C_{VOC\ removed} = {}^{a}C_{CO2\ in\ effluent\ gas\ and\ effluent\ liquid} + {}^{b}C_{VSS\ in\ effluent\ liquid} + {}^{c}C_{Total\ organic\ carbon\ in\ effluent\ liquid} + {}^{d}C_{VSS\ washed\ out\ through\ backwashing} + C_{Biomass\ retained\ in\ the\ reactor}$. A typical cellular composition for a heterogeneous microorganism can be represented as $C_5H_7O_2N$.

** Nitrogen balance: $N_{Nitrogen\ utilized} = N_{nitrogen\ used\ for\ biomass\ growth} + N_{nitrogen\ serve\ as\ electron\ acceptor}$. Since the net accumulation of attached biomass in the reactor is not equal to be zero, $N_{nitrogen\ used\ for\ biomass\ growth} = {}^{e}N_{VSS\ in\ effluent\ liquid\ and\ VSS\ washed\ out\ through\ backwashing} + {}^{f}N_{Biomass\ retained\ in\ the\ reactor}$.

*** Estimated from $C_{unaccounted}$ in an assumption that the carbon unaccounted in the experiment is equal to the carbon retained in the reactor.

4.4.2. Biological activity

In biological processes, the removal of organic carbon is brought by two principal processes, namely, oxidation and synthesis (Rittmann and McCarty 2001). The overall reaction for aerobic biodegradation of toluene under steady state condition is summarized as seen in Table 4-2. A mass balance check seen in Table 4-1 shows that for aerobic biodegradation of toluene, 72.3 percent of the carbon equivalent in toluene removal was used for CO_2 production. Hence, based on equation 4-4 in Table 4-2, f_s = 0.3016, and f_e = 1 - 0.3016 or 0.6984. The overall reaction for aerobic biodegradation of toluene at an organic loading rate of 46.9 g/m^3·hr under steady state condition without the accumulation of intermediate products and nitrate used as nitrogen source is , thus, given by:

$$C_7H_8 + 6.2854\,O_2 + 0.3878\,NO_3^- + 0.3878\,H^+ \rightarrow 0.3878\,C_5H_7O_2N + 2.8366\,H_2O + 5.061\,CO_2 \quad (4\text{-}5)$$

Equation 4-5 provides the general overall biodegradation reaction for toluene if it is assumed that no denitrification is taking place. Since biological activity varies along the biofilter depth and

with sequential date of operation, the rationale for biological activity based on the overall reaction as represented by equation 4-5 is inevitably questioned.

In order to evaluate temporal and spatial changes in biological activity along the biofilter, CO_2 production was compared with toluene removal at different bed media depth as a function of sequential time following backwashing (see Figure 4-2). At the top portion of bed media (above 0.12 L_o), the molar ratio of CO_2 to toluene removed was initially 4.1 and it increased exponentially with sequential time. The ratios also increased along bed media. At the lower portions of bed media (0.62 L_o and above), the ratio decreased exponentially with the sequential time. It is worthwhile noting that limitation of nutrient and oxygen could develop along the bed depth. However, since sufficient nutrient were supplied and excess nitrate was measured in the effluent liquid, nutrients limitation could be negligible. Oxygen limitation generally depends on the VOC concentration and other factors such as medium types and biofilm structure (Zhu et al. 2004). As discussed by Smith et al. (2002), oxygen limitation begins to be a problem beyond an inlet concentration of 593 ppmv for toluene at 32^oC, indicating that oxygen limitation was not a problem in this study. It is, therefore, speculated from Figure 4-2 that cell synthesis was preferable in the upper section of the biofilter while toluene oxidation dominated in the lower section. One possible explanation for this speculation is that less cell synthesis was involved in the lower section of the biofilter due to substrate limitation. During the experimental runs, more than 60 % of the inlet toluene was degraded within the upper sections (above 0.37 L_o) while the lowest section (beyond 0.87 L_o) of the media contributed only 0.05 % of toluene removal. As discussed by Hwang and Tang (1997), local biological growth rate would be lower in the lower section of the biofilter due to low substrate concentration. Cherry and Thompson (1997) observed that without nutrient limitation, biomass subsequently grew until the substrate was used up, while biomass growth ceased in case of substrate limitation.

It is also noted from Figure 4-2 that the molar ratios of CO_2 production to toluene removed along the biofilter depth approached a similar value with sequential time. As observed by Song and Kinney (2000), cell synthesis would be initially preferred in the inlet section of the biofilter. However after a certain period when biomass grows sufficiently, toluene oxidation process predominated in the whole bed. As biomass became locally concentrated in the inlet section, the dominated oxidation process would subsequently be brought by substrate availability due to deeper biofilm formation.

Table 4-2 Half reaction and overall reaction for aerobic biodegradation of toluene under steady state condition without the accumulation of intermediate products: NO_3^- is the preferred nitrogen source

Half reaction	
R_a	$1/4\ O_2 + H^+ + e^- \rightarrow 1/2\ H_2O$ (4-1)
R_c	$1/28\ NO_3^- + 5/28\ CO_2 + 29/28\ H^+ + e^- \rightarrow 1/28\ C_5H_7O_2N + 11/28\ H_2O$ (4-2)
R_d	$1/36\ C_7H_8 + 14/36\ H_2O \rightarrow 7/36\ CO_2 + H^+ + e^-$ (4-3)
Overall reaction ($R = f_e R_a + f_s R_c - R_d$)	
R	$C_7H_8 + 9f_e O_2 + 36/28\ f_s NO_3^- + 36\ (f_e + 29/28\ f_s - 1)H^+ \rightarrow$ $36/28\ f_s C_5H_7O_2N + (18\ f_e + 99/7\ f_s - 14)H_2O + (7 - 45/7\ f_s)CO_2$ (4-4)

R, overall reaction; R_a, electron acceptor half reaction; R_c, cell synthesis half reaction; R_d, donor half-reaction (written as oxidation), $f_e + f_s = 1.0$ (f_e, fraction used to generate energy; f_s, fraction converted into cell synthesis).

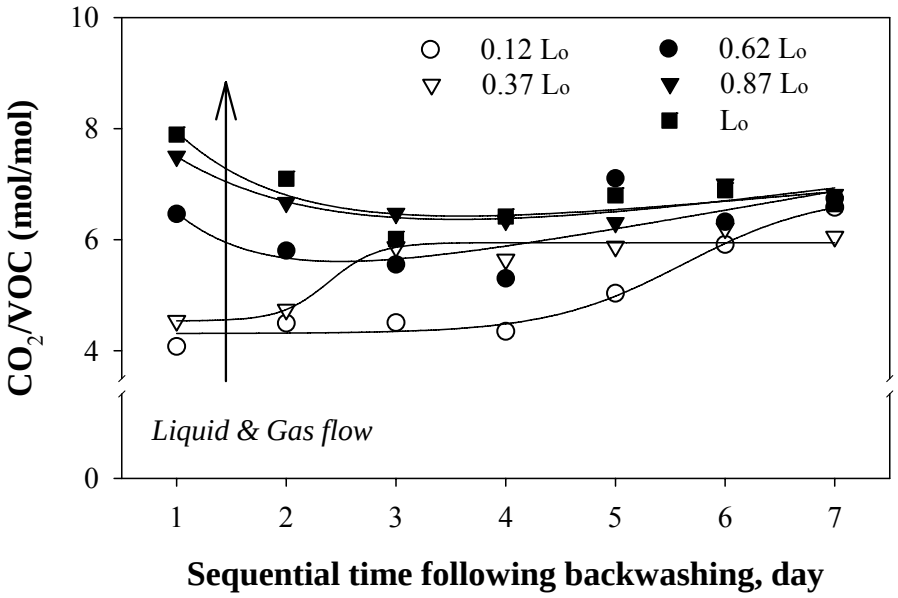

Figure 4-2 Molar ratio of CO_2 produced to toluene removed with bed media depth following the backwashing: The symbols represent the average experimental value and the error bars represent the standard deviation for three cycles of backwashing. (L_o = 60 cm bed media depth).

4.4.3. Biomass distribution

The profiles obtained for total biomass and biofilm EPS components, showing the concentrations of VS, total carbohydrates, and proteins as a function of the depth of bed media in the biofilter, are provided in Figure 4-3. These profiles are provided for the two experimental strategies (backwashing and starvation) and are compared to those after 7-day operation. The profile after 7-day operation was obtained just prior to backwashing or starvation.

It is seen from Figure 4-3a that a decrease in the amount of total biomass along the bed media was noticed after 7-day operation, i.e., less biomass grew in the bottom section of the biofilter. This behavior confirms the previous speculation that the synthesis process was preferable in upper section of the biofilter. A concentration decrease of biofilm EPS in VS along the bed media was also noticed after 7-day operation as seen in Figure 4-3b and c. The total carbohydrate/VS changed from 31.4 ± 3.6 mg/g to 21.9 ± 3.8 mg/g, and Proteins/VS changed from 1.8 ± 0.4 mg/g to 1.5 ± 0.9 mg/g. It is speculated that EPS production is higher in the upper section of the biofilter where higher levels of electron donors are available in comparison to the subsections due to high microbial viability. In contrast to the observation after 7-day operation, backwashing of bed media achieved an even distribution of the EPS components as well as total biomass. These results support the findings in previous studies (Kim et al. 2005b; Smith et al. 1996; Sorial et al. 1998), which indicated that periodic backwashing with medium fluidization was very effective in preventing accumulation of excess biomass.

It is also seen from Figure 4-3a that 2-days of starvation provided a spatial decrease in total biomass compared to that for 7-day operation. As discussed by Cox and Deshusses (2002), the decrease in biomass subjected to starvation would result from biomass death and lysis, endogenous respiration of microbial cultures in the system, predation by higher organisms, and shear by the liquid flow or gas flow. It is interesting to note that after starvation (see Figure 4-3b

and c), the ratio of EPS components to total biomass increased along the depth of bed media. In the lower section, the ratios after starvation were greater than those after 7-day operation. One possible explanation is that the release of lysis products made soluble EPS components increase along the bed media. In a study of the activated sludge in a membrane bioreactor (Lobos et al. 2005), an increase in soluble proteins concentration was observed during the starvation phase. Zhang and Bishop (2003) observed that the cells produced new EPS and gradually consumed the newly produced EPS during a starved state. They also found that the rate of the EPS carbon hydrates utilization were much faster than that of the EPS proteins during EPS biodegradation. From this point of view, an increasing tendency of EPS proteins along media bed depth was much larger than that of EPS carbohydrates when the biofilter was exposed to a starved state. Overall, the starved state was subsequently attributed to a decrease in biomass within media bed, which could indicate that starvation can be considered as another means of biomass control. In the previous study (Kim et al. 2005a), stable 99 % removal performance was observed for the periodic starvation strategy (2 days of starvation for a week) for toluene loadings up to 18.8 $g/m^3 \cdot hr$ demonstrating that starvation can be practically utilized as biomass control at low loading rate where the biofilter does not potentially encounter clogging problem due to accumulation of excess biomass.

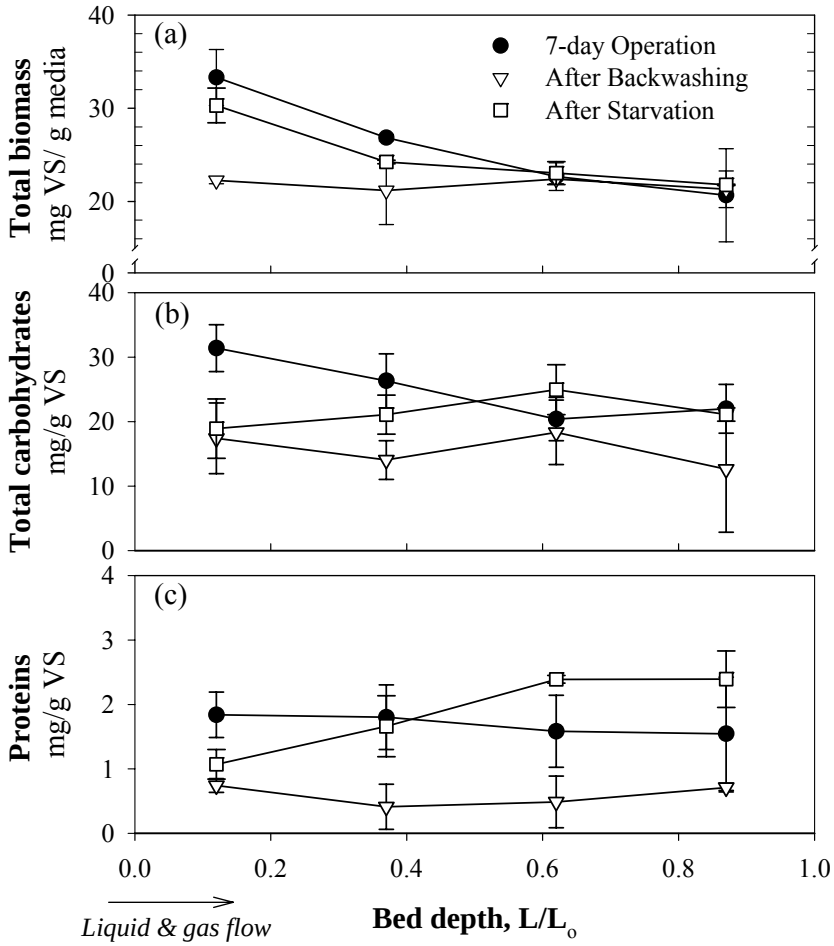

Figure 4-3 Biomass distribution as a function of the media depth: (a) Volatile solids as total biomass; (b) Total carbohydrates; (c) Proteins. The symbols represent the average experimental value and the error bars represent the standard deviation for the different cycles of each experimental strategy (L_o = 60 cm bed media depth).

4.4.4. CO_2 production during starvation

During starvation, CO_2 evolution as an estimate of the biological activity was explored (see Figure 4-4). In Figure 4-4a, the net CO_2 production rate (P_o) was plotted as a function of the sequential time of starvation. Figure 5a indicates that the net CO_2 evolution significantly decreased during the first 2 hours after shut down of toluene loading. A gradual decrease is noticed thereafter. This indicates that during starvation, mixed cultures experienced endogenous respiration and microbial activity was slowly exhausted. It is speculated that initially, easy biodegradable EPS was rapidly consumed and then microorganisms steadily lost their activity. The other possible explanation is that toluene adsorbed in biomass itself may be first consumed and then biodegradable EPS was gradually consumed.

Figure 4-4b shows the corresponding contribution to CO_2 production along the bed media. The percent CO_2 produced at a specific bed media depth is defined by the following equation:

$$\%\ CO_2\ produced_{i+1} = \frac{P_{i+1} - P_i}{P_o} \times 100 \qquad (4\text{-}6)$$

where, P_i, net carbon production rate at a sampling port (i) along bed media; P_{i+1}, net carbon production rate at a sampling port ($i+1$) along bed media; P_o, net carbon production rate in effluent gas.

Initially, approximately 32.5 % of the total CO_2 produced was detected up to 0.12 L_o of the bed media. The contribution in the top portion gradually decreased to approximately 21.6 % in 48 hours. Relatively, constant contribution was observed at bed depth of 0.37 L_o. In the case of the lower section of the biofilter (> 0.37 L_o), the contribution gradually increased from approximately 33 % to 47 %. This behavior correlates with the increase in EPS components along the bed media during starvation (see Figure 4-3). It is speculated that higher CO_2 production evolved from endogenous respiration. It is interesting to note that during the two days of starvation, the

microbial activity was not totally exhausted. This observation subsequently influenced the biofilter reacclimation to the original performance (see Figure 4-5). As seen in Figure 4-5, the response after substrate starvation was significantly different from that after backwashing. In case of starvation, the biomass retained in the system played a significant role in high removal efficiency of the substrate. This behavior would be due to initial adsorption of toluene on biomass. After that, vigorous microbial activity attributed to the biofilter recovery to high removal performance as compared to backwashing. The biofilter response after restart-up following starvation was not only affected by the amount of biomass and EPS materials, but also by the microbial activity that remained in the system.

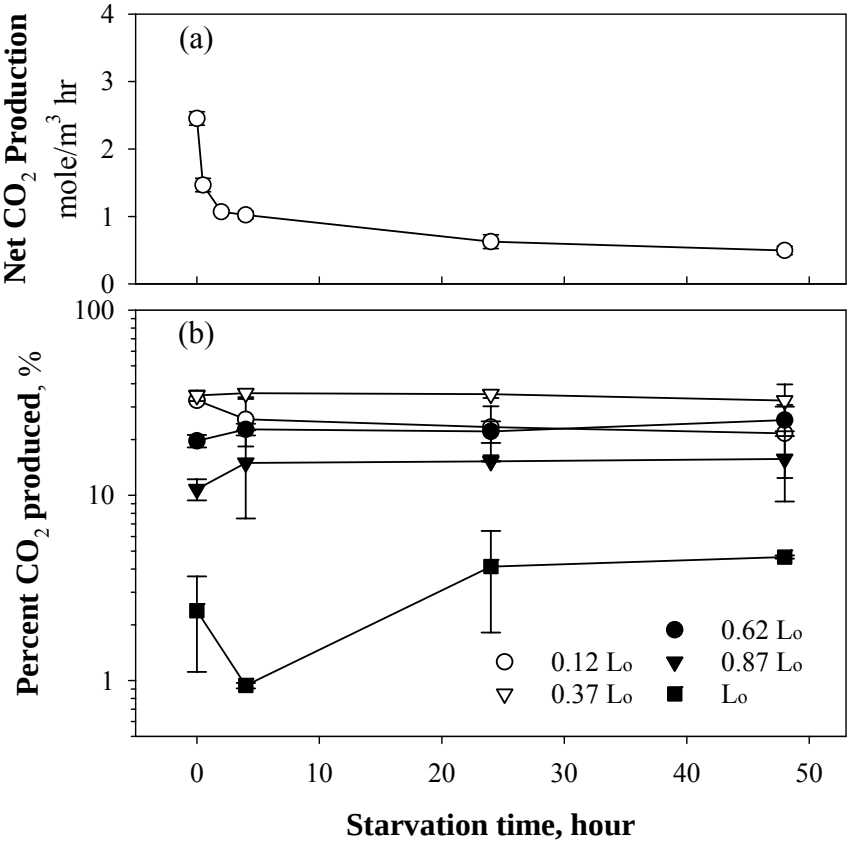

Figure 4-4 CO_2 production during starvation period: (a) CO_2 in effluent; (b) Percent Contribution to CO_2 production along the media depth. Gas and liquid flows were downward through the media (L_o = 60 cm bed media depth). The symbols represent the average experimental value and the error bars represent the relative error for two cycles

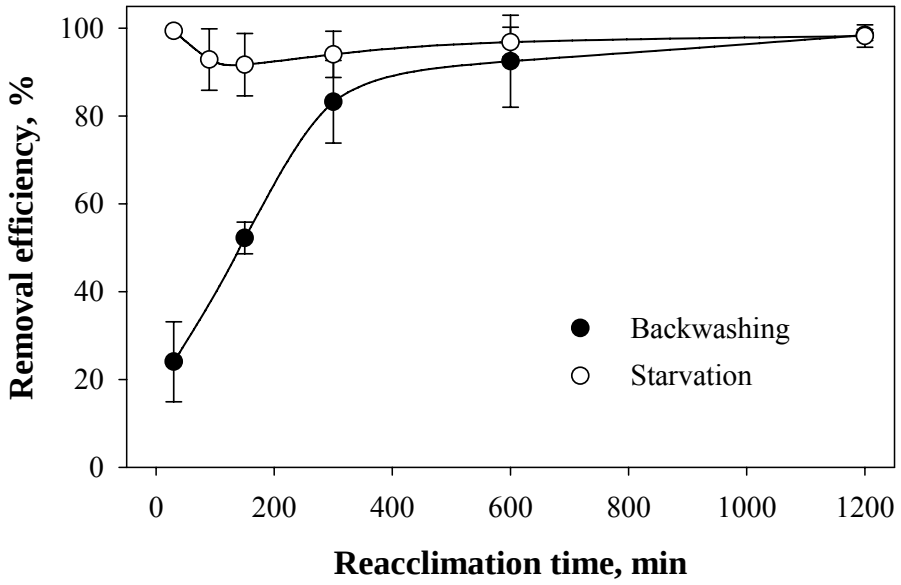

Figure 4-5 Biofilter response after the restart-up following backwashing and starvation: The symbols represent the average experimental value and the error bars represent the standard deviation for the different cycles of each experimental strategy

4.5. Conclusions

Biofilter performance was strongly affected by microbial activity and biomass distribution. Periodic backwashing was effective in inducing even spatial distribution of biomass along the bed media, achieving long-term stable efficient biofilter performance. Cell synthesis was preferable to substrate oxidation in order to maintain sufficient biomass amount in the system. However, substrate oxidation became predominant in the whole biofilter bed with time due to local nutrient and substrate limitation in deep biofilm.

The substrate starvation condition influenced the decrease in the total biomass along the bed media, suggesting that starvation can be considered as another means of biomass control in case of low organic loadings. The presence of sufficient biomass and microbial activity played important role in biofilter reacclimation when biofilter was exposed to starvation conditions.

4.6. References

APHA/AWWA/APCF. (1998). Standard methods for the examination of water and wastewater, American Public Health Association/American Water Works Association/Water Pollution Control Federation, Washington, D.C.

Cherry, R. S., and Thompson, D. N. (1997). "Shift from growth to nutrient-limited maintenance kinetics during biofilter acclimation." Biotechnology and Bioengineering, 56(3), 330-339.

Cox, H. H. J., and Deshusses, M. A. (2002). "Effect of starvation on the performance and re-acclimation of biotrickling filters for air pollution control." Environmental Science & Technology, 36(14), 3069-3073.

Daniels, L., Hanson, R. S., and Phillips, J. A. (1994). "Chemical analysis." Methods for general and molecular bacteriology, P. Gerhardt, ed., American Society for Microbiology, Washington, D.C. :, 512-553.

Delhomenie, M. C., Bibeau, L., Gendron, J., Brzezinski, R., and Heitz, M. (2003). "A study of clogging in a biofilter treating toluene vapors." Chemical Engineering Journal, 94(3), 211-222.

Devinny, J. S., Deshusses, M. A., and Webster, T. S. (1996). Biofiltration for air pollution control, Lewis Publishers, Boca Raton, FL.

du Plessis, C. A., Kinney, K. A., Schroeder, E. D., Chang, D. P. Y., and Scow, K. M. (1998). "Denitrification and nitric oxide reduction in an aerobic toluene-treating biofilter." Biotechnology and Bioengineering, 58(4), 408-415.

Hwang, S. J., and Tang, H. M. (1997). "Kinetic behavior of the toluene biofiltration process." Journal Of The Air & Waste Management Association, 47(6), 664-673.

Iliuta, I., and Larachi, F. (2004). "Transient biofilter aerodynamics and clogging for VOC degradation." Chemical Engineering Science, 59(16), 3293-3302.

Kim, D., Cai, Z., and Sorial, G. A. (2005a). "Behavior of trickle bed air biofilter for toluene removal: effect of non-use periods." Environmental Progress, 24(2), 155-161.

Kim, D., Cai, Z., and Sorial, G. A. (2005b). "Evaluation of trickle bed air biofilter performance under periodic stressed operating conditions as a function of styrene loading." Journal of the Air & Waste Management Association, 55(2), 200-209.

Kim, D., Cai, Z., and Sorial, G. A. (2005c). "Impact of interchanging VOCs on the performance of trickle bed air biofilter." Chemical Engineering Journal, 113(2-3), 153-160.

Konopka, A., Zakharova, T., and Nakatsu, C. (2002). "Effect of starvation length upon microbial activity in a biomass recycle reactor." Journal of Industrial Microbiology & Biotechnology, 29(5), 286-291.

Lobos, J., Wisniewski, C., Heran, M., and Grasmick, A. (2005). "Effects of starvation conditions on biomass behaviour for minimization of sludge production in membrane bioreactors." Water Science and Technology, 51(6-7), 35-44.

Martin, F. J., and Loehr, R. C. (1996). "Effect of periods of non-use on biofilter performance." Journal of the Air & Waste Management Association, 46(6), 539-546.

Metris, A., Gerrard, A. M., Cumming, R. H., Weigner, P., and Paca, J. (2001). "Modelling shock loadings and starvation in the biofiltration of toluene and xylene." Journal of Chemical Technology and Biotechnology, 76(6), 565-572.

Rittmann, B. E., and McCarty, P. L. (2001). Environmental biotechnology : principles and applications, McGraw-Hill, Boston :.

Smith, F. L., Sorial, G. A., Suidan, M. T., Biswas, P., and Brenner, R. C. (2002). "Development and demonstration of an explicit lumped-parameter biofilter model and design equation incorporating Monod kinetics." Journal of the Air & Waste Management Association, 52(2), 208-219.

Smith, F. L., Sorial, G. A., Suidan, M. T., Breen, A. W., Biswas, P., and Brenner, R. C. (1996). "Development of two biomass control strategies for extended, stable operation of highly efficient biofilters with high toluene loadings." Environmental Science & Technology, 30(5), 1744-1751.

Song, J. H., and Kinney, K. A. (2000). "Effect of vapor-phase bioreactor operation on biomass accumulation, distribution, and activity: Linking biofilm properties to bioreactor performance." Biotechnology and Bioengineering, 68(5), 508-516.

Sorial, G. A., Smith, F. L., Suidan, M. T., Pandit, A., Biswas, P., and Brenner, R. C. (1998). "Evaluation of trickle-bed air biofilter performance for styrene removal." Water Research, 32(5), 1593-1603.

Trulear, M. G., and Characklis, W. G. (1982). "Dynamics of biofilm processes." Journal Water Pollution Control Federation, 54(9), 1288-1301.

Weber, F. J., and Hartmans, S. (1996). "Prevention of clogging in a biological trickle-bed reactor removing toluene from contaminated air." Biotechnology and Bioengineering, 50(1), 91-97.

Zhang, X. Q., and Bishop, P. L. (2003). "Biodegradability of biofilm extracellular polymeric substances." Chemosphere, 50(1), 63-69.

Zhu, X. Q., Alonso, C., Suidan, M. T., Cao, H. W., Kim, B. J., and Kim, B. R. (1998). "The effect of liquid phase on VOC removal in trickle-bed biofilters." Water Science and Technology, 38(3), 315-322.

Zhu, X. Q., Suidan, M. T., Pruden, A., Yang, C. P., Alonso, C., Kim, B. J., and Kim, B. R. (2004). "Effect of substrate Henry's constant on biofilter performance." Journal of the Air & Waste Management Association, 54(4), 409-418.

CHAPTER 5

ADSORPTION ISOTHERM

5.1. Abstract

Gas phase adsorption of toluene, methyl ethyl ketone (MEK), and methyl isobutyl ketone (MIBK) on two types of activated carbons, BPL – bituminous base and OVC – coconut base, were investigated in this study. Single and ternary adsorption isotherms were determined by employing a simple constant volume method, which was utilized by using Tedlar gas sampling bags as a constant volume batch reactor. For the single solute adsorption, Freundlich and Myers adsorption equations were found to adequately correlate the experimental adsorption data. The pore size distribution of adsorbents was found to affect their adsorption capacities; its effect was dependant on the solute concentration. The ternary adsorption experimental isotherms were accurately predicted by using the well-known model, i.e., ideal adsorbed solution theory (IAST).

5.2. Introduction

Adsorbents have been widely used for removing organic contaminants from the environment – air, water, and wastewater (Chiang et al. 2001; Lordgooei and Kim 2004; Monneyron et al. 2003). Activated carbon has long been recognized as one of the most versatile adsorbents due to its high porosity and the resulting high surface area (Prakash et al. 1994; Yang 2003). The performance of the adsorption process is strongly affected by both the adsorbent and adsorbate characteristics. Fundamental studies of adsorption have long been the objectives of many researchers (Chiang et al. 2001; Lordgooei and Kim 2004; Prakash et al. 1994; Yang 2003).

The design and efficient operation of an adsorption process require beforehand the adsorption capacity, which is often obtained from experimental isotherm data (Allen et al. 2004;

Chiang et al. 2001; Nirmalakhandan and Speece 1993). Experimental methods for obtaining the gas phase equilibrium isotherm data can be divided into three categories: dynamic adsorption column method (Lin et al. 1996); gravimetric method (Cal et al. 1997; Paulsen and Cannon 1999; Ramirez et al. 2004); and constant volume method (Brosillon et al. 2001; Golden and Sircar 1994; Monneyron et al. 2003). By using the dynamic adsorption column, one can obtain adsorption equilibrium derived fundamentally from mass balances around the adsorption bed. However, its prediction is complicated because kinetics concepts (e.g., film diffusion, surface diffusion, and pore diffusion) should be also incorporated into the mass balances (Sontheimer et al. 1988). In an adsorption fixed column test, Lin et al. (1996) predicted adsorption isotherms from kinetic adsorption/desorption experiments. They then compared the adsorption isotherm predictions to experimental data based on a micro gravimetric balance and column experiments. Higher predictive errors (5% on average with a maximum of 13%) were obtained for adsorption capacity measured in the column experiments while excellent agreement (less than 4%) was obtained from the gravimetric method. It is worthwhile noting that the gravimetric method using an electrobalance is typically designed only for single solute adsorption. Given the above limitation, further measurements are required for multi-component adsorption. Cal et al. (1997) tested mixture-component adsorption by using the gravimetric balance to measure the total mass adsorbed and a multi-ported hang-down tube for gas sampling at the inlet and the outlet. Even if one expects relatively accurate adsorption isotherm data by the gravimetric method, this method requires complicated experimental equipment which is rather expensive. The third adsorption isotherm determination is the constant volume method. This method is commonly used for obtaining adsorption isotherms for single solute and multi-component solute (Monneyron et al. 2003). A batch reactor is employed and calculations procedures are relatively simple.

The adsorption isotherm approach presented in this study is a simple constant volume method utilized by using Tedlar gas sampling bags as a constant volume batch reactor. Gas phase adsorption isotherms for both the single solute and multi-component solute were determined. For this purpose, two different activated carbons, i.e., bituminuous based BPL and coconut based OVC, were tested for three single solutes, namely, toluene, methyl ethyl ketone (MEK), and methyl isobutyl ketone (MIBK) and their ternary mixture. The ternary adsorption experimental isotherm data were verified against the well-known model in predicting the multi-component adsorption, i.e., ideal adsorbed solution theory (IAST) that was originally developed by (Myers and Prausnitz 1965). Furthermore, the pore size distribution of the adsorbents was evaluated to assess its effects on the adsorption capacities for the solutes of concern

5.3. Materials and Methods

5.3.1. Adsorbate

Three commercially available volatile organic compounds, toluene, MEK, and MIBK (Fisher Scientific, Fair Lawn, NJ) were used as single solutes and as three-component mixtures. The properties of these adsorbates are summarized in Table 5-1.

Table 5-1 Adsorbates main characteristics

	Toluene	MEK	MIBK
Formula	C_7H_8	C_4H_8O	$C_6H_{12}O$
Molecular weight, g/mol	92.14	72.11	100.16
Molar volume, 25°C (cm^3/mol)	106.87	90.1	125.81
Kinetic diameter, Å	5.8	5.2	7.35
Vapor pressure, 25°C (kPa)	3.79	12.6	2.0
Dipolar moment, 3.162×10^{-25} $(J\ m^3)^{1/2}$	0.4	3.3	2.8

5.3.2. Adsorbent

Two kinds of activated carbon, Bituminous based BPL and Coconut based OVC (Calgon Carbon Corporation, Pittsburgh, PA), were used for this study. These adsorbents will be referred to as BPL and OVC in this manuscript. Prior to use in the study, the adsorbents were dried in an oven at 110 ^{o}C for two days to remove any moisture present and then stored in a desiccator until use. The physical properties of adsorbents are listed in Table 5-2.

Table 5-2 Physical characteristics of adsorbents used in this study (Calgon carbon corporation)

	BPL	OVC
Surface area, m^2/g	1050-1150	1150-1250
Bulk density, g/cm^3	0.48	0.44
Particle density, g/cm^3	0.85	0.85
Pore volume, cm^3/g	0.80	0.72

5.3.3. Isotherm Procedure

The adsorption isotherms that relate the concentration of volatile organic compounds (VOCs) in the adsorbed state versus its gas phase concentrations were determined by using the constant volume method. Each isotherm point was obtained by using a "Gas Sampling Bag", which is a ten liter Tedlar gas sample bag (SKC inc., Eighty Four, PA). Each bag has two ports. One is used for pumping air/gas and the other port, which has a threaded cap with septa, is used to insert the adsorbent and later for sampling purposes. Different masses of the adsorbents were carefully weighed to the nearest 0.1 mg and placed inside each bag through the port provided. Masses of the adsorbents ranged from 4 to 50 mg per bag for the single-solute isotherms and the ternary systems. Each bag was then filled accurately with 6 liters of hydrocarbon-free and moisture-free compressed air by using a calibrated 6-liter canister, which can withstand pressure up to 10 atm. At a pressure of 1 atmosphere, this canister contains an air volume of 6 L. When

more air was allowed into the canister until a 2 atmospheres pressure was reached at the same temperature, the canister would hold an air volume of 12 L. The pressure inside the canister was recorded by a digital pressure gauge (Cole parmer, Vernon Hills, IL). When the outlet valve of the canister, which was connected to the exhaust port of the bag, is opened it allowed the air to expand until a final pressure of 1 atmosphere was reached. Therefore, an air volume of 6 L was embodied in each isotherm bag. To obtain the desired initial concentration in the bag, a known volume of gaseous VOC was injected into the bag (through the septum) by use of a gas-tight syringe (VICI Precision Sampling, Inc.) with a side-port needle, which lead to an intial concentration of 3.0 to 15.0 mmol/m^3 for each set of the single solute isotherm and 0.8 to 5.5 mmol/m^3 for the ternary adsorption. The quantity of VOC injected depended on the initial gas-phase concentration desired in the bag. The gaseous VOC was prepared by injecting pre-calculated volume of liquid VOC (0.3 to 1.5 mL) into a 6 L air inside another bag. The initial concentration combinations for determining the experimental adsorption isotherms are summarized in Table 5-3.

For each set of single solute isotherm, three different initial concentrations were considered in order to ensure true equilibration had been attained. For ternary adsorption, two different compositions of multi-component VOC were considered. One was defined from U.S. Environmental Protection Agency (EPA) Toxic Release Inventories (TRIs) (1998-2001). The approximate molar ratio of the mixture was assumed to be 6:3:1 (toluene: MEK: MIBK). The other was equal-molar ratio of each component.

Each set of bags under study was accompanied by blank bags (without any adsorbent) that contained the same initial VOC concentration that was used in the isotherm bags. These procedural blanks served to quantify adsorption of VOC due to the bag alone. All of the bags were equilibrated in a room that has a constant temperature of 20±1 °C. After a one-hour

equilibration period, the blank bags were sampled and analyzed. The measured values were recognized as the initial concentration for each set of bags. Through initial testing, it was found that six days were enough for attaining equilibrium. Gas samples were taken and analyzed to determine the equilibrium gas phase concentrations of VOCs on day 7. The bags were turned over every day to ensure proper contact of the adsorbent with the VOC. The percent loss of VOCs in the blank bags after an equilibration period of six days were 23.1±1.6, 13.0±1.6, and 8.4±1.8 for toluene, MEK, and MIBK, respectively. In an evaluation test of Tedlar bags conducted by Wang et al. (1996), it was demonstrated that the losses of the VOCs were mostly due to sorption losses to the bag alone. Therefore, the obtained isotherm data were compensated for the loss of VOCs due to adsorption on the bags surface. In this study, the percentage VOC loss was independent on the initial concentration of VOC and the type of adsorbent.

Table 5-3 Initial concentration combination for the adsorption isotherms

Isotherm set	Adsorbate	Adsorbent	Initial concentration ($mmol/m^3$)		
	Single solute adsorption				
Run no. 1	Toluene	BPL	8.75	6.65	3.01
Run no. 2	Toluene	OVC	11.43	6.65	3.68
Run no. 3	MEK	BPL	15.00	7.59	3.26
Run no. 4	MEK	OVC	14.54	7.89	3.26
Run no. 5	MIBK	BPL	13.68	6.2	2.91
Run no. 6	MIBK	OVC	10.95	6.94	3.85
	Ternary adsorption				
Run no. 7	Toluene	BPL	5.48		
(Combination 1)	MEK	BPL	2.56		
	MIBK	BPL	0.84		
Run no. 8	Toluene	BPL	2.90		
(Combination 2)	MEK	BPL	3.10		
	MIBK	BPL	2.90		

5.3.4. Analytical Procedure

The determination of the adsorbate concentrations in the gas phase was made by a GC equipped with FID. Details about GC analysis are found in Appendix III. Tristar 3000 (Micromeritics, Norcross, GA) was used to investigate the pore size distribution, using liquid nitrogen adsorption and desorption isotherms. The samples were purged with nitrogen gas for 2 hours at 150°C using Flow prep 060 (Micromeritics, Norcross, GA).

5.3.5. Theoretical Models

Single Solute Adsorption Isotherm: The Freundlich equation and Myers isotherm equation Sorial et al., (1993) were used for correlating the experimental isotherm data. The Freundlich isotherm equation is represented by

$$q_{e,i} = k_i \cdot C_{e,i}^{1/n_i} \qquad (5\text{-}1)$$

where, k_i and $1/n_i$ are regression parameters; $C_{e,i}$ is equilibrium adsorbate concentration in the gas phase; $q_{e,i}$ is adsorbate concentration adsorbed on the adsorbent.

The gas phase concentration, $C_{e,i}$, was determined by gas chromatograph and the loading, $q_{e,i}$, was calculated from a mass balance on each isotherm bag by using the following equation

$$q_{e,i} = \frac{(C_{o,i} - C_{e,i}) \cdot V}{m} \qquad (5\text{-}2)$$

where, $C_{o,i}$ is initial gas phase concentration of solute i; m is the mass of adsorbent; The adsorbate volume represented by V is 6 L.

The drawback of using the Freundlich equation is that it does not follow Henry's law equation at low coverage. This criterion is very important when predicting the multicomponent

adsorption data by IAST because the model utilizes the Gibbs adsorption equation that requires isotherm data at low coverage.

The experimental adsorption isotherm data were plotted on logarithmic plots (see Figure 5-1, e.g., MEK adsorption on OVC), the regressed adsorption isotherm was then developed and the experimental data were validated by using the 99 % confidence interval (SigmaPlot 9.0, Systat Software, Inc., 2004). The validated isotherm data were also correlated by the Myers isotherm equation which is presented by

$$C_{e,i} = \frac{q_{e,i}}{H_i} \cdot \exp(K_i q_{e,i}^{P_i}) \qquad (5\text{-}3)$$

where, H_i, K_i, and P_i are regression parameters.

The Myers isotherm equation has the property of satisfying Henry's law at low concentration. Thus, it is more suitable for multi-component computations than the Freundlich-type isotherm equation. Details about Myers isotherm equation can be found elsewhere (Lu and Sorial 2004; Sorial et al. 1993).

Ternary Adsorption Isotherm: If the adsorbed phase is thermodynamically ideal, the equilibrium relationship for an adsorbed mixture can be driven from the pure component isotherms. Based on this hypothesis, Myers and Prausnitz developed the IAST, to describe competitive adsorption for gas mixtures (Myers and Prausnitz 1965). The IAST basically utilizes three equations. One is the Raoult's law equivalence equation for an adsorption system, the other is the Gibbs adsorption equation, and the third is based on the assumption of an ideal adsorbed solution. A detailed description of the IAST equations can be found elsewhere (Lu and Sorial 2004; Sorial et al. 1993).

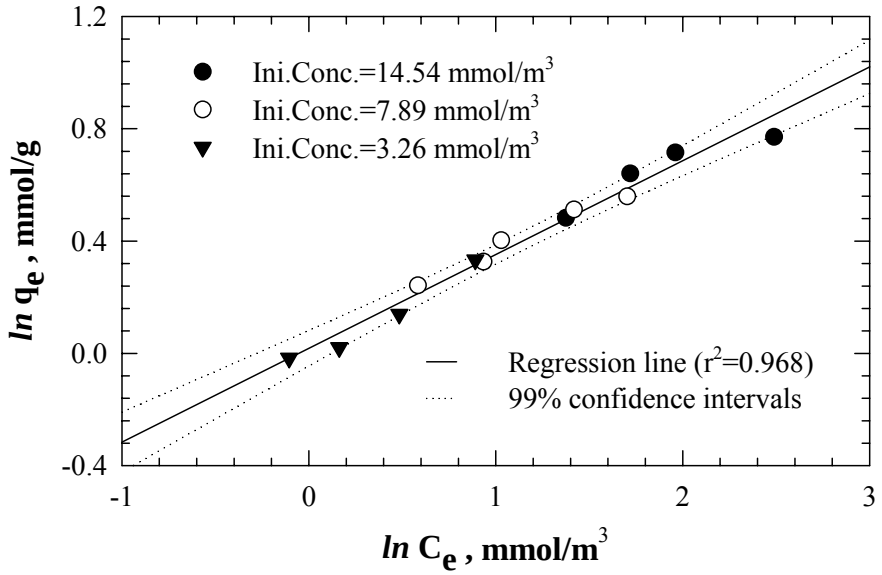

Figure 5-1 MEK adsorption on OVC

5.4. Results and Discussion

5.4.1. Single Solute Isotherm

Single solute gas phase adsorption isotherms for toluene, MEK, and MIBK, on two adsorbents, i.e., BPL and OVC, were investigated at the room temperature (20±1 ^{o}C). Three sets of different initial concentration for each isotherm were incorporated for checking the reliability of adsorption isotherm. Figure 5-1 represents the single solute adsorption of MEK on OVC adsorbent. Analysis of the data in Figure 5-1 reveals that the accuracy of adsorption isotherm was confirmed by using the three sets of initial concentration. The three sets of the experimental were within the 99 % confidence interval of the linear regression performed in a log-log scale. Similar results were obtained for the other solutes studied on the two adsorbents (data are not shown). The R square values for the linear regression (logarithmic Freundlich equation) are presented in Table 5-4.

For all the compounds studied, the isotherm curves obtained on BPL and OVC were typically type 1 according to International Union of Pure and Applied Chemistry (IUPAC) classification (1985). The single solute adsorption isotherms for the three adsorbates are given in Figure 5-2 together with the correlated isotherm models, i.e., Freundlich isotherm and Myers isotherm. The correlation of the experimental data to the two isotherm equations was done by using non-linear least square regression algorithm for minimizing the total relative error (Ramirez et al. 2004). The total relative error is defined by:

$$Total\ relative\ error\,(\%) = \frac{1}{N_I}\sum_{i=1}^{N_I}\left(\frac{1}{N_{T,i}}\sum_{j=1}^{N_{T,i}}\left[\frac{|\,q_m - q_e\,|}{q_e}\times 100\right]\right) \quad (5\text{-}4)$$

where q_m = modeled adsorbate concentration adsorbed on the adsorbent; q_e = experimental adsorbate concentration adsorbed on the adsorbent; N_T = number of data points; N_i = number of adsorption isotherms

The obtained results for both isotherm equations are presented in Table 5-4. It is seen from Table 5-4 that the total relative error was less than 10 % for all cases, implying good agreement between the model and the experimental data. The adsorption capacities of the two adsorbents increased with an increase in molecular weight, molar volume, and kinetic diameter of the adsorbates studied, but decreased with an increase in their vapor pressures (see Table 5-1).

Figure 5-3 shows the ratio of the adsorption capacities of the two adsorbents, (BPL/OVC), for the three adsorbates. The adsorbents capacities were compared by using the Freundlich predicted adsorbed phase concentration, q_e. It is seen from Figure 5-3 that as the equilibrium solute concentration was increased, BPL provided much higher adsorption capacity for MIBK, while it provided lower adsorption capacity for MEK. In case of toluene, BPL gave a slightly higher adsorption capacity. It is also interesting to observe that, at MIBK concentration of about 0.1 mmol/m^3 or below, the adsorption capacity of OVC was higher than BPL. The process of gas

phase adsorption is influenced by both the adsorbate properties and the adsorbents properties. The pore size distribution of the adsorbent strongly affects adsorption (Chiang et al. 2001; Lu and Sorial 2004). At high solute concentration, the activated carbon in which large pores predominate has higher capacity than those with predominant small pores. However, at low concentration, the large pore activated carbon has a lower capacity (Cheremisinoff and Ellerbusch 1978). Figure 5-4 clearly indicates that BPL has higher pore volume for the pore size diameters (2 - 200nm) as compared to OVC. This property is in accordance with the experimental data for toluene and MIBK. However, this result contradicted the observation of MEK adsorption. It is speculated that the abnormal phenomenon was caused by a strong dipolar moment as compared to the other adsorbates. In the physical adsorption, adsorption of gas molecules on activated carbon is also dominated by interaction potentials of adsorbate on the adsorbent surface: the van der Waals forces interaction; electrostatic interactions comprising polarization; dipole moment and quadrupole moment interaction (Ruthven 1984). For a gas molecule that has strong dipole moment, the adsorption of this gas molecule can be increased because the field dipole interaction term becomes significant (Yang 2003). This property may play a role in the adsorption potential of MEK within the smaller pore volume of OVC.

Table 5-4 Freundlich and Myers isotherm equations parameters for single solute system

		Freundlich Isotherm			
		K $(mmol/g)/(mmol/m^3)^{1/n}$	1/n	R^{2*}	TRE** %
Toluene	BPL	1.742	0.314	0.976	3.7
	OVC	1.542	0.272	0.961	2.8
MEK	BPL	0.756	0.298	0.971	3.1
	OVC	1.018	0.334	0.968	3.4
MIBK	BPL	2.824	0.241	0.927	9.2
	OVC	2.136	0.094	0.958	2.7
		Myers Isotherm			
		H m^3/g	K $(mmol/g)^{-p}$	P	TRE %
Toluene	BPL	2.474×10^5	10.722	0.181	3.8
	OVC	1.549×10^4	8.201	0.272	2.9
MEK	BPL	6.737×10^1	5.149	0.441	3.4
	OVC	4.483×10^3	8.379	0.219	3.3
MIBK	BPL	5.839×10^3	5.248	0.356	9.4
	OVC	2.583×10^5	6.504	0.775	2.8

* The R-square value in the linear regression

** Total relative error

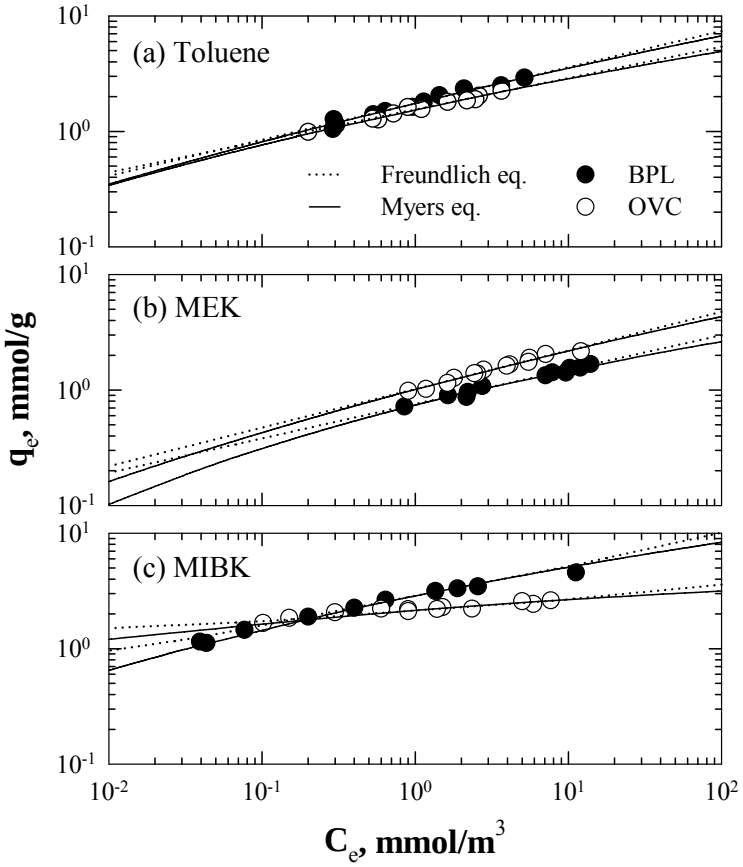

Figure 5-2 Adsorption isotherms for single solute system

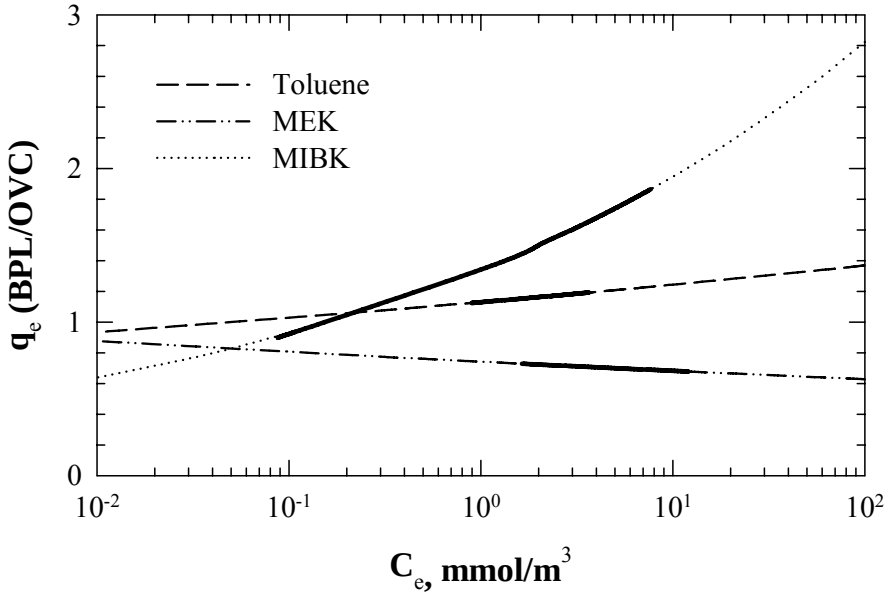

Figure 5-3 Comparison of activated carbon adsorption capacities for the three VOCs (Solid curves indicates the experimental observation for each solute).

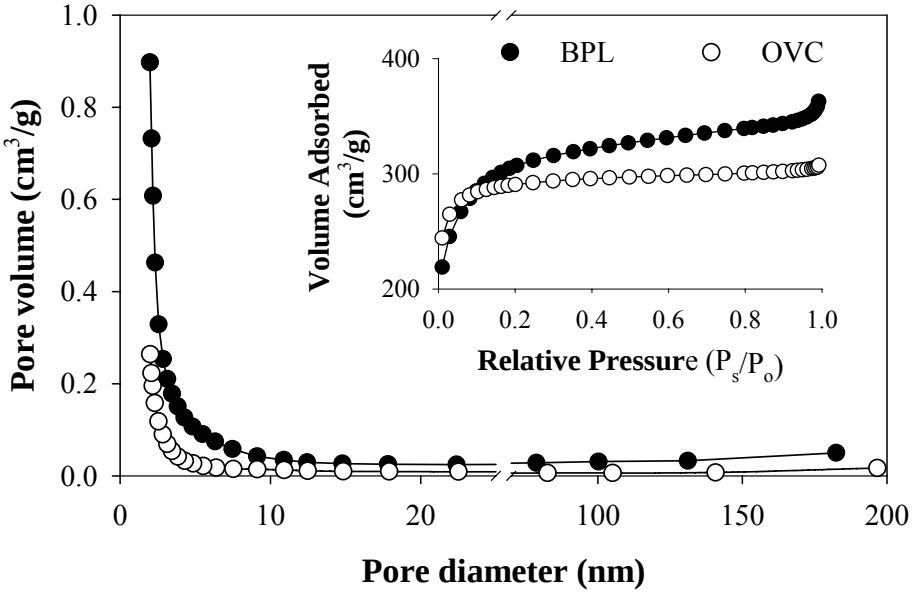

Figure 5-4 Pore size distribution of BPL and OVC

5.4.2. Ternary Isotherm

In this study, since toluene was the major component among VOCs of concern in the U.S. EPA TRIs (1998-2001) and since in the single solute isotherms BPL gave higher adsorption capacity for toluene than OVC in the range of concentration considered, BPL was hence chosen for the ternary adsorption. Sorial et al. (1993) demonstrated that the Freundlich equation represents well typical single solute adsorption data over a restricted range of concentration, but the IAST using the Freundlich equation showed high deviations from the experimental data. It is worthwhile noting that, at extremely low concentration the Freundlich equation does not satisfy Henry's law. Consequently, this will strongly influence the integration of the Gibbs adsorption equation in the IAST.

The IAST, using the Myers isotherm equation for correlating the single solute data, predicted reasonably well the two concentration combinations for the ternary system (see Figure 5-5). The TRE values for the ternary system are shown in the legend of Figure 4-5. It is worthwhile noting that, Smith (1991) observed that the predictive ability of the IAST was dependant on the solute concentration. However, in some studies conducted by Sorial et al. (1993) and Lu and Sorial (2004), high predictive ability of the IAST was revealed in the solute concentration range of 10 - 10^4 mmol/m^3. Considering the range of solute concentration (10^{-2} - 10 mmol/m^3) used in this study, Figure 5-5 together with the reported TRE values reveals the effectiveness of IAST predictions.

For single-solute isotherms, BPL activated carbon gave the lowest adsorption capacity for MEK as compared to toluene and MIBK. Figure 5-5 shows that MEK was outcompeted more at high concentrations by toluene and MIBK than at low concentration. This behavior is usually observed for the least competitive adsorbate in multi-component adsorption which is also well predicted by IAST. Factors that affect overall adsorption of multi-component adsorption include

the relative molecular size and configuration, the relative adsorptive affinities, and the relative concentrations of the solute (Ruthven 1984). Hence, competitive adsorption is most likely to occur since the available surface area of the activated carbon will be occupied, to varying degrees, by all the adsorbate components.

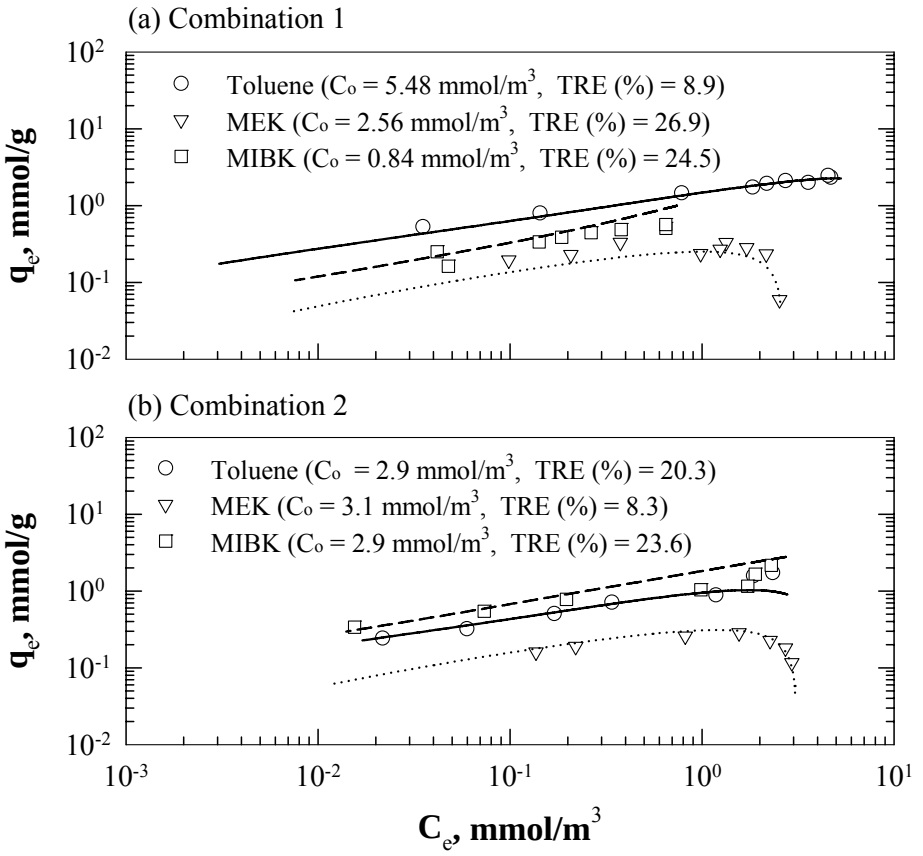

Figure 5-5 Ternary adsorption of toluene, MEK, and MIBK on BPL.
(IAST simulation curve: —— Toluene, ····· MEK, - - - - - - MIBK; TRE: total relative error (%))

5.5. Conclusions

Single and ternary solute gas phase adsorption isotherms were conducted in this study to evaluate the effectiveness of a simple constant volume method, which was utilized by using Tedlar gas sampling bags as a constant volume batch reactor. Three initial concentrations of the single solutes and two different combinations of the ternary system were evaluated in this study. The single solute adsorption isotherms based on the three initial concentrations of the adsorbates were adequately represented by both the Freundlich and the Myers isotherm equations. The total relative errors between the observed and the modeled data were less than 10 %. The adsorption capacity of bituminous base (BPL) and coconut base (OVC) activated carbons for the solutes studied was strongly dependent on the physical properties of the adsorbent and the adsorbate. The pore size distribution of the adsorbents was found to affect their adsorption capacities. Its effect was dependant on the solute concentration. The experimental results of the ternary systems for the two combinations studied were further confirmed by using the IAST. Accurate predictions of the IAST were achieved by using the Myers equation for correlating the single solute data.

5.6. References

Allen, S. J., McKay, G., and Porter, J. F. (2004). "Adsorption isotherm models for basic dye adsorption by peat in single and binary component systems." *Journal of Colloid and Interface Science*, 280(2), 322-333.

Brosillon, S., Manero, M. H., and Foussard, J. N. (2001). "Mass transfer in VOC adsorption on zeolite: Experimental and theoretical breakthrough curves." *Environmental Science & Technology*, 35(17), 3571-3575.

Cal, M. P., Rood, M. J., and Larson, S. M. (1997). "Gas phase adsorption of volatile organic compounds and water vapor on activated carbon cloth." *Energy & Fuels*, 11(2), 311-315.

Cheremisinoff, P. N., and Ellerbusch, F. (1978). *Carbon adsorption handbook*, Ann Arbor Science Publishers, Ann Arbor, MI.

Chiang, Y. C., Chaing, P. C., and Huang, C. P. (2001). "Effects of pore structure and temperature on VOC adsorption on activated carbon." *Carbon*, 39(4), 523-534.

Golden, T. C., and Sircar, S. (1994). "Gas adsorption on silicalite." *Journal of Colloid and Interface Science*, 162(1), 182-188.

Lin, T. F., Little, J. C., and Nazaroff, W. W. (1996). "Transport and sorption of organic gases in activated carbon." *Journal of Environmental Engineering-ASCE*, 122(3), 169-175.

Lordgooei, M., and Kim, M. S. (2004). "Modeling volatile organic compound sorption in activated carbon. I: Dynamics and single-component equilibrium." *Journal of Environmental Engineering-ASCE*, 130(3), 212-222.

Lu, Q. L., and Sorial, G. A. (2004). "Adsorption of phenolics on activated carbon - impact of pore size and molecular oxygen." *Chemosphere*, 55(5), 671-679.

Monneyron, P., Manero, M. H., and Foussard, J. N. (2003). "Measurement and modeling of single- and multi-component adsorption equilibria of VOC on high-silica zeolites." *Environmental Science & Technology*, 37(11), 2410-2414.

Myers, A. L., and Prausnitz, J. M. (1965). "Thermodynamics of mixed-gas adsorption." *J AIChE*, 11(1), 121-127.

Nirmalakhandan, N. N., and Speece, R. E. (1993). "Prediction of activated carbon adsorption capacities for organic vapors using quantitative structure-activity relationship methods." *Environmental Science & Technology*, 27(8), 1512-1516.

Paulsen, P. D., and Cannon, F. S. (1999). "Polytherm model for methylisobutylketone adsorption onto coconut-based granular activated carbon." *Carbon*, 37(2), 249-260.

Prakash, J., Nirmalakhandan, N., and Speece, R. E. (1994). "Prediction of activated carbon adsorption-isotherms for organic vapors." *Environmental Science & Technology*, 28(8), 1403-1409.

Ramirez, D., Sullivan, P. D., Rood, M. J., and Hay, K. J. (2004). "Equilibrium adsorption of phenol-, tire-, and coal-derived activated carbons for organic vapors." *Journal of Environmental Engineering-ASCE*, 130(3), 231-241.

Ruthven, D. M. (1984). *Principles of adsorption and adsorption processes*, A Wiley-Interscience publication, New York.

Smith, E. H. (1991). "Evaluation of multicomponent adsorption equilibria for organic mixtures onto activated carbon." *Water Research*, 25(2), 125-134.

Sontheimer, H., Crittenden, J. C., and Summers, R. S. (1988). *Activated carbon for water treatment*, DVGW-Forschungsstelle, Engler-Bunte- Institut, Universitat Karlsruhe (TH), Karlsruhe, Germany :.

Sorial, G. A., Suidan, M. T., Vidic, R. D., and Maloney, S. W. (1993). "Competitive adsorption of phenols on gac .1. Adsorption equilibrium." *Journal of Environmental Engineering-ASCE*, 119(6), 1026-1043.

Wang, Y., Raihala, T. S., Jackman, A. P., and StJohn, R. (1996). "Use of Tedlar bags in VOC testing and storage: Evidence of significant VOC losses." *Environmental Science & Technology*, 30(10), 3115-3117.

Yang, R. T. (2003). *Adsorbents: fundamentals and applications*, John Wiley & Sons, Inc., Hoboken, NJ.

CHAPTER 6

2-FIXED BED ADSORPTION

6.1. Abstract

2-step cycle of adsorption and desorption in a 2-bed adsorption unit was proposed to attenuate contaminant load fluctuation. Pore and surface diffusion model (PSDM) was used to predict adsorption and desorption profiles which can provide a design curve to estimate an operating parameter, i.e., EBRT for the adsorption bed. The adsorption system consisted of two fixed beds which are alternately pressurized and depressurized, in which a 2-step cycle, i.e., adsorption and desorption was simply achieved. The operating adsorption and desorption cycles for the adsorption system yielded constant loading conditions on the biofilter. This chapter also provided the operating conditions for the 2-bed adsorption unit.

6.2. Introduction

In this chapter, a two fixed beds adsorption system was proposed to yield consistent loading conditions on the biofilter. Basically, pore and surface diffusion model (PSDM) embedded in Adsorption Design Software (AdDesignS^{TM}) was used to predict the adsorption and desorption behavior. A simple procedure for two fixed beds adsorption design is presented in this chapter and then the effluent response to cyclic operation in the adsorption system was investigated.

Pore and surface diffusion model (PSDM) embedded in AdDesignS^{TM} software (Mertz et al. 1999) was used to predict the adsorption and desorption behavior in the adsorption system. The mechanisms incorporated in this model are: 1) Homogenous surface diffusion: This parameter is estimated by calibrating the desorption data. 2) Film transfer resistance at the adsorbent surface. 3) Advection dominates axial transport in bed. 4) Local equilibrium exists at the adsorbent

surface. For this study, adsorption equilibrium was described by the Freundlich equation where the Freundlich parameters were obtained through an isotherm study (see Chapter 5). The kinetic parameters, surface diffusion coefficient and film transfer coefficient were calculated by using empirical equation embedded in the software. Detailed methodology of the model is described in the manual of AdDesignS^{TM} software (Mertz et al. 1999).

6.3. 2-Bed Adsorption Concept

The 2-bed adsorption unit applied in this study was based on the concept of pressure swing adsorption (PSA). PSA is a very versatile technology for separation and purification for gas mixtures (Ruthven et al. 1994; Sircar 2002). It includes separate feeding (adsorption), depressurization, purging (desorption & regeneration) and repressurization steps. When the adsorption rate of solutes on adsorbent is hypothetically equal to their desorption rate, the concept of PSA would be simplified into a 2-step, i.e., feeding and purging. Figure 6-1 shows a typical two-bed with 2-step cycle for 2-bed adsorption unit in this study. Each step includes the feeding phase (adsorption) and the purging phase (desorption). The purging phase functions as regeneration. The only driving force necessary for contaminant desorption is the naturally occurring decrease in contaminant gas pressure imposed on the waste stream. The required design capacity for this unit (e.g., adsorption capacity of an adsorbent for an adsorbate) was mainly based on the results obtained in Chapter 5.

The net effect of the 2-bed adsorption unit is to flatten and reduce the VOC concentration in the treated air which makes it amenable for biofiltration. Through the 2-cycle operation, the 2-bed adsorption unit serves to buffer contaminant loading of the biofilter. The secondary effect of the 2-bed adsorption unit is that it can act as a polishing unit during the initial acclimation period of the biofilter. Furthermore, the 2-bed adsorption could serve as a feeding source for the biofilter

without any feeding phase when the biofilter is exposed to non-use periods as a shut down for factory retooling or equipment repair, or during weekends and holidays.

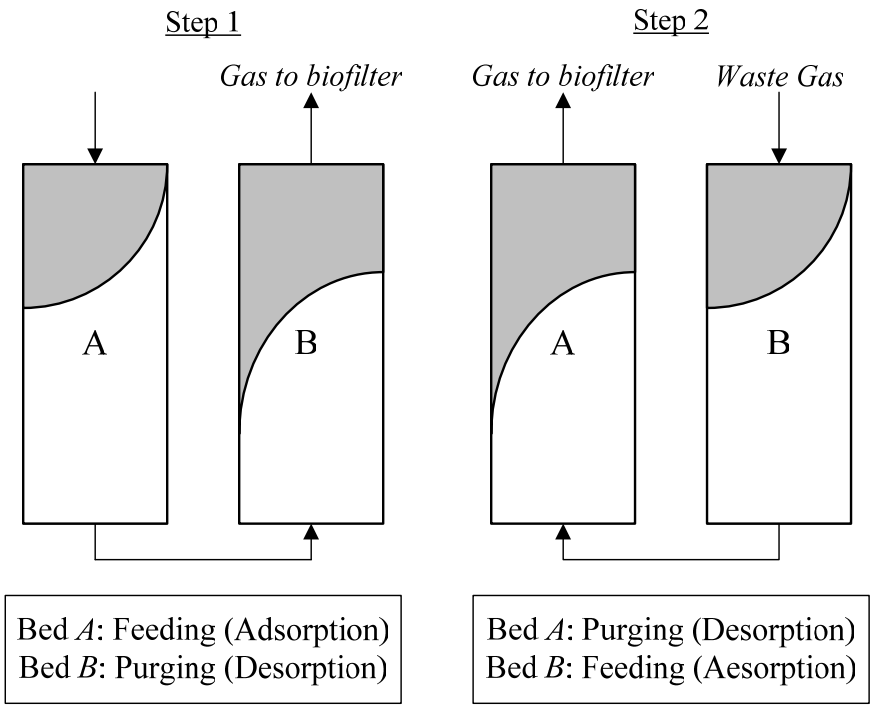

Figure 6-1 Two-bed with 2-step cycle for adsorption system

6.4. Materials and Methods

The schematic diagram of the 2-bed adsorption process is presented in Figure 6-2. The system was designed for operation in a 2-step cycle, i.e., feeding (adsorption) and purging (desorption) within two adsorption beds. The design methodology proposed by Moe and Li (2004) for determining EBRT was accepted in this study and is demonstrated in section 6.5. The employed EBRT for 2-bed adsorption unit was designed to be 5.6 sec (at air flow rate of 2.22 L/min). The total volume of the two cylindrical adsorption beds was 2.06×10^{-4} m^3. Each bed was constructed of stainless steel with an external diameter of 2.54 cm (1 inch) and a length of 20.3

cm (8 inch). The beds were packed with 165g of bituminous based BPL activated carbon (Calgon Carbon Co, apparent density = 0.85 g/mL). The selection of the adsorbent was discussed in Chapter 5.

The air supplied to the system was purified with complete removal of water, oil, carbon dioxide, VOCs, and particles by Balston FTIR purge gas generator (Paker Hannifin Corporation, Tewksbury, MA). Liquid VOC was injected via syringe pumps (Harvard Apparatus, model NP-70-2208, Holliston, MA) into the air stream where it vaporized, and entered the equalizing vessel before the system. To simulate transient loading conditions in the industry, a square wave change of toluene inlet concentration was considered as shown in Figure 6-3.

Cyclic operation was generated through an electrically operated 4-way solenoid valve (ASCO 8342G 701, Florham Park, NJ), which was controlled by an electronic timer (Digi 42A-120; GRASSLIN Controls Corp., Mahwah, NJ). The cycle duration was set at 8 hours which provided each bed to have 4-hour feeding and 4-hour purging. Sampling ports were installed for both the feed and exhaust gases. An additional air valve was installed to introduce the supplemental fresh air within two adsorption beds for reducing gas pressure in the other fixed bed where desorption occurs, if necessary.

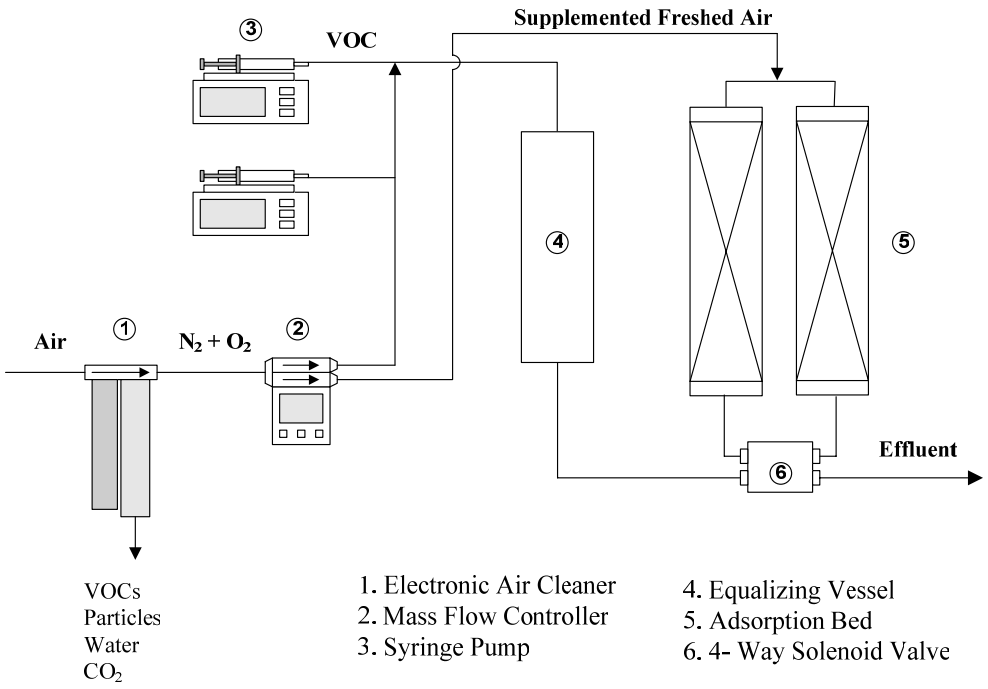

Figure 6-2 Schematic diagram for 2-bed adsorption experiment

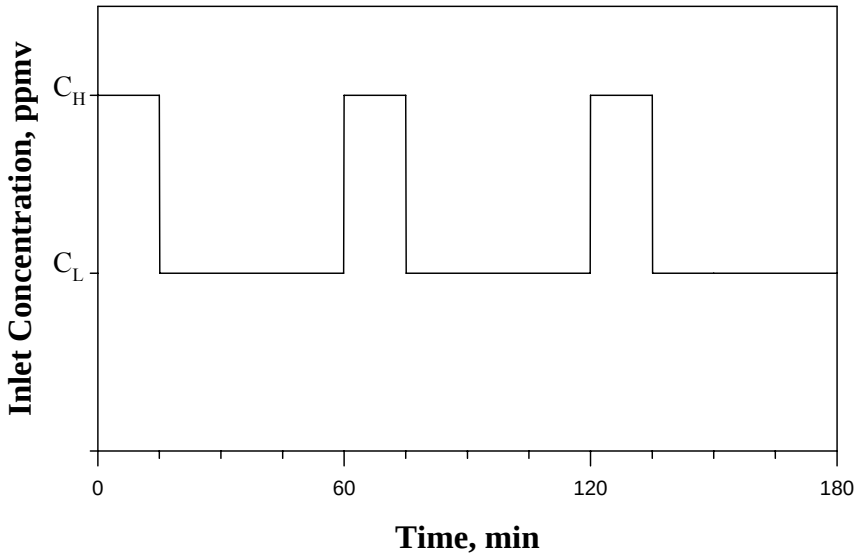

Figure 6-3 Theoretical feeding condition for a square wave change of inlet concentration (C_L=200 ppmv, C_H=400ppmv)

6.5. Results and Discussion

6.5.1. Determination of Dimension of Adsorption Bed

Pore and surface diffusion model (PSDM) was used to develop a design curve that can provide guidance in reactor sizing. This method was originally proposed by Moe and Li (2004) for determining the EBRT for a single bed of carbon column.

Simulations using the PSDM were performed by using AdDesignS^{TM} software under transient loading condition (see Figure 6-3). In the model simulation, the gas flow rate was set at 2.22 L/min. The corresponding EBRT of bed column ranged from 0.05 to 1.9 sec. A summary of model input parameters is presented in Appendix V. The design curve developed in this study is depicted in Figure 6-4. The data presented were obtained at quasi-steady state under the fluctuating loading condition defined. The data values indicate the ratios of the effluent concentration (as to maximum or minimum) to the inlet concentration with respect to employed EBRT.

It is shown in Figure 6-4 that the difference between normalized maximum and minimum effluent concentrations comes to be negligible as the EBRT increases. It is, therefore, determined that load equalization can be accomplished when the EBRT is designed at 0.6 sec or longer. For feasible fabrication and safety maintenance of the adsorption unit, the EBRT in the 2-bed adsorption was designed to be 5.6 sec (at air flow rate of 2.22 L/min) with corresponding total volume of two cylindrical beds of 2.06×10^{-4} m^3. It is therefore expected that a cycle of adsorption and desorption will be performed within each bed in the 2-bed adsorption unit.

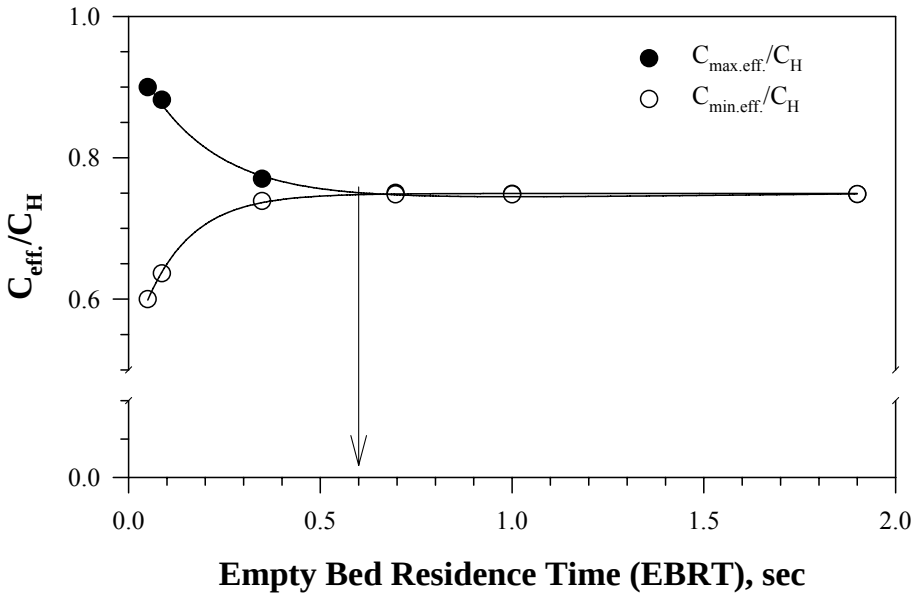

Figure 6-4 Design curve to determine operating EBRT in adsorption bed: Data were obtained at quasi-steady state under the fluctuating loading condition defined previously; $C_{max.eff.}$, maximum effluent concentration; $C_{min.eff.}$, minimum effluent concentration; C_H, Maximum inlet concentration

6.5.2. Adsorption and Desorption of 2-Bed Adsorption Unit

Adsorption and desorption of toluene vapors were studied in the 2-bed adsorption unit without utilizing the cyclic operation, i.e., conducted as if they were one adsorption bed. Figure 6-5 provides the data collected for both the adsorption and desorption cycles together with the simulation results obtained by using Adsorption Design Software (AdDesignSTM). It is seen from Figure 6-5 that both the adsorption and desorption experimental data agreed well with the simulated data. Furthermore, Figure 6-5 clearly shows that the desorption time was much longer than the breakthrough time. The long desorption time suggests that utilizing multiple adsorber beds with cyclic adsorption/desorption operation will be more effective than single beds.

Figure 6-6 represents desorption rate data collected from one adsorber bed with flow switching. The feed flow with time, T_f , was upward and the purging flow with time, T_p, was downward. The data were collected for T_f at 1, 2, 4, and 6 hr and T_p was varied in such a way to provide the ratio of T_f / T_p to be ranging between 0 and 1.0. Figure 6-6 indicates that the desorption rate apparently decreased as the purging time increased regardless of the different feeding times used. Furthermore, the desorption rate (R_D; mg/min) can be empirically expressed in term of the relative purge/feed time (R_t) as follows:

$$R_D = 1.538 + 0.468 e^{-2.892 R_t} \qquad (6\text{-}1)$$

Also R_D can be written as $d(M_D)/d(T_p)$, where M_D is the net mass desorbed during T_P. Integration of equation (1) gives:

$$M_D = 1.538 T_p - 0.162 T_f \left(e^{-2.892 T_p / T_f} - 1\right) \qquad (6\text{-}2)$$

where M_D is the net mass desorbed. It is worthwhile to note that the above equation is only valid when the adsorber bed is not exhausted. If the feed and purge times are identical then the net mass desorbed during the purging process is given by:

$$M_D = 1.691 T_p \qquad (6\text{-}3)$$

Hence, R_D is 1.691 mg/min, demonstrating that the desorption rate is independent on the cycle duration if the purging and feeding times are identical. Based on the results obtained, the operating conditions for 2-bed adsorption unit were defined in Table 6-1.

Figure 6-7 demonstrates effluent responses from a 2-bed adsorber unit with a cyclic adsorption/desorption operation and a non-cyclic single bed adsorption for square wave changes of toluene inlet concentration (see Figure 6-3). The data clearly indicate that the effluent from the 2-bed adsober was more attenuated below the critical inlet concentration (250 ppmv, determined in Chapter 3) to the biofilter. The effluent concentration was varying between 173±2 ppmv and

236±4 ppmv for the two bed adsorber unit. While for the single bed adsorber unit the effluent concentration was varying between 231±2 ppmv to 268±4 ppmv which is less amenable to effective biodegradation in the biofilter since the inlet concentration to the biofilter exceeded the critical value. Furthermore it is seen that for the 2-bed adsorption unit prior to steady state conditions, toluene was observed in the effluent just after 4 hrs whereas for a single bed adsorber unit more than 17 days were required before any breakthrough to occur which will provide a long non-use period for the biofilter and might highly impact the retention of microbial activities.

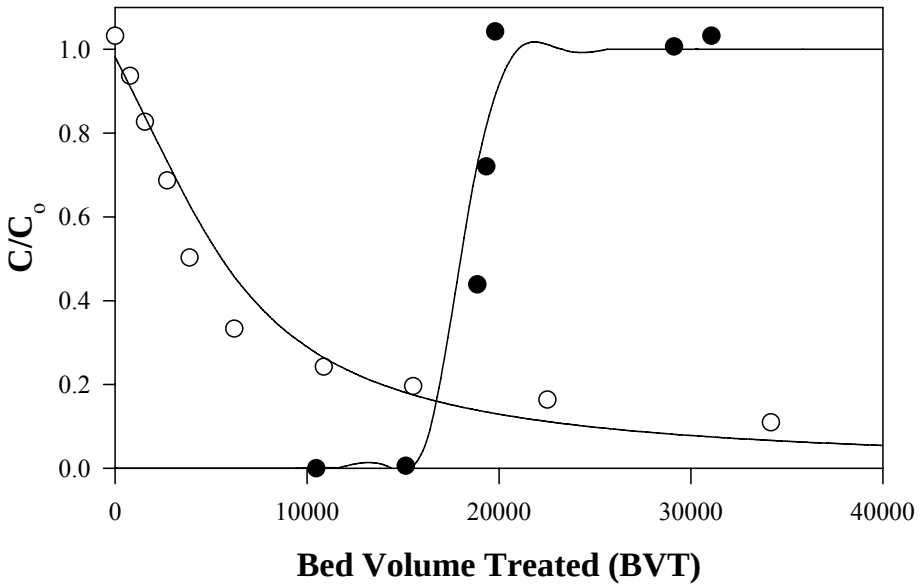

Figure 6-5 Adsorption and desorption profiles for non-cyclic operation in the adsorption process: Adsorption was conducted at consistent feeding of toluene concentration of 3000 ppmv at 4 L/min of air flow; the individual data were experimentally observed for adsorption and desorption; the data for solid line were obtained from the simulation by using AdDesignS^{TM}.

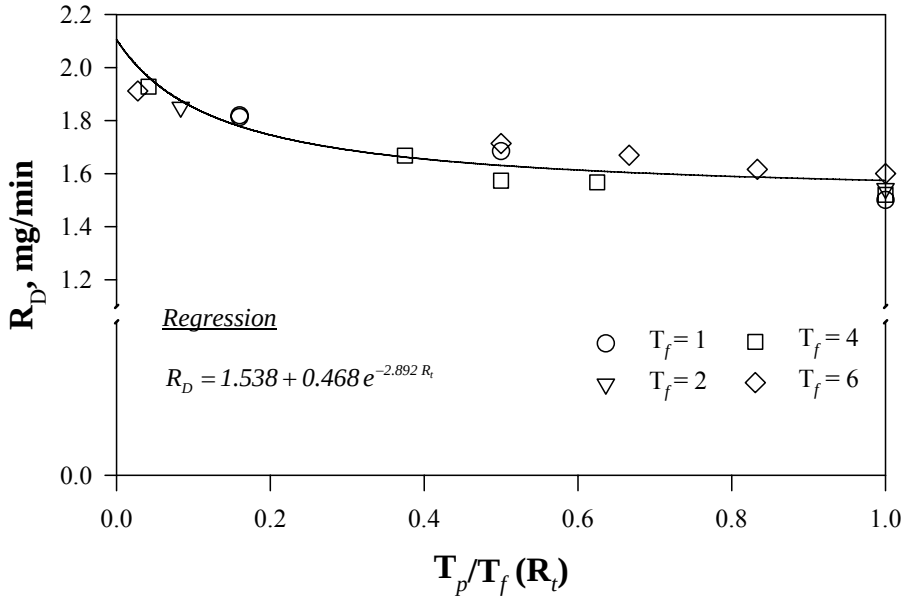

Figure 6-6 Desorption rates (R_D) during purging phase for cyclic operation as a function of a ration of purging time (T_p) to feeding time (T_f): Toluene feeding concentration was consistent 250 ppmv at 2.22 L/min of air flow.

Table 6-1 Operating conditions for 2-bed adsorption unit

Adsorbent	Bituminous based BPL activated carbon
Adsorbate	Toluene
Air flow, L/min	2.22[a]
Adsorber	2 beds
	1 inch (OD) × 8 inch (L) / bed
Duration of 2-step cycle for feeding (adsorption) and purging (desorption), hrs	
	8 (4/adsorption + 4/desorption, each bed)

[a.] determined from the setup value of air flow rate for the biofilter.

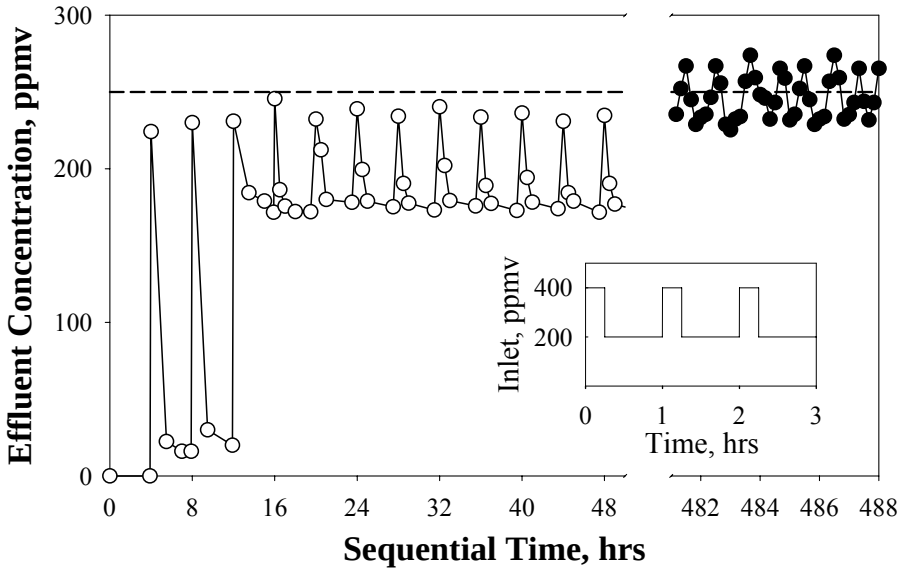

Figure 6-7 Effluent responses to cyclic operation and non-cyclic operation in 2-bed adsorption: Cyclic operation (○); non-cyclic operation (●); and the doted line indicates the critical inlet concentration (250 ppmv) to the biofilter at the employed EBRT of 1.23 min, which was determined in Chapter 3.

6.6. Conclusions

Pore and surface diffusion model (PSDM) was used to predict adsorption and desorption profiles, which can provide a design curve to estimate an operating parameter, i.e., EBRT. The adsorption system consisted of two fixed beds which are alternately pressurized and depressurized, in which a 2-step cycle, i.e., adsorption and desorption was simply achieved. The operating adsorption and desorption cycles for the adsorption system yielded constant loading conditions that can be treated effectively in a biofiltration.

6.7. References

Mertz, K. A., Gobin, D., Hand, D. W., Hokanson, D. R., and Crittenden, J. C. (1999). *Adsorption Design Software for Windows (AdDesignS^{TM})*, Michigan Technological University, Houghton, MI.

Moe, W. M., and Li, C. N. "A design methodology for activated carbon load dampening systems for biofilters treating intermittent VOC concentrations." 2004 *USC-CSC-TRG Conference on Biofiltration for Air Pollution Control*, Santa Monica, California, 89-96.

Ruthven, D. M., Farooq, S., and Knaebel, K. S. (1994). *Pressure swing adsorption*, VCH Publishers, Weinheim, New York.

Sircar, S. (2002). "Pressure swing adsorption." *Industrial & Engineering Chemistry Research*, 41(6), 1389-1392.

CHAPTER 7

INTEGRATED TREATMENT SCHEME OF A BIOFILTER AND A 2-FIXED BED ADSORPTION

7.1. Abstract

A 2-bed adsorption unit packed with granular activated carbon was installed in series before a biofilter. Toluene was tested to investigate the feasibility of adsorption and desroption cycle for stabilizing biofilter performance fluctuation. The results obtained revealed that the net effect of the 2-bed adsorption was an attenuation of the toluene concentration that makes it amenable for biofiltration. It was concluded in this study that the 2-step cycle in 2-bed adsorption could serve successfully as a polishing unit to abate the initial acclimation for the biofilter, a buffering unit to dampen the biofilter performance fluctuation during a square wave change of toluene inlet concentration, and a feeding source for the biofilter without any feeding phase when the biofilter is exposed to non-use periods. The results also demonstrated that the integrated treatment scheme compared to a stand alone biofilter attained a high biological activity for toluene biodegradation and an extended highly efficient operation for dynamic toluene loadings.

7.2. Introduction

In this chapter, a 2-fixed bed adsorption unit was integrated in series with a biofilter. The role of 2-step cycle of adsorption unit in biofilter performance was investigated. The experimental plan was, therefore, designed to evaluate the overall performance of an integrated process scheme consisting of a 2-adsorption unit followed by a biofilter under dynamic loadings of toluene. The results obtained were compared to that of a stand alone biofilter (control).

7.3. Materials and Methods

7.3.1. Experimental Setup

The experimental work was performed on two lab-scale reactors for controlling toluene as single contaminant. One system consisted of a 2-bed adsorption unit followed by a biofilter (hearafter named as integrated unit). The other system was a control unit, in which a biofilter was solely involved. The systems were maintained at a constant operating temperature of 20 ^{o}C in a constant temperature chamber. The experimental setup is shown in Figure 7-1.

The air supplied to the system was purified with complete removal of water, oil, carbon dioxide, VOCs, and particles by Balston FTIR purge gas generator (Paker Hannifin Corporation, Tewksbury, MA). The air flow to the system was set up at the rate of 2.22 L/min, regulated by a mass flow controller (MKS Model 247C four-channel read-out mass flow controller, Andover, Mass.). Liquid VOC was injected via syringe pumps (Harvard Apparatus, model NP-70-2208, Holliston, MA) into the air stream where it vaporized, and entered the equalizing vessel before it is evenly divided into the control unit and the integrated unit.

Details about the setup of adsorption unit are founded in Chapter 6, section 6.4. The biofilter setup was demonstrated in Chapter 2, section 2.3.1. The biofilters were seeded with an aerobic microbial culture pre-acclimating to toluene, which had been obtained form a previous operation of the biofilter (Kim et al. 2005b). The employed EBRT for each biofilter was 1.23 min. *In-situ* upflow backwashing was coordinated as biomass control strategy for removing excess biomass in the biofilter. Each biofilter was backwashed at a rate of one hour once a week. The details about the backwashing methodology are found in Chapter 2, section 2.3.5.

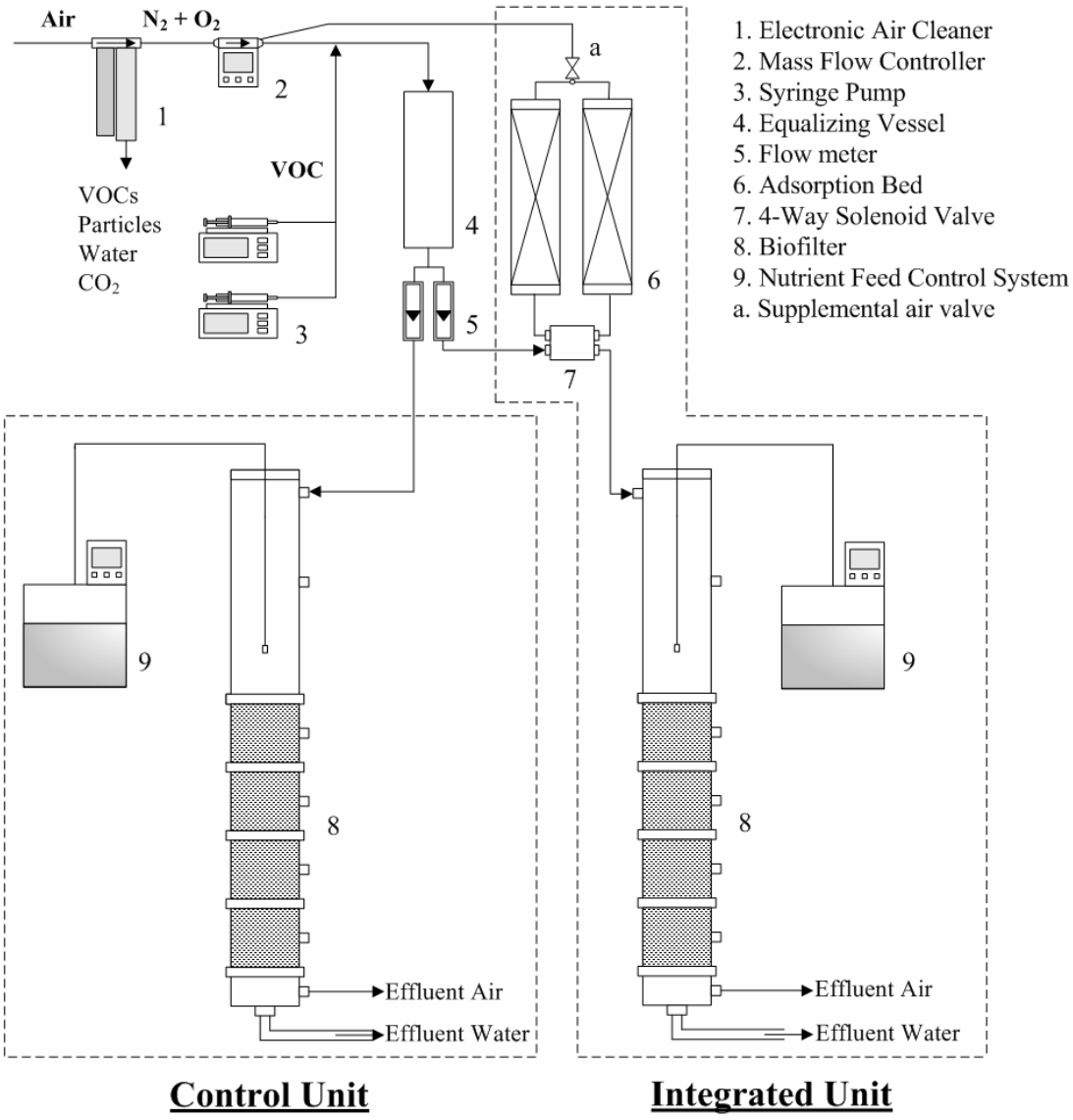

Figure 7-1 Schematic diagram for the experiment of the integrated treatment scheme of a biofilter preceded by a 2-fixed bed adsorption unit

7.3.2. Toluene Feeding Condition

Different types of square wave changes of inlet concentration were considered to simulate transient emission in the chemical industry (see Table 7-1). Two syringe pumps were used for this purpose. Syringe pumps were controlled by an electronic timer (Digi 42A-120; GRASSLIN Controls Corp., Mahwah, NJ). Basically, the average loading rate applied in the present study is subjected to the critical inlet loading of 3.52 kg COD/m^3·day (46.9 g/m^3·hr, corresponding inlet concentration of 250 ppmv at 2.22 L/min air flow) to the toluene biofilter determined in Chapter 3.

Table 7-1 Toluene feeding conditions of square wave change of inlet concentration

	Type A	Type B	Type C	Type D
Hourly average loading rate*, g/m^3·hr	46.9	46.9	56.3	65.9
Frequency of square wave per hour	1	1	1	2
Inlet concentration				
Peak concentration, ppmv	400	700	400	600, 400
Duration, min/hour	15	6	30	15, 15
Base concentration, ppmv	200	200	200	200
Mode of feeding**	C	C	C	D

* For Type A and B, an hourly average loading rate applied in the present study is subjected to the critical inlet loading (46.9 g/m^3·hr) to the toluene biofilter. Correspondingly, the critical inlet concentration to the toluene biofilter was found to be 250 ppmv at 2.22 L/min of air flow rate. Types C and D are designed to have higher loading rates compared with the critical loading.

** Daily continuous feeding (C); Daily discontinuous feeding (D): toluene loading interval = 10 hours/day, meaning 10-hour square wave change of toluene concentration followed by 14-hours starvation without toluene loading each day. During the 14-hour starvation, pure air and liquid continued to flow through the system as the same rate as during the loading period.

7.3.3. Analytical Methods

Gas phase samples for toluene analysis and CO_2 analysis were analyzed by using a gas chromatograph (GC) equipped with a flame ionization detector (FID) and a thermal conductivity detector (TCD), respectively. Liquid phase samples were analyzed for nitrate, total carbon (TC), inorganic carbon (IC), and volatile suspended solid (VSS) concentration. Nitrate was determined by using a Shimadzu UV mini 1240 UV-VIS spectrophotometer (Shimadzu Corp., Tokyo, Japan). TC and IC were determined by using a Shimadzu TOC 5000 analyzer (Shimadzu Corp., Tokyo, Japan). Details about analytical methods are summarized in Appendix III.

7.4. Results and Discussion

7.4.1. Toluene Removal Performance

The integrated unit and a stand alone biofilter serving as a control unit were initially operated under a square wave type 'A' feeding condition (see Table 7-1) for 48 days. The overall toluene removal efficiency and effluent concentration for the two units are provided in Figure 7-2 as logarithmic plots in order to compare them over a wide range of time. It is seen from Figure 7-2 that the integrated unit did not require any initial acclimation period for maintaining over 99 % removal while the control unit required more than 10 days (240 hours). This observation demonstrated the ability of the 2-bed adsoption unit to serve as a polishing unit during initial acclimation of the biofilter. This goal was achieved by abating toluene release from the adsorption unit. However, it is worthwhile to note that the integrated unit provided temporary drops to approximately 92 % removal efficiency after day 2. One possible explanation for this is that the base concentration exiting the adsorption unit increased suddenly after 12-hr operation (see Figure 6-7 in Chapter 6), which induced load fluctuation in the biofilter.

After the initial10 days of operation, the effluent concentrations from the integrated unit ranged from the detection limit of 0.5 ppmv to approximately 5 ppmv and the corresponding removal efficiencies were comparatively stable at the 99 % level with some temporary drops to about 97.5 %. The temporary drops in removal efficiency were mainly caused during acclimation after periodic media backwashing for biomass control. Immediately after backwashing, toluene removal efficiency dropped below 80 %, and then it recovered to the 99 % level in less than 10 hours. In contrast the control unit showed large fluctuations in the effluent during the same operational period. Frequent drops in removal efficiency below 90 % were observed consequent to the peak square wave concentration (400 ppmv) of toluene feeding.

Figure 7-3 shows a typical daily performance of both systems under a square wave type 'A' feeding condition. It is clearly seen from Figure 7-3 that the effluent performance of the integrated unit was apparently independent on the feed toluene loading. However, subsequent to cyclic operation in the 2-bed adsorption unit, temporary peaks of the effluent were seen with concentration below 5 ppmv. On the other hand, the control unit provided effluent performance strongly contingent on the feeding wave concentration.

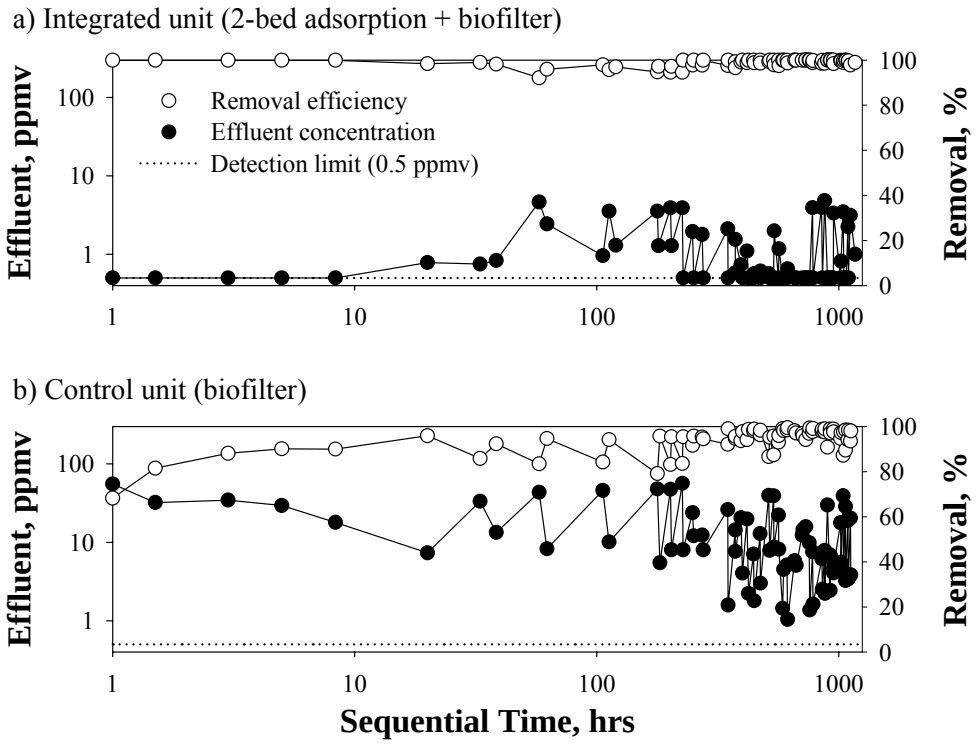

Figure 7-2 Overall toluene removal performance (feeding condition: Type A)

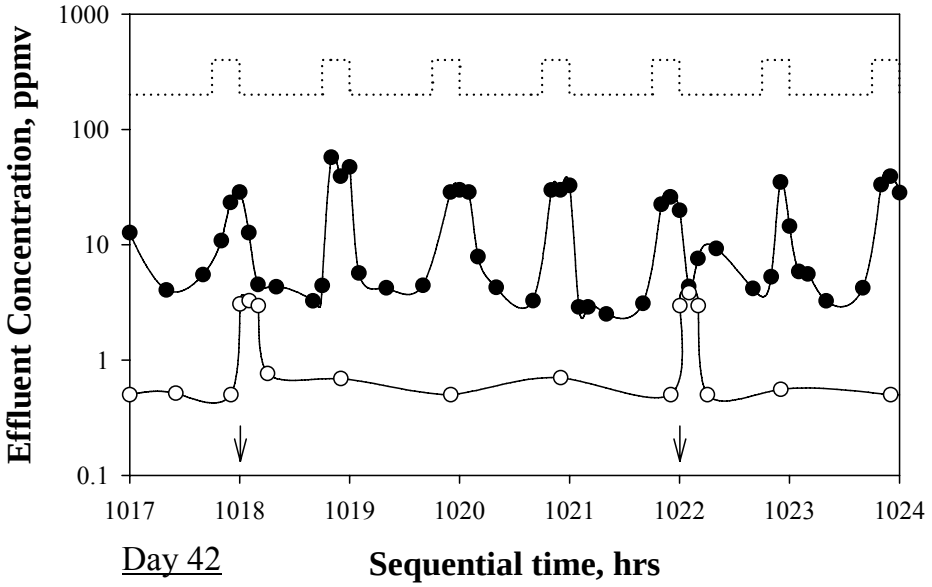

Figure 7-3 Effluent performance on Day 42 (feeding condition: Type A). A dotted line indicates the square wave changes of inlet concentration; effluent concentrations in control unit (●) and in integrated unit (○). Arrows indicate changes of air direction for cyclic operation in 2-bed adsorption.

7.4.2. Carbon Mass Balance

The cumulative carbon of toluene consumed (C_{inlet}) in both systems (integrated and control unit) was compared to the cumulative carbon produced (C_{outlet}) within the biofilter during the experimental period for the feeding square wave condition type 'A'. It is seen from Figure 7-4 that the carbon recovery in the control unit was 97.4 %, which is reasonably good within the experimental accuracy, while the carbon recovery in the integrated unit was 81.4 %. This indicates that the difference between the integrated unit and the control unit resulted from the accumulation of toluene in the adsorption beds, which is estimated to be 23.525 g toluene (11.17 mole C of inlet toluene for 48 days × 16 % (difference in carbon recovery between the two units)). The theoretical toluene adsorption capacity on BPL activated carbon used in the present study is 0.335 g toluene/g activated carbon (as observed in Chapter 5). Thus, the toluene holding capacity in the 2-bed adsorption unit with 165 g of adsorbent is 55.275 g toluene. It is, therefore, interesting to note that adsorption beds were adsorbing 42.6 % of the theoretical toluene holding capacity during the experimental period. On the other hand, the accumulation of toluene in the adsorption beds based on Equation 6-3 (in Chapter 6) is 30.15 g toluene for the experimental period, which indicates that the adsorbed toluene was 54.5 % of the theoretical toluene holding capacity in the adsorption unit. The difference of percentile saturation between the two estimations is reasonably good within the experimental accuracy.

When the buffering capacity of the adsorption system is exhausted, regeneration of the adsorbents needs to be undertaken. In the present study, further regeneration could be achieved by using the supplemental valve air installed within the adsorption unit (see Figure 7-1). This allows further reduction in gas pressure of the desorbing adsorbent bed. An increase in the running cost of the system is however unavoidable for this purpose. However, it is worthwhile to note that repeated periods of non-use, such as weekend and holidays are common in most

chemical industries. These non-use periods can be considered as a method for regeneration whereby the adsorption system can be used only for desorbing the contaminants to the biofilter. Considering equation 6-2 in Chapter 6 (if T_f =4 hrs, and T_p=2 days), a 2-day of non-use allows 8.1 % of the theoretical toluene holding capacity within the beds to be released. Thus, the integrated unit can be assigned for treating waste air from discontinuous process bearing transient emission together with weekend recess. This would effectively retain the buffer capacity of the adsorbent unit when the process industry is back to normal shift hours. Furthermore, it should be noted that the biofilter recovery after non-use is one of the important factors for assessing biofilter performance.

It is interesting to notice from Figure 7-5 that after non-use periods, the integrated unit had superior reacclimation performance compared with the control unit. There was no apparent reacclimation time in the integrated system because the biological activity in the biofilter had been supported by incessantly substrate release from the adsorption system. On the other hand, the control unit was exposed to substrate starvation condition whereby longer reacclimation was encountered. The important implication of this result is that the 2-bed adsorption unit can also effectively function as a feeding source for the biofilter without any feeding phase during non-use periods.

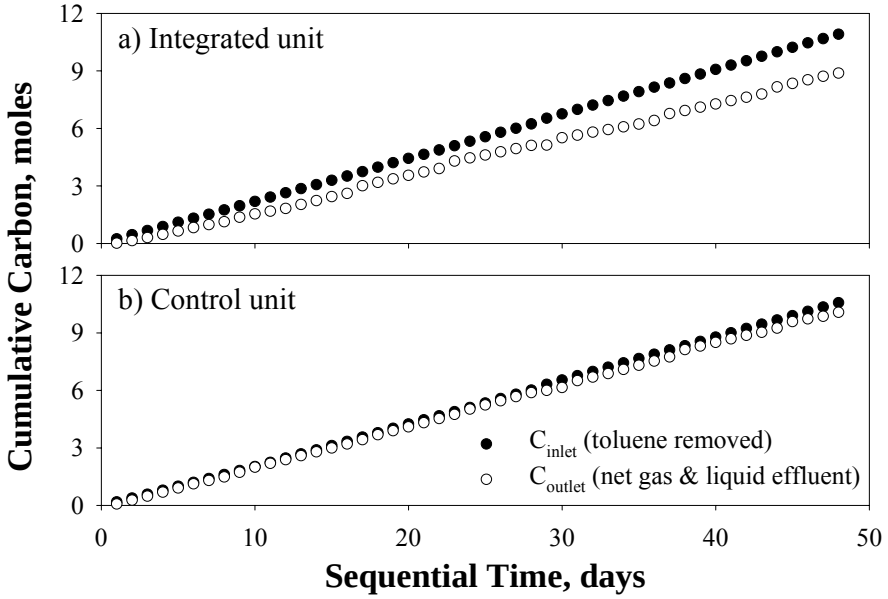

Figure 7-4 Carbon recovery (feeding condition: Type A). The cumulative carbon produced (C_{outlet}) is estimated as the net analysis of effluent carbon in the gas and liquid stream coupled with the VSS loss from the biofilter by assuming that a typical cellular composition for a heterogeneous microorganism can be represented by $C_5H_7O_2N$.

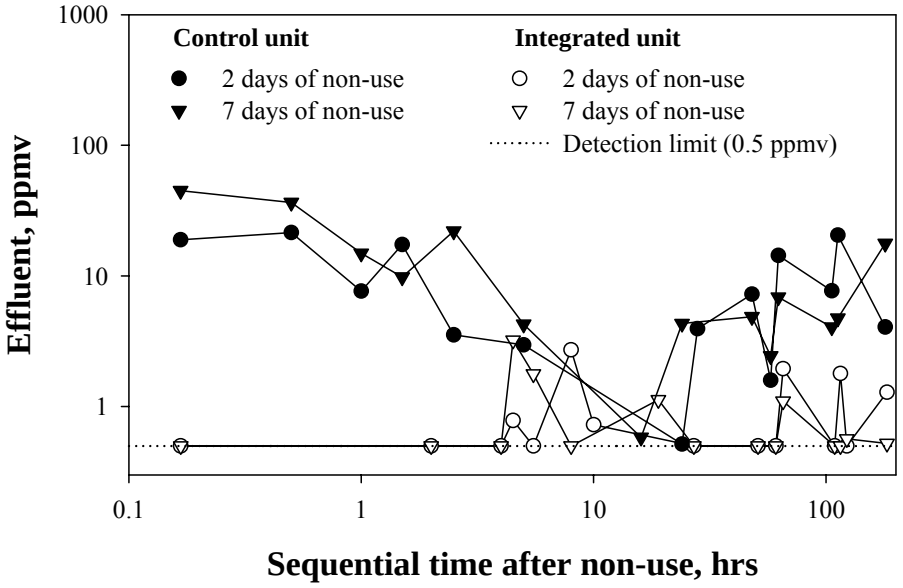

Figure 7-5 Effluent performances after non-use period (feeding condition: Type A). During non-use period without toluene loading, pure air passed through the system.

7.4.3. Evaluation of the Integrated Treatment Scheme

Having demonstrated the effectiveness of the integrated unit for Type "A" square wave (see Table 7-1), its operation was further extended to different feeding conditions (see Table 7-1) - higher peak concentration (Type B); more frequent peak concentration (Type C); and higher & more frequent peak concentration (Type D). The effluent responses to different feeding conditions are summarized in Figure 7-6a. Interestingly, it was observed for Type "D" square wave (daily discontinuous feeding) that no acclimation periods were apparently observed in the integrated unit, while about 2 hours of acclimation in the control unit was perceived after 14-hour starvation each day (data is presented in the next section). Hence the comparison provided in Figure 7-6a was based on using an 8-hour Time Weighted Average (TWA) effluent. If one considers toluene exposure to the occupational environment, it had been noted that the majority of people suffered acutely from mucous membrane irritation beyond a level of 5 mg VOC/m^3 (Molhave et al. 1984). Thus the exposure limit of 5 mg VOC/m^3 had been adopted by the American Industrial Hygiene Association (AIHA) (Hines et al. 1993). It is seen from Figure 7-6a that the integrated unit treated favorably the waste gas contaminated with toluene below this level (5 mg/m^3) for all cases. This behavior was not achieved by the control unit over any experimental period. The 8-hour TWA of the effluent from the control unit was 34.7±15.7, 31.7±16.4, 10.9±8.4, and 116.2±54.4 mg/m^3 for the feeding conditions of Types A, B, C, and D, respectively.

In order to determine the differences in biological activity for each unit, the first order kinetic constants as an estimate of biological activity were designated as follows (Ottengraf 1986)

$$\frac{C_e}{C_i} = \exp\left(-\frac{L K_1}{m U_a}\right) \qquad (7\text{-}1)$$

where C_e and C_i are the effluent and influent toluene concentrations to the biofilter, L is the height in the biofilter (60 cm), K_1 is the first order reaction rate constant (an estimate of microbial activity), m is the distribution coefficient for the VOC between liquid and gas phases which is 0.280 - dimensionless Henry's law constant, and U_a is the superficial velocity (0.00816 m/s). As seen in Figure 7-6b, estimates of microbial activity were calculated for peak loading and base loading at each feeding condition. It is seen from Figure 7-6b that more vigorous and stable biological activities were achieved by integrating the adsorption system with the biofilter. It is further seen from Figure 7-6b that the biological activities in the control unit deteriorated as the degree of load fluctuation increased. This supports the contention that any change in the substrate flux strongly affects the biological activity (Cox and Deshusses 2002; Kim et al. 2005a).

An interesting result is the comparison of total volume between the integrated unit and the single biofilter. To achieve the same treatment goal (over 99 % removal) as in the integrated unit, the reactor volume consisted of a single biofilter can be calculated by using equation 7-2,

$$V = \frac{C_{i,p} \cdot Q_i}{L_C} \qquad (7\text{-}2)$$

where, L_C is the critical loading to attain the 100 % removal of contaminant ($g/m^3 \cdot hr$), $C_{i,p}$ is the peak concentration for the inlet contaminant (g/m^3), Q_i is the air flow rate (m^3/hr), and V is the biofilter bed volume (m^3). The results obtained are summarized in Table 7-2, of which comparison indicates that the reduction in total volume of the system can be achieved by integrating the adsorption into the biofilter. It should be noted that biomass accumulation will accelerate when organic loading rate increases, specifically in the inlet section of the biofilter as observed in Chapter 4. Since excess accumulation of biomass can cause severe biofilter operating

problems such as clogging and pressure drop in the bed, the overall biofilter performance is unlikely to improve only if the reactor is scaled up.

Finally, the results of this study suggest that the competitiveness of the integrated treatment scheme greatly increases as the peak of contaminant concentration increases, and much lower investment and treatment costs will be projected for large scale of waste gas treatment.

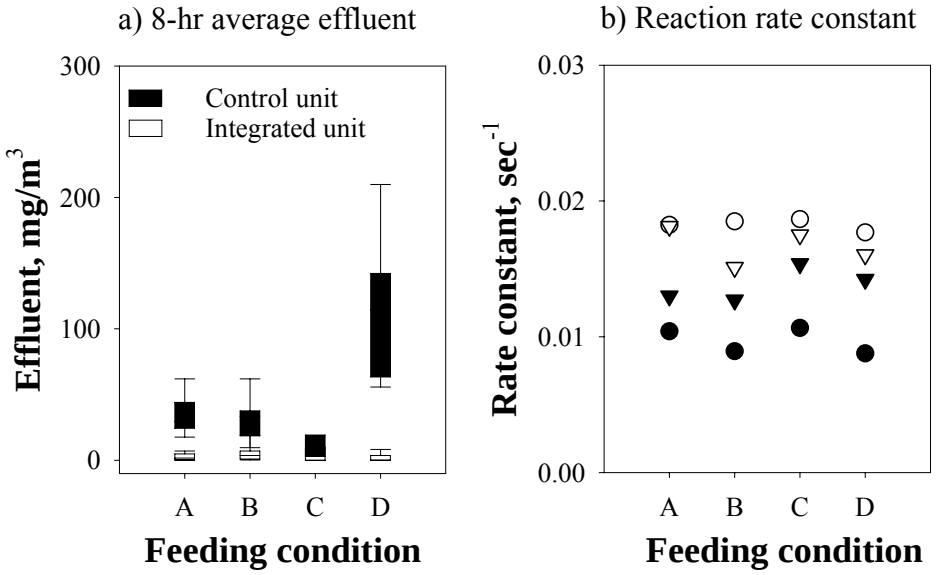

Figure 7-6 The effluent response and biological activity with respect to feeding conditions. a) 8-hr average effluent concentration: The box plot provides the 8-hour average effluent concentration across the range of experimental periods, stretching from the lower hinge (defined as the 5th percentile) to the upper hinge (the 95th percentile). b) First order reaction rate constant (an estimate of biological activity): The data presented represent the average values for peak loadings (○, integrated unit; ●, control unit) and base loading (▽, integrated unit; ▼, control unit) at each feeding condition.

Table 7-2 Reactor volume consisted of a single biofilter required [*]

Feeding Condition	Type A	Type B	Type C	Type D
Peak concentration ($C_{i,p}$), ppmv	400	700	400	600
(g/m^3)	(1.53)	(2.68)	(1.53)	(2.30)
Biofilter bed volume required (V), m^3 [**]	0.00435	0.00761	0.00435	0.00653
$V / V_{integrated}$ [***]	1.5	2.6	1.5	2.2

[*] Reactor volume consisted of a single biofilter to achieve the same treatment goal as in the integrated treatment scheme of a 2-fixed bed adsorption followed by a biofilter.

[**] Using equation 7-2, L_C = 46.9 $g/m^3 \cdot hr$ (defined in Chapter 3); Q_i = 0.133 m^3/hr (2.22L/min)

[***] $V / V_{integrated}$ denotes the ratio of the single biofilter volume to the integrated system volume for providing the same treatment goal. The volume of the integrated unit ($V_{integrated}$) is calculated to be 0.00293 m^3 = 0.000206 m^3 (a 2-fixed bed adsorption unit) + 0.00272 m^3 (a biofilter with 46.9 $g/m^3 \cdot hr$ of the critical loading for toluene removal).

7.4.4. Role of Backwashing in the Performance of Integrated Unit

To investigate the role of backwashing as biomass control in the performance of integrated treatment scheme, the removal performances of the integrated unit and the control unit with time after backwashing were evaluated under the feeding wave condition type "D". The results obtained are shown in Figure 7-7. The data presented denotes the average values for a period of three cycles of backwashing. As seen in the integrated unit, no acclimation periods were apparently observed and subsequently over 99 % removal efficiencies were consistently attained during the experimental period. However, for the control unit, more than 2 hours of acclimation was observed on day 1 when backwashing was conducted, and also about 2 hours of acclimation was perceived after 14-hour starvation each day. After acclimation, subsequent removal performance in the control unit fluctuated with removal efficiencies ranging from 85 % to 99 %. The difference of performance between the two units clearly indicates that the adsorption unit provided an important role in stabilizing the biofilter performance.

After a period of three cycles of backwashing, the two units continued to be operated without any biomass control. As shown in Figure 7-8, the overall performances of both units were found to deteriorate with time. Prolonged operation primarily resulted in formation of biomass not actively involved in contaminant removal, and subsequently the biofilter subject to excessive biomass formation faces clogging with decreasing contaminant removal efficiency (Cox and Deshusses 1998; Smith et al. 1996). This indicates that the control of biomass was necessary for attaining stable, long term high removal efficiencies for the biofilter. For this reason, periodic backwashing of the biofilter with medium fluidization was coordinated in this study. It is worthwhile to note that in the integrated unit, the deterioration impact was much less as compared to the control unit due to less contaminant loading on the biofilter in the integrated unit. Overall, when the integrated unit of a fixed 2-bed adsorption followed by a biofilter was

coordinated with periodic backwashing as biomass control, removal efficiencies above 99 % were consistently attained.

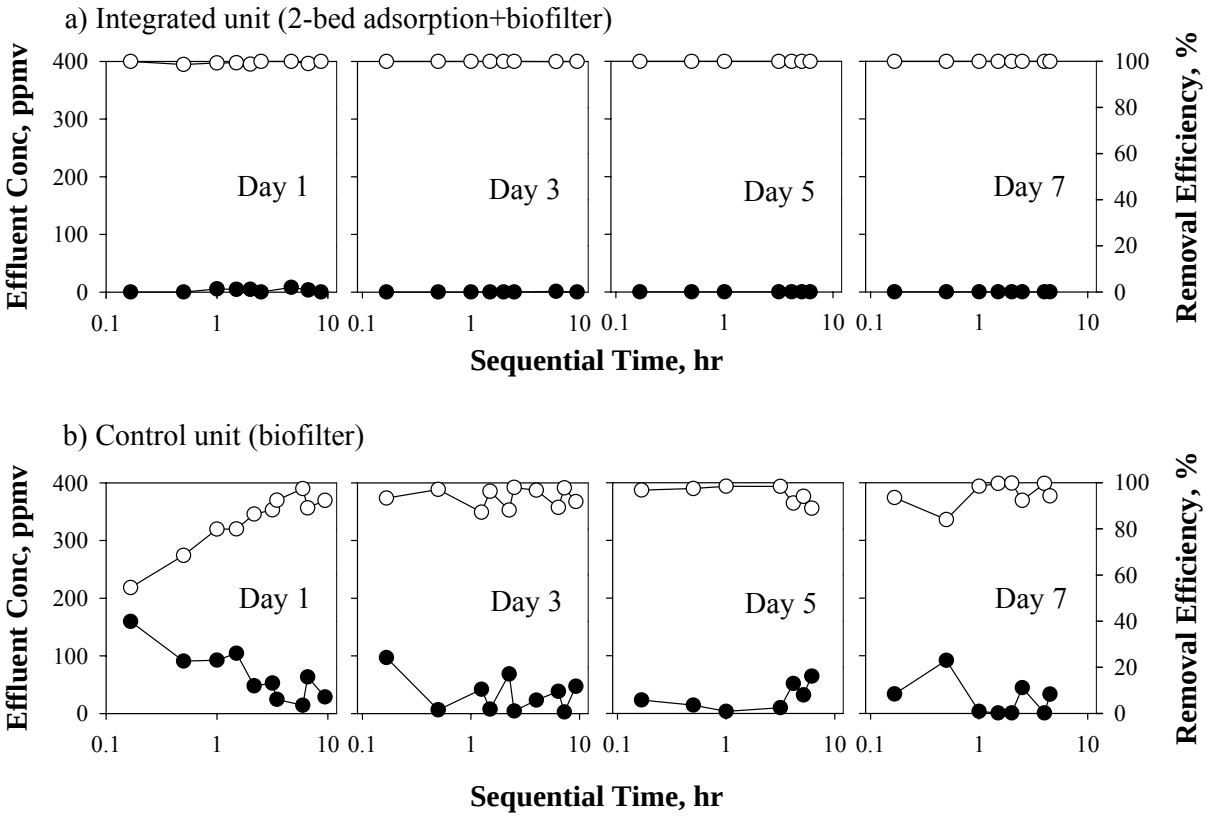

Figure 7-7 Overall removal performances of integrated unit and control unit with time after backwashing: Effluent concentrations, ppmv (●); Percent removal, % (○); the data presented are the averages each day (10 hours/day) for three cycles of backwashing, which was conducted once a week.

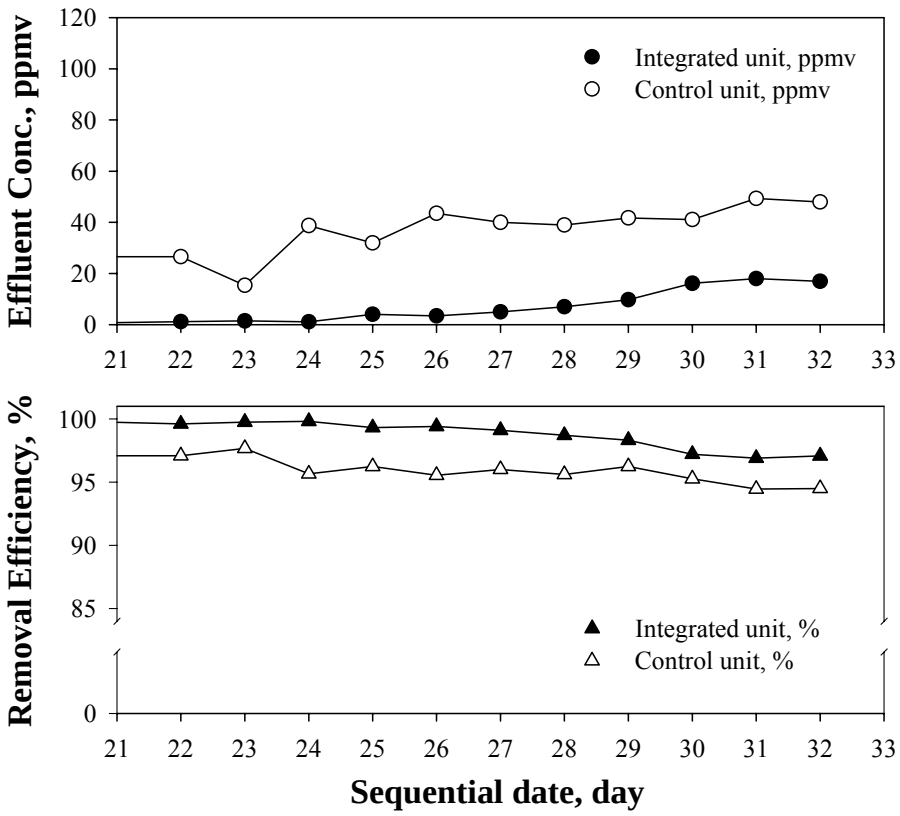

Figure 7-8 Overall toluene removal performances without backwashing: The data are the 8-hour average for each day. After 14-hour starvation each day, the 2-hour of reacclimation period for the control unit was excluded in the calculation.

7.5. Conclusions

As a final engineering observation, the results of the present study are particularly true when waste gas emissions appear to be similar to the different square wave options explored in the present study. The present study demonstrates that the net effect of the 2-bed adsorption was VOC concentration stabilization that makes it amenable for effective stable biodegradation. The conclusions that can be drawn from this study are as follows:

1. The 2-step cycle of adsorption and desorption in the 2-bed adsorption successfully performed particular functions as a polishing unit to abate the initial acclimation for the biofilter; as a buffering unit to mitigate the biofilter performance during load fluctuation; as a feeding source for the biofilter without any feeding phase when the biofilter is exposed to non-use periods as a shut down during weekends and holidays.
2. When periodic backwashing as biomass control was coordinated in operation of the integrated unit, extended and stable performance with highly efficient removal was performed.
3. The integrated treatment scheme of a biofilter preceded by a 2-fixed bed adsorption attained higher biological activity for toluene biodegradation, and treated favorably the waste gas contaminated with toluene in terms of VOC exposure to the occupational environment.
4. Details of the reactor volume suggest that capital expenses can be minimized by achieving a careful design and operation of the integrated unit.

7.6. References

Cox, H. H. J., and Deshusses, M. A. (1998). "Biological waste air treatment in biotrickling filters." *Current Opinion in Biotechnology*, 9(3), 256-262.

Cox, H. H. J., and Deshusses, M. A. (2002). "Effect of starvation on the performance and re-acclimation of biotrickling filters for air pollution control." *Environmental Science & Technology*, 36(14), 3069-3073.

Hines, A. L., Ghosh, T. K., Loyalka, S. K., and Warder, R. C. (1993). Indoor air quality and control, PTR Prentice Hall, Englewood cliffs, NJ.

Kim, D., Cai, Z., and Sorial, G. A. (2005a). "Evaluation of trickle bed air biofilter performance under periodic stressed operating conditions as a function of styrene loading." *Journal of the Air & Waste Management Association*, 55(2), 200-209.

Kim, D., Cai, Z., and Sorial, G. A. (2005b). "Impact of interchanging VOCs on the performance of trickle bed air biofilter." *Chemical Engineering Journal*, 113(2-3), 153-160.

Molhave, L., Bach, B., and Pederson, O. F. "Human reactions during exposures to low concentrations of Organic Gases and Vapors known as normal indoor air pollutants." *3rd for international conference on indoor air quality and climate*, Stockholm, Sweden.

Ottengraf, S. P. P. (1986). "Exhaust gas purification." Biotechnology, H. J. Rehm and G. Reed, eds., VCH Verlagsgesellschaft, Weinheim, Germany.

Smith, F. L., Sorial, G. A., Suidan, M. T., Breen, A. W., Biswas, P., and Brenner, R. C. (1996). "Development of two biomass control strategies for extended, stable operation of highly efficient biofilters with high toluene loadings." *Environmental Science & Technology*, 30(5), 1744-1751.

CHAPTER 8

CONCLUSION AND SUMMARY

Biofiltration systems have recently emerged as an attractive option for controlling volatile organic compounds (VOCs) emissions from industrial processes due to their cost effectiveness. However, biofiltration technology faces a number of challenges. Typically, most off-gas or treatment schemes for VOCs that originate in industrial processes have variable flowrates and contaminant concentration that limit the handling efficiency of the biofiltration system. As a solution to the handling limitation in biofilter performance, this study was proposed to develop an integrated technology to achieve stable contaminant removal efficiency by combining the buffering capacity of a two-bed cyclic adsorption/desorption unit with a Trickle Bed Air Biofilter (TBAB). Three major phases of this research included the characterization of biofilter performance under the adverse operating conditions, development of adsorption process of 2-column unit, and application of an integrated technology to the removal of VOCs. The following conclusions can be drawn from this study:

Phase I: Biofilter performance was operated under different operating conditions, i.e., backwashing, and two different non-use periods (starvation and stagnant period), as a function of VOCs loading. Experimental findings supported the handling limitation of performance of the current biofiltration system. This indicates that the limitation of current biofiltration system demands an innovative VOC control technology. Specific findings that can be drawn from this study include the following:

1. High performance (over 99% removal) of the biofilter had been observed for all experimental strategies (periodic backwashing, starvation, and stagnant) for toluene loading

up to 3.52 kg COD/m^3·day (corresponding to an inlet concentration of 250 ppmv); for styrene loading up to 1.27 kg COD/m^3·day (100 ppmv); for MEK loading up to 3.52 kg COD/m^3·day (250 ppmv); for MIBK loading up to 2.17 kg COD/m^3·day (100 ppmv). When higher VOCs loadings were employed, the coordinated biomass control, i.e., backwashing was subsequently unavoidable for attaining consistently high removal efficiency. As VOCs loadings increased, reacclimation of the biofilter to reach the 99 % removal efficiency following backwashing or the nonuse periods was delayed: which was a critical factor in biofilter performance.

2. The biofilter response after restart-up after non-use periods was strongly dependent on the active biomass in the biofilter. The substrate starvation condition influenced the decrease in the total biomass along the bed media, suggesting that starvation can be considered as another means of biomass control in case of low organic loadings. The presence of sufficient biomass and microbial activity played an important role in biofilter reacclimation when the biofilter was exposed to starvation conditions.
3. No significant difference between the effects of the two different strategies (starvation and stagnant) for non-use periods on biofilter performance was observed during the period of this study. As a final engineering view, significant energy saving would be made by shutting down the air blower and liquid pump during a period of non-use. However, operators should notice that long-term of the shut down cause problems of anaerobic condition in the biofilter bed, i.e., changes in microbial community, biofilm decay, and odor generation.
4. Biofilter performances linked with VOCs removal and biomass growth strongly depended on the physicochemical properties of VOCs treated. Most of all, the availability of VOCs into biofilm, which can be described by Octanol-water partition coefficient and Henry's

constant, was a critical factor to understand VOCs removal in the biofilter. In this study, high correlation ($r^2 = 0.922$) between Octanol-water partition coefficient and critical loading rate to the biofilter was found.

5. Large biomass yield was found in the biofilters treating oxygenated compounds (MEK and MIBK) as compared to aromatic compounds (toluene and styrene). Nitrate utilization was a strong function of the substrate loading rate, and was different according to the substrates treated. The ratio of nitrate utilization to nitrate usage for biomass yield increased as loading rates of oxygenated compounds increased. However, oxygen limitation and development of denitrification due to deeper biofilm formation could be driven at higher VOC loading rates. Correspondingly, the substrate inhibition of microbial growth and activity was observed as substrate loading rates increased.
6. Biofilter performance was strongly affected by microbial activity and biomass distribution. Periodic backwashing was effective in inducing even spatial distribution of biomass along the bed media, achieving long-term stable efficient biofilter performance. Cell synthesis was preferable to substrate oxidation in order to maintain sufficient biomass amount in the system. However, substrate oxidation became predominant in the whole biofilter bed with time due to local nutrient and substrate limitation in deep biofilm.

Phase II: Based on the adsorption isotherm of VOCs of concern, a two-fixed bed adsorption system proposed was designed and experimentally evaluated. Specific conclusions that can be drawn from this study include the following:

1. Single and ternary adsorption isotherms were determined by employing a simple constant volume method, which was utilized by using Tedlar gas sampling bags as a constant volume batch reactor. For single solute adsorption, Freundlich and Myers adsorption

equations were found to adequately correlate the experimental adsorption data. The pore size distribution of adsorbents was found to affect their adsorption capacities; its effect was dependant on the solute concentration. The ideal adsorbed solution theory (IAST) using the Myers equation for correlating the single solute data was found to accurately predicts the ternary adsorption isotherms.

2. Pore and surface diffusion model (PSDM) was used to predict adsorption and desorption profiles, which can provide a design curve to estimate an operating parameter, i.e., EBRT. The adsorption system consisted of two fixed beds which are alternately pressurized and depressurized in a 2-step cycle, where adsorption and desorption was simply achieved. The operating adsorption and desorption cycles for the adsorption system yielded constant loading conditions that can be treated effectively in a biofiltration system.

Phase III: An integrated treatment scheme of a two-fixed bed adsorption unit followed by a TBAB unit was evaluated under the transient toluene loading conditions, i.e., square wave changes of toluene inlet concentration. The results obtained revealed that the net effect of the 2-bed adsorption was VOC concentration stabilization that makes it amenable for effective stable biodegradation. The conclusions that can be drawn from this study are as follows:

1. The 2-step cycle of adsorption and desorption in the 2-bed adsorption successfully performed particular functions as a polishing unit to abate the initial acclimation for the biofilter; as a buffering unit to mitigate the biofilter performance during load fluctuation; as a feeding source for the biofilter without any feeding phase when the biofilter is exposed to non-use periods as a shut down during weekends and holidays. When a periodic backwashing as biomass control was coordinated in operation of the integrated unit, extended and stable performance with highly efficient removal was performed.

2. The integrated treatment scheme of a biofilter preceded by a 2-fixed bed adsorption attained higher biological activity for toluene biodegradation, and treated favorably the waste gas contaminated with toluene in terms of VOC exposure to the occupational environment.
3. Details of the reactor volume suggest that capital expenses can be minimized by achieving a careful design and operation of the integrated unit.

CHAPTER 9

Recommendations for Future Works

Biofilters operating in industry are generally exposed to other compounds or multi-component contaminants, particularly when assigned to the treatment of waste air (e.g. chemical or petroleum industry). Waste streams from industrial processes can also include chlorinated compounds. Cometabolism is significantly responsible for the degradation of chlorinated compounds (Alexander 1999), which would be of interest in a biofilter system. Furthermore, part of the challenge for successful biofiltration is that contaminants with low water solubility and high Henry's law constant are present in waste stream. Kim et al. (2004) demonstrated that hydrophilic compounds were degraded easily and deposited additional cell mass in the biofilter, while degradation of hydrophobic compounds was retarded until the biological cultures produced sufficient RNA or enzyme/protein to utilize these compounds. Mohseni and Allen (1999) found that the presence of a hydrophilic VOC in waste streams significantly decreased the removal rate of a hydrophobic compound in the biofilter. Maximum removal performance of different classes of organic compounds in the biofilter followed the sequence of alcohols > esters > ketones > aromatics > alkanes (Deshusses and Johnson 2000). The sequence well correlates with their Henry's law constants. Thus, an increase in the bioavailability of VOCs may enhance the rate of biodegradation if mass transfer is limiting. As a means for enhancing solubility, surfactants can be introduced in the biofiltration system. Nonionic and anionic surfactants have been intensively studied to enhance mobilization and bioavailability of hydrophobic compounds in contaminated soils and sediments. However, only a few studies have been conducted for gas treatment bioreactors. Woertz and Kinney (2004) found that a nonionic surfactant enhanced toluene degradation in the fungal biofilter by simulating bud formation in *E. lecanii-corni*.

Dhamwichukorn *et al*. Dhamwichukorn et al. (2001) reported that addition of a surfactant mixture increased α-pinene removal to 94 % in the thermophilic biofilter, in which its removal was only 26 % without addition of a surfactant. In a study of Mireles et al. (2001), the effect of a bio- and chemical surfactant on biofilm formation and attachment were investigated. Similar to investigations conducted for soil remediation, surfactant could have a microbial attachment inhibition to the biofilm. However, this function of the surfactant may serve effectively in retarding the accumulation of excess biomass in the biofilter. It is, therefore, expected to be successful in the defining a surfactant that will serve a dual purpose. The first is to improve biofilter performance for the removal of hydrophobic VOCs as a means in increasing its bioavailability and the second is to retard the accumulation of excess biomass in the biofilter.

When the integrated treatment scheme of a biofilter and adsorption is exposed to multi-component contaminants, competitive sorption can occur in the adsorption unit. As a result, adsorbents may exhibit differing buffering capacities for different contaminants. VOCs adsorption to adsorbents is governed by both adsorbents and VOCs properties. The pore and surface diffusion model (PSDM) can be successful in qualitatively and quantitatively predicting the pattern of VOC concentrations exiting the adsorption bed for the multi-component gas stream. An appropriate basis for design and analysis of the adsorption system should be established beforehand in the application.

Reference

Alexander, M. (1999). *Biodegradation and bioremediation*, Academic Press, San Diego, CA.

Deshusses, M. A., and Johnson, C. T. (2000). "Development and validation of a simple protocol to rapidly determine the performance of biofilters for VOC treatment." *Environmental Science & Technology*, 34(3), 461-467.

Dhamwichukorn, S., Kleinheinz, G. T., and Bagley, S. T. (2001). "Thermophilic biofiltration of methanol and alpha-pinene." *Journal Of Industrial Microbiology & Biotechnology*, 26(3), 127-133.

Kim, D., Cai, Z., and Sorial, G. A. "Impact of Interchanging VOCs on the performance of trickle-bed air biofilter." *USC-CSC-TRG Conference on Biofiltration for Air Pollution Control*, Santa Monica, California, 35-41.

Mireles, J. R., Toguchi, A., and Harshey, R. M. (2001). "Salmonella enterica serovar typhimurium swarming mutants with altered biofilm-forming abilities: Surfactin inhibits biofilm formation." *Journal Of Bacteriology*, 183(20), 5848-5854.

Mohseni, M., and Allen, D. G. (1999). "Transient performance of biofilters treating mixtures of hydrophilic and hydrophobic volatile organic compounds." *Journal of the Air & Waste Management Association*, 49(12), 1434-1441.

Woertz, J. R., and Kinney, K. A. (2004). "Influence of sodium dodecyl sulfate and tween 20 on fungal growth and toluene degradation in a vapor-phase bioreactor." *Journal Of Environmental Engineering-Asce*, 130(3), 292-299.

Appendix I: Composition of the various components in the buffered nutrient solution

Component	Chemical Compound	Concentration (mg/l)
B^{3+}	$Na_2B_4O_7 \cdot 10H_2O$	0.0019
Ca^{2+}	$CaCl_2 \cdot 2H_2O$	0.2699
Co^{2+}	$CoCl_2 \cdot 6H_2O$	0.0104
Cu^{2+}	$CuCl_2 \cdot 2H_2O$	0.0113
Fe^{3+}	$FeCl_3$	0.0159
K^+	$KHSO_4$	1.7427
Mg^{2+}	$MgCl_2 \cdot 6H_2O$	0.4338
Mn^{2+}	$MnCl_2 \cdot 4H_2O$	0.0194
Cl^-	- [a]	1.8512
SO_4^{2-}	$KHSO_4$	4.28
Mo^{6+}	$(NH_4)_6Mo_7O_{24}$	0.0167
NH_4^+		0.0027
Zn^{2+}	$ZnCl_2$	0.0232
Na^+	- [b]	- [c]
NO_3^-	$NaNO_3$	- [c]
PO_4^{2-}	$NaH_2PO_4 \cdot H_2O$	- [c]
CO_3^-	$NaHCO_3$	- [d]
p-Aminobenzoic acid	$C_7H_7NO_2$	0.0011
Biotin	$C_{10}H_{16}N_2O_3S$	0.0004
Cyanocobalamin (B12)	$C_{63}H_{88}CoN_{14}O_{14}P^-$	0.00002
Folic acid	$C_{19}H_{19}N_7O_6$	0.0004
Nicotinic acid	$C_6H_5NO_2$	0.0011
Panothenic acid.	$C_{18}H_{32}CaN_2O_{10}$	0.0011
Pyriodoxine hydrochloride	$C_8H_{12}ClNO_3$	0.0023
Riboflavin	$C_{17}H_{20}N_4O_6$	0.0011
Thiamin hydrochloride	$C_{12}H_{18}Cl_2N_4OS$	0.0011
Thioctic acid	$C_8H_{14}O_2S_2$	0.0011

[a] $CaCl_2 \cdot 2H_2O$, $CoCl_2 \cdot 6H_2O$, $CuCl_2 \cdot 2H_2O$, $FeCl_3$, $MgCl_2 \cdot 6H_2O$, $MnCl_2 \cdot 4H_2O$, $ZnCl_2$,

[b] $NaNO_3$, $NaH_2PO_4 \cdot H_2O$, $NaHCO_3$

[c] flexible as VOCs loading rate: COD/N = 50:1 ; N/P = 4:1

[d] buffer solution

Appendix II: Properties of Compounds Studied

	Toluene	Styrene	Methyl ethyl ketone (MEK)	Methyl isobutyl ketone (MIBK)
Formula	C_7H_8	C_8H_8	C_4H_8O	$C_6H_{12}O$
Molecular Weight (g/mole)	92.14	104.15	72.1	100.16
Water Solubility (mg/L)	546	230	256,000	19,100
Vapor Pressure (mmHg, 20 ^oC)	22	5.12	77.5	15
Henry's Constant (atm m^3/mole, 25^oC)	6.74×10^{-3}	2.61×10^{-3}	4.66×10^{-5}	1.49×10^{-5}
(dimensionless)	0.28	0.109	0.00194	0.00062
K_{ow} ($logK_{ow}$) [a]	2.58	3.16	0.28	1.09
K_{oc} (ml/g)	300	920	4.5	19
Specific gravity	0.867	0.906	0.805	0.789
Air Saturated Conc.				
(g/m^3, 20^oC)	110	31	-	27
(g/m^3, 30^oC)	184	52	-	53
EC50 (mg/L) [b]	23	5.5	3426	80
List [c]	PCNH	CNH	CNH	NH
Chemical Abstract NO.	108-88-3	100-42-5	78-93-3	108-10-1

[a] Octanol-water partition coefficient

[b] Ecotoxicity (EC50, mg/L) of VOCs to photobacterium phosphoreum by the Microtox® test

[c] P = priority pollutant (designated under the Clean Water Act); C = hazardous substance list (designate under CERCLA); N = Appendix IX chemicals (designated under RCRA); H = hazardous air pollutant (designated under the Clean Air Act Amendments).

Appendix III: Analysis Methods for Gas and Liquid Samples

VOCs Analyses for Gas Phase Samples

GC Analysis. The concentrations of VOCs as gas phase were determined by using a GC (HP 5890, Series II, Hewlett Packard, Palo Alto, CA) with a flame ionization detector (FID), and a 30-m length, 0.25-mm I.D., 0.25-μm Film thickness narrow bore column (DB 624, J&W Scientific, Folsom, CA). The GC oven temperature was programmed from 40 °C to 120 °C at a rate of 20 °C/min with a 2-min hold at 40 °C and a 2-min hold at 120 °C. The carrier gas (N_2) flow rate was set at 2.3 mL/min. The FID detector was used with N_2 make-up gas at a flow rate of 20 mL/min, a fuel gas flow (H_2) of 30 mL/min, and an oxidizing gas flow (air) of 300 mL/min. The detector temperature was 250 °C. Detection limits for VOCs concentration were 0.5, 0.5, 0.25, and 0.25 ppmv for toluene, styrene, MEK, and MIBK, respectively.

Gas Sampling. Gas phase samples for VOC analysis were taken with gas-tight syringes (500 μL) through low-bleed and high-puncture-tolerance silicone gas chromatograph (GC) septa installed in the sampling ports.

VOC Standard and Calibration. Gaseous VOCs standards were prepared in a static gas dilution bottle (SGDB). Neat multi-component VOCs of concern as liquid phase was prepared. 10 μL of the neat multi-component VOC was added to a calibrated bottle to achieve 1.0 μg/mL of vapor standard. 40 mL of the1.0 μg/mL vapor standard was added to another bottle in order to achieve 0.02 μg/mL of standard. All volumes were verified by weight by using an analytical balance. In the SGDB, the injected VOC vaporized within 2 hours. Taking out different volume of VOC as vapor from each of the two prepared bottles, the calibration points were established by GC analysis (see Table A). The density and purity of chemical products were considered in all concentration calculations listed in Table 1. Once the calibration curve was established, a check

standard was injected prior to analysis in order to confirm calibration. Recalibration was done every other month. A reference standard was also prepared to ensure the accuracy of the standard prepared above. 1.0 μg/mL and 0.1 μg/mL of the reference standard were used to verify the accuracy of the standard. 1.0 μg/mL of the reference standard was prepared by using the same method for preparing the standard. 8 mL of 1.0 μg/mL of standard was added to another bottle to achieve 0.1 μg/mL of the reference standard.

Table A. The Standard Concentration and Calibration Levels for bag samples

VOCs in SGDB (μg/mL)	VOCs Volume Injected Into GC (μl)	VOCs Calibration Level (ng on column)	Concentration* (mg/L, ppmv)
0.02	50	1	0.002, 0.5
0.02	100	2	0.004, 1
0.02	250	5	0.01, 2.5
0.02	500	10	0.02, 5
0.02	1000	20	0.04, 10
1.0	25	25	0.05, 12.5
1.0	50	50	0.1, 25
1.0	100	100	0.2, 50
1.0	250	250	0.5, 125
1.0	500	500	1.0, 250

* based on 500 μL sample volume

CO_2 Gas Analysis

GC Analysis. CO2 concentration in the gas phase were measured by chromatographic separation on a 2.4-m HayeSep Q, 80/100 column using a GC (HP 5890, Series II, Hewlett Packard, Palo Alto, CA) equipped with a thermal conductivity detector (TCD) (Hewlett Packard, Palo Alto, CA). The GC oven temperature was programmed from 50 °C to 80 °C at 10 °C/min with a 3.2 min hold at 50 °C and a 1.5 min hold at 80 °C. The carrier gas (He) flow rate was set at 30 mL/min, and the TCD detector was used with He make-up gas at A flow rate of 35 μL/min. Detection limit for CO_2 concentration was 300 ppmv

Gas Sampling. Gas phase samples for CO_2 analysis were taken with gas-tight syringes (1000 μL) through low-bleed and high-puncture-tolerance silicone gas chromatograph (GC) septa installed in the sampling ports.

Nitrate Analysis for Liquid Samples

The nitrate concentration was determined by using a Shimadzu UVmini 1240 UV-VIS spectrophotometer (Shimadzu Corp., Tokyo, Japan) as the following.

1. PREPARE STOCK SOLUTION
   A. Dry potassium nitrate (KNO_3) in an oven at 105°C for 24 h.
   B. Dissolve 0.7218 g in distilled or deionized water of high purity and dilute to 1000ml; 1.00ml=100μg NO_3^- -N (100mg/l), preserve with 2ml $CHCl_3$.
   C. Dilute the above solution 100ml to 1000ml with water; 1.00ml=10.0μg NO_3^- -N (10mg/l), preserve with 2ml $CHCl_3$.
2. PREPARE SAMPLES
   A. Dilute (0, 1.00, 2.00, 4.00, 5.00, 10.0, 20.0, 25.0, 30.0, 35.0ml) of 10mg/l stock solution to 50ml to get (0, 0.2, 0.4, 1.0, 2.0, 4.0, 5.0, 6.0, 7.0 mg/l) standard samples
   B. Add 1 ml 1N HCl solution and mix thoroughly
   C. Take 50 ml clear sample, filtered if necessary, add 1 ml 1N HCl solution and mix thoroughly
3. SPECTROPHOTOMETRIC MEASUREMENT
   A. Read absorbance against redistilled water set at **zero** absorbance
   B. Use a wavelength of 220 nm to obtain NO_3^- reading
   C. Use a wavelength of 275 nm to determine interference due to dissolved organic matter
4. PREPARE CALIBRATION CURVE AND SAMPLES CALCULATION
   A. Subtract two times the absorbance reading at 275 nm from the reading from 220 nm to obtain absorbance due to NO_3^-
   B. Construct a standard curve by plotting absorbance from A against NO_3^--N concentration of standard.
   C. Use corrected sample absorbances, obtain sample concentrations directly from standard curve.

NOTE: if correction value is more than 10% of the reading at 220 nm, do not use this method

TC & IC Analyses for Liquid Samples

TC and IC were analyzed by using a Shimadzu TOC 5000 analyzer (Shimadzu Corp., Tokyo, Japan). Samples were filtered through 0.45 μm nylon filters (Micron Separation, Westboro, MA) prior to the analysis.

1. ORGANIC CARBON STOCK SOLUTION PREPARATION
   A. Dissolve 2.1254g anhydrous primary-standard-grade potassium biphthalate, $C_8H_5KO_4$ in carbon-free water and dilute to 1000ml, 1.00ml=1.00mg carbon;
   B. Prepare 5 different concentrations (1.0, 5.0, 10.0, 20.0 and 30.0 mg/l) from A solution with super-Q water;
2. INORGANIC CARBON STOCK SOLUTION PREPARATION
   A. Dissolve 4.4122g anhydrous sodium carbonate, Na_2CO_3 in water and add 3.497g anhydrous sodium bicarbonate $NaHCO_3$, dilute to 1000ml; 1.00 ml= 1.00mg carbon
   B. Prepare 5 different concentrations (1.0, 5.0, 10.0, 20.0 and 30.0 mg/l) from A solution with super-Q water;
3. CALIBRATION CURVE IN TOC
   A. Blank Super-Q water
   B. Five TC standards (start with the lowest concentration). Acidify the standard with 12 N HCl, sparge for 3 min and then do 5 injections with a max of 10 injections per standard. The samples that are acidified and purged will provide the non-purgeable organic carbon (NPOC)
   C. Use the standards measured results to draw the calibration curve of TOC
4. CALIBRATION CURVE IN IC
   A. Blank Super-Q water
   B. Five IC standards (start with the lowest concentration). Do 5 injections with a max of 10 injections per standard.
   C. Use the standards measured results to draw the calibration curve of IC

VSS Analysis for Liquid Samples

The VSS concentrations in the effluent and backwashing solution were determined according to Standard Methods 2540 G.

1. Prepare VSS filter papers
   A. Select 4.7-cm diameter 1.5- μm glass fiber filter papers and pans for 3 samples for each analysis.
   B. Place each filter on the filter screen, rough side up, and suck water through each, 2 times.
   C. Place each pan with filter paper in the 550°C over for 60 minutes.
   D. Place fresh desiccant in the scale, and in the desiccator.
   E. Remove from the oven, place in a desiccator for 30 minutes to cool.
   F. Weigh each pan, and leave in the desiccator for later use.

2. Filter the VSS samples
   A. Put a mixing bar into the sample bottle and stir on stirrer.
   B. Rinse all filtering equipment with DI water, and drain excess.
   C. Assemble the filter apparatus, with a clean 500mL filter flask.
   D. Put a fresh, tared filterin the filter assembly.
   E. Fill a 100mL graduated cylinder with fresh, mixed sample.
   F. Filter the 100mL, and "by eyeball" decide how much additional sample to filter through this paper
   G. Record the total amount filtered for this VSS sample
   H. Return the filter paper to the pan. Check that any torn filter material is scrapped form the filter, and added to the filter in the pan.
   I. Place the pan aside, under a protective cover.
   J. Repeat this procedure for each sample.

3. (Desiccation): Put all the filter pans in the 103°C oven for 2 hours.
4. Remove all pans from the oven, Place in the desiccator for 30 minutes, and weigh.
5. (Ignition): Put all filter pans in the 550°C oven for 60 minutes.
6. Remove all pan from the oven, Place in the desiccator for 30 minutes, and Weight.
7. Calculate VSS as mg/L.

Appendix IV: Kinetics analysis for VOC removal with biofilter depth

The removal performances as a function of depth in the biofilter were studied on day following the backwashing and the non-use periods for each VOC. The obtained data were used to develop the first-order removal rate as a function of depth in the biofilter for each experimental strategy. To avoid misinterpretation of the data because of the possibility of biodegradation occurring above the media bed along the reactor freeboard walls at the top of the biofilter and in the bottom disengagement chamber used for separation between water and air, the kinetic analyses were conducted by using the data from sampling ports within the media. The data below detection limit were excluded in the analysis. By plotting the semi-logarithmic scale of the ratio of residual concentration to inlet concentration as a function of depth in the biofilter, the first order reaction rate constants were obtained from the slops of the regression lines. The results obtained are depicted in Figure A ~ D for toluene, styrene, MEK, and MIBK, respectively.

Figure A. Reaction rate as a function of toluene loadings and experimental strategies

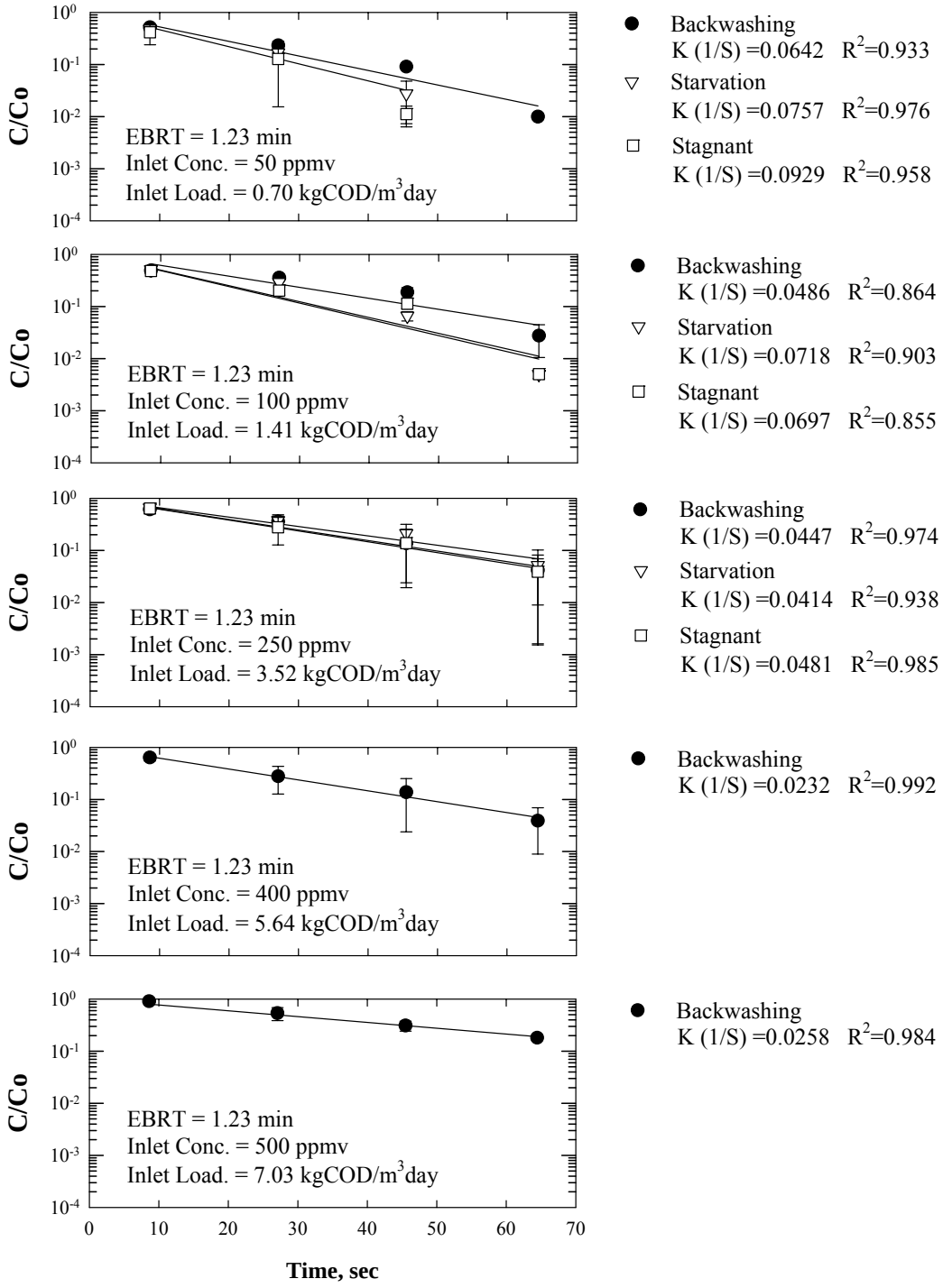

Figure B. Reaction rate as a function of styrene loadings and experimental strategies

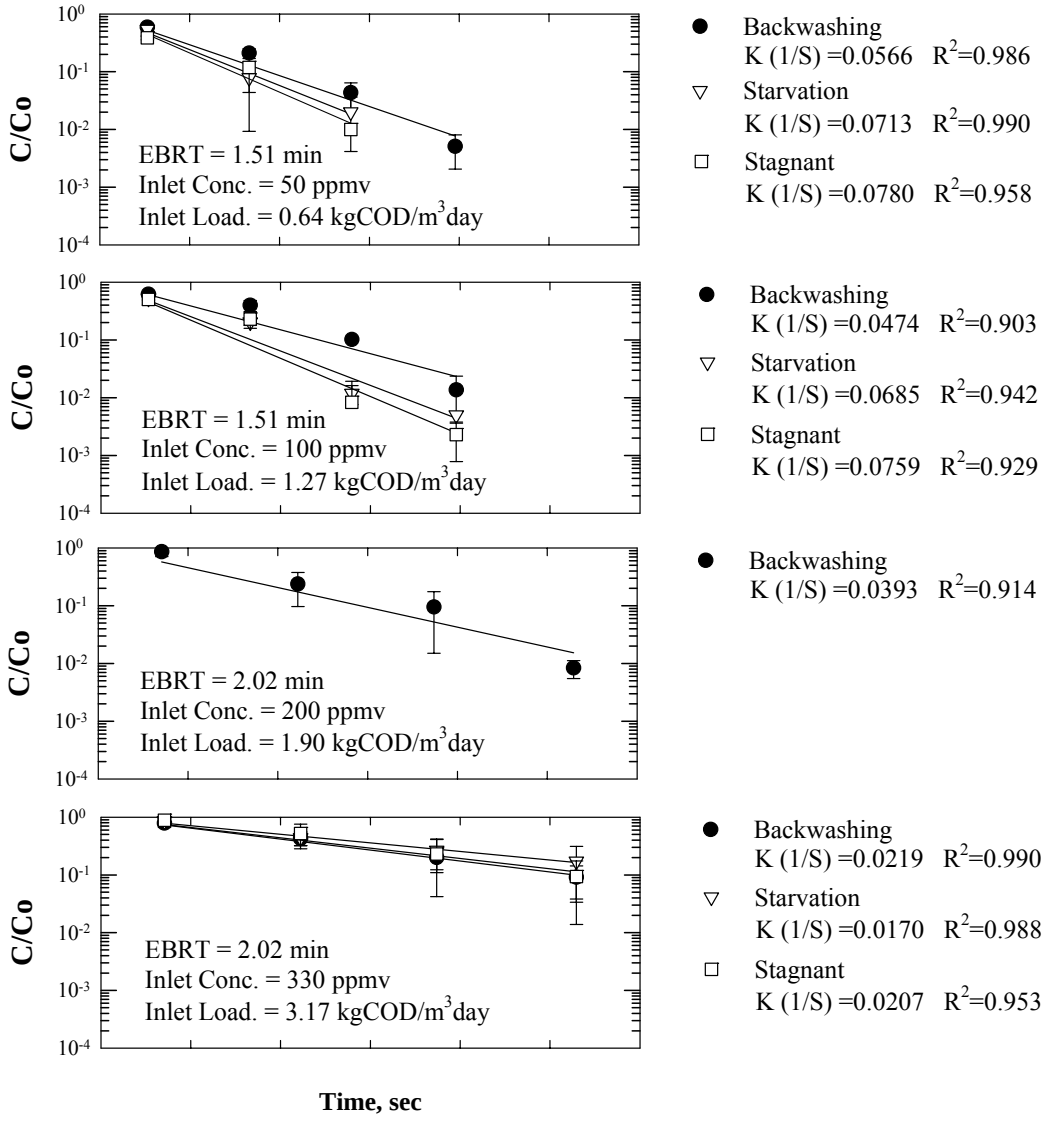

Figure C. Reaction rate as a function of MEK loadings and experimental strategies

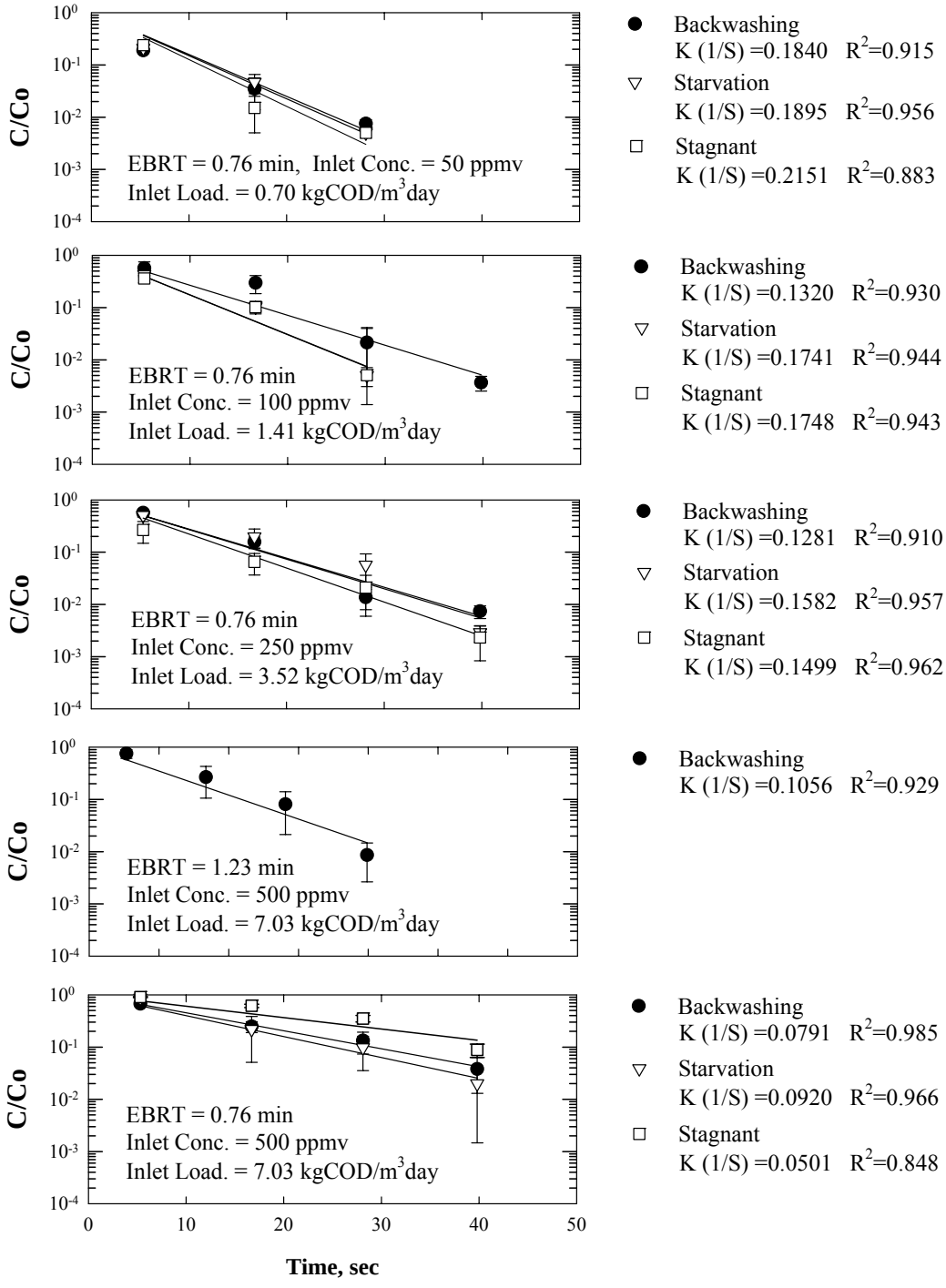

Figure D. Reaction rate as a function of MIBK loadings and experimental strategies

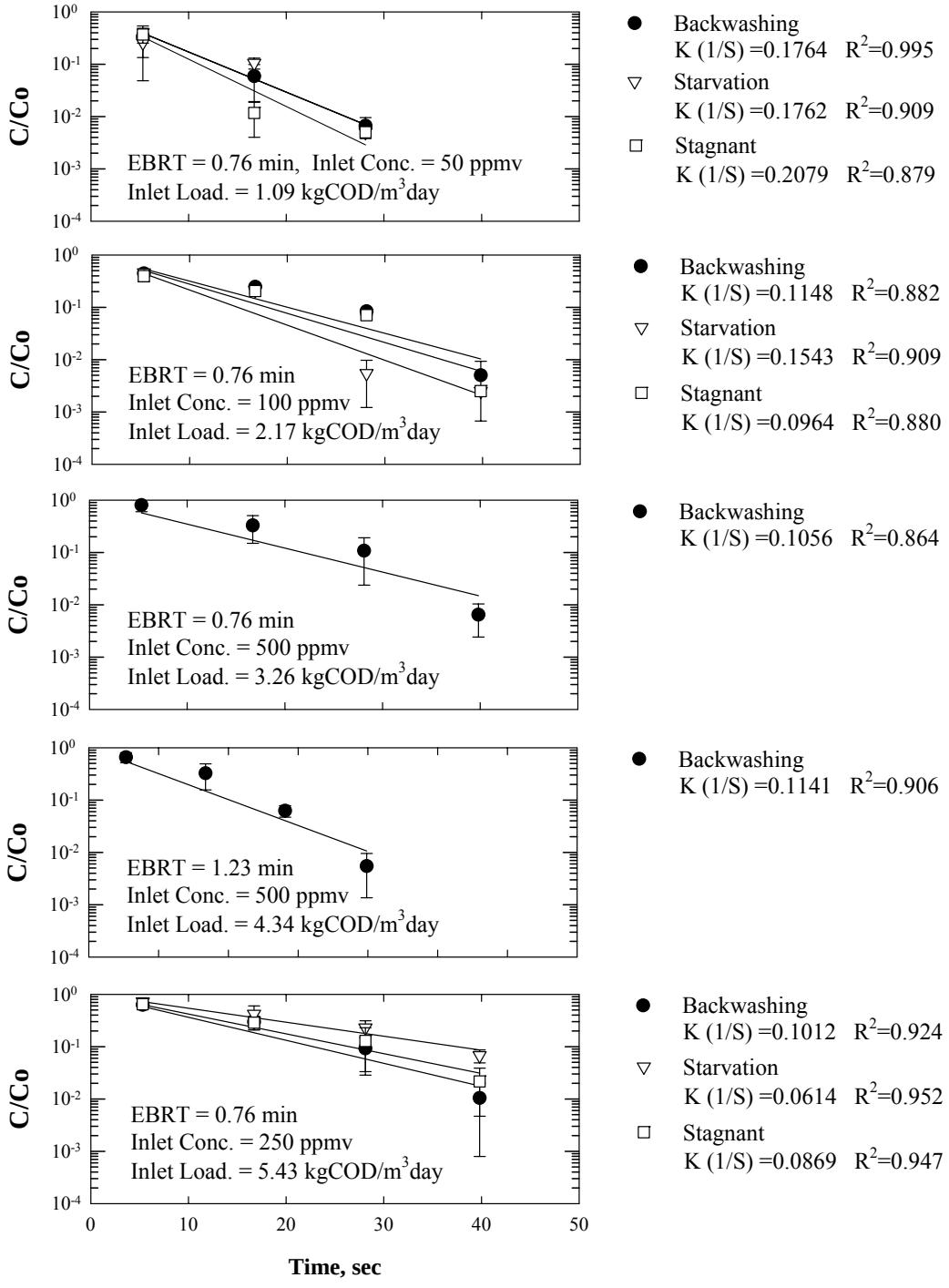

Appendix V: Input parameters for Adsorption Simulation used in AdDesignS™

Parameter	Value	Unit
Fixed Bed Properties		
Bed Length	0.5 ~14 [a]	cm
Bed Diameter	2.54 [a]	cm
Bed Mass	2.1 ~ 81.8 [b]	g
Flowrate	2.22 [a]	L/min
Adsorbent Properties		
Name	Calgon BPL 6×16	
Apparent Density	0.85 [c]	g/mL
Particle Radius	0.186 [c]	cm
Porosity	0.595 [c]	
Particle Shape Factor	0.72 [c]	
Component Properties: Toluene		
Freundlich Isotherm Parameters		
K	339 [d]	$(mg/g)(L/mg)^{1/n}$
1/n	0.314 [d]	
Kinetic Paramters		
Film Diffusion	1.02 [e]	cm/s
Surface Diffusion	3.58×10^{-6} [f]	cm^2/s
Pore Diffusion	8.08×10^{-2} [f]	cm^2/s
Surface to pore diffusion flux ratio	16 [e]	
Tortuosity	1 [e]	
Air Properties		
Pressure	1 [a]	atm
Temperature	20 [a]	^oC

[a.] Defined by user: Values for bed diameter, flowrate, air pressure, and temperature were fixed. Flowrate was predefined from the setup value of air flow rate for the toluene biofilter. Variable values for bed length were defined for generating different EBRTs.

[b.] Assumed that bed was well packed with adsorbents and calculated by apparent density of adsorbent

[c.] Data provided by Calgon carbon

[d.] Experimentally measured in Chapter 5 of adsorption isotherm

[e.] Based on the study performed by Moe and Li (2004 USC-CSC-TRG Conference, 89-96)

[f.] Calculated by AdDesignS™